AN AERODYNAMIC INVESTIGATION OF A LOW ASPECT RATIO WING

Leonard B. McCommon

Air Force Institute of Technology
Wright-Patterson Air Force Base, Ohio

December 1975

KEEP UP TO DATE

Between the time you ordered this report—which is only one of the hundreds of thousands in the NTIS information collection available to you—and the time you are reading this message, several *new* reports relevant to your interests probably have entered the collection.

Subscribe to the **Weekly Government Abstracts** series that will bring you summaries of new reports *as soon as they are received by NTIS* from the originators of the research. The WGA's are an NTIS weekly newsletter service covering the most recent research findings in 25 areas of industrial, technological, and sociological interest—invaluable information for executives and professionals who must keep up to date.

The executive and professional information service provided by NTIS in the **Weekly Government Abstracts** newsletters will give you thorough and comprehensive coverage of government-conducted or sponsored research activities. And you'll get this important information within two weeks of the time it's released by originating agencies.

WGA newsletters are computer produced and electronically photocomposed to slash the time gap between the release of a report and its availability. You can learn about technical innovations immediately—and use them in the most meaningful and productive ways possible for your organization. Please request NTIS-PR-205/PCW for more information.

The weekly newsletter series will keep you current. But *learn what you have missed in the past* by ordering a computer **NTISearch** of all the research reports in your area of interest, dating as far back as 1964, if you wish. Please request NTIS-PR-186/PCN for more information.

WRITE: Managing Editor
5285 Port Royal Road
Springfield, VA 22161

Keep Up To Date With SRIM

SRIM (Selected Research in Microfiche) provides you with regular, automatic distribution of the complete texts of NTIS research reports *only* in the subject areas you select. SRIM covers almost all Government research reports by subject area and/or the originating Federal or local government agency. You may subscribe by any category or subcategory of our WGA **(Weekly Government Abstracts)** or **Government Reports Announcements and Index** categories, or to the reports issued by a particular agency such as the Department of Defense, Federal Energy Administration, or Environmental Protection Agency. Other options that will give you greater selectivity are available on request.

The cost of SRIM service is only 45¢ domestic (60¢ foreign) for each complete microfiched report. Your SRIM service begins as soon as your order is received and processed and you will receive biweekly shipments thereafter. If you wish, your service will be backdated to furnish you microfiche of reports issued earlier.

Because of contractual arrangements with several Special Technology Groups, not all NTIS reports are distributed in the SRIM program. You will receive a notice in your microfiche shipments identifying the exceptionally priced reports not available through SRIM.

A deposit account with NTIS is required before this service can be initiated. If you have specific questions concerning this service, please call (703) 451-1558, or write NTIS, attention SRIM Product Manager.

This information product distributed by

NTIS U.S. DEPARTMENT OF COMMERCE
National Technical Information Service
5285 Port Royal Road
Springfield, Virginia 22161

UNCLASSIFIED

SECURITY CLASSIFICATION OF THIS PAGE (When Data Entered)

REPORT DOCUMENTATION PAGE	READ INSTRUCTIONS BEFORE COMPLETING FORM
1. REPORT NUMBER: GAE/AE/75D-15	2. GOVT ACCESSION NO.
	3. RECIPIENT'S CATALOG NUMBER: AD-A021 733
4. TITLE (and Subtitle): AN AERODYNAMIC INVESTIGATION OF A LOW ASPECT RATIO WING	5. TYPE OF REPORT & PERIOD COVERED: MS Thesis
	6. PERFORMING ORG. REPORT NUMBER
7. AUTHOR(s): Leonard V. McCommon, Captain, USAF	8. CONTRACT OR GRANT NUMBER(s)
9. PERFORMING ORGANIZATION NAME AND ADDRESS: Air Force Institute of Technology (AFIT-EN), Wright-Patterson AFB, Ohio 45433	10. PROGRAM ELEMENT, PROJECT, TASK AREA & WORK UNIT NUMBERS: Project 19900105
11. CONTROLLING OFFICE NAME AND ADDRESS: Air Force Flight Dynamics Laboratory, Prototype Division (AFFDL/PTB), Wright-Patterson AFB, Ohio 45433	12. REPORT DATE: December, 1975
	13. NUMBER OF PAGES: 126
14. MONITORING AGENCY NAME & ADDRESS (if different from Controlling Office)	15. SECURITY CLASS. (of this report): Unclassified
	15a. DECLASSIFICATION DOWNGRADING SCHEDULE

16. DISTRIBUTION STATEMENT (of this Report)

Approved for public release; distribution unlimited

PRICES SUBJECT TO ...

17. DISTRIBUTION STATEMENT (of the abstract entered in Block 20, if different from Report)

18. SUPPLEMENTARY NOTES

Approved for public release; IAW AFR 190-17

JERRY C. HIX, Captain, USAF
Director of Information

19. KEY WORDS (Continue on reverse side if necessary and identify by block number)

Aerodynamics of a low aspect ratio wing
Wing investigation
Stability investigation

20. ABSTRACT (Continue on reverse side if necessary and identify by block number)

This study consisted of modeling and testing a high-speed, low-aspect ratio flying wing with the intention of determining its lift, drag, and static stability characteristics. The model was tested at Mach numbers of 0.70 to 0.86 in the Air Force Flight Dynamics Laboratory's Trisonic Gasdynamic Facility located at Wright-Patterson Air Force Base, Ohio. Six different configurations of stabilizing fins were tested in addition to

DD FORM 1 JAN 73 1473 EDITION OF 1 NOV 65 IS OBSOLETE

UNCLASSIFIED

SECURITY CLASSIFICATION OF THIS PAGE (When Data Entered)

the basic configuration of the wing without fins. The results of the tests indicated that the proposed aircraft can be made statically stable; the degree of stability being dependent on center of gravity location and angle of attack. Wind tunnel test results are presented in graphical and tabular form for use in future design studies of similar aerodynamic configurations.

AN AERODYNAMIC INVESTIGATION OF A LOW ASPECT RATIO WING

THESIS

GAE/AE/75D-15 Leonard V. McCommon
Captain USAF

Approved for public release; distribution unlimited.

GAE/AE/75D-15

AN AERODYNAMIC INVESTIGATION OF A LOW ASPECT RATIO WING

THESIS

Presented to the Faculty of the School of Engineering
of the Air Force Institute of Technology
Air University
In Partial Fulfillment of the
Requirements for the Degree of
Master of Science

By
Leonard V. McCommon, B.S.
Captain USAF
Graduate Aero-Mechanical Engineering
December 1975

Preface

The purpose of this report was to determine certain aerodynamic characteristics of a newly proposed high-speed aircraft. This aircraft, a low-aspect ratio wing designed to provide low detectability at high altitudes, was believed to possess an inherent lack of stability due to its proposed stabilizer location. It was my intention to determine if the proposed aircraft is aerodynamically feasible, especially from a lateral stability standpoint.

I wish to thank my thesis advisor, Major Roger A. Crawford, of the Aero-Mechanical Engineering Department of the United States Air Force Institute of Technology. Without his instruction both in and out of the classroom my difficulties in this task would have been many times multiplied.

I wish also to acknowledge the outstanding craftsmanship of Mr. John Brohas and Mr. Jack Tiffany, of the AFIT Training Aids Division. With the rather poor drawings I sometimes submitted, they returned an excellent model.

Finally, I wish to thank my wife, Judy K., for tolerating me in my moments of despair while preparing this report.

LEONARD V. McCOMMON

TABLE OF CONTENTS

LIST OF FIGURES

LIST OF TABLES

Notations

A	Aspect ratio
a	Three-dimensional lift curve slope
$\bar{a}_o$	Mean two-dimensional lift curve slope for wing
a.c.; A.C.	Aerodynamic center
α	Angle of attack
α_o	Angle of attack for zero lift
A_M	Model cross-section area
A_T	Test section cross-section area
b	Wing span
c	Chord
C_D	Drag coefficient
c.g.; C.G.	Center of Gravity
C_L	Three-dimensional lift coefficient
C_l	Rolling moment coefficient
C_{l_ψ}	Derivative of C_l with respect to ψ
C_M; C_m	Pitching moment coefficient
$C_{M_{C.G.}}$	Pitching moment coefficient about C.G.
$C_{M_{\bar{c}/4}}$	Pitching moment coefficient about .25 MAC
C_n	Yawing moment coefficient
C_{n_ψ}	Derivative of C_n with respect to ψ
c.p.	Center of pressure
C_R	Root chord of wing
C_Y	Side force coefficient
C_{Y_ψ}	Derivative of C_Y with respect to ψ

D	Drag
F	Degree Fahrenheit. Force
γ	Ratio of specific heat of air at constant pressure to that at constant volume
L	Lift
$L/D\|_{max}$	Maximum lift to drag ratio
M	Mach number. Moment
MAC; $\bar{c}$	Mean aerodynamic chord
M_{CR_D}	Critical Mach number
M_{DD}	Drag divergence Mach number
M_m	Mach number occurring on model
M_T	Free stream test section Mach number
P	Pressure
P_o	Total pressure
P_s	Static pressure
ψ	Yaw angle about the z axis
q	Dynamic pressure
R	Reynolds number
S	Planform area
T_o	Total temperature

Abstract

This study consisted of modeling and testing a high-speed, low-aspect ratio flying wing with the intention of determining its lift, drag, and static stability characteristics. The model was tested at Mach numbers of 0.70 to 0.86 in the Air Force Flight Dynamics Laboratory's Trisonic Gasdynamic Facility located at Wright-Patterson Air Force Base, Ohio. Six different configurations of stabilizing fins were tested in addition to the basic configuration of the wing without fins. The results of the tests indicated that the proposed aircraft can be made statically stable; the degree of stability being dependent on center of gravity location and angle of attack. Wind tunnel test results are presented in graphical and tabular form for use in future design studies of similar aerodynamic configurations.

AN AERODYNAMIC INVESTIGATION OF A LOW ASPECT RATIO WING

I. Introduction

This study addresses the problem of determining aerodynamic characteristics of a flight vehicle proposed by the Air Force Flight Dynamics Laboratory (AFFDL). The vehicle, designated as the Spade in this report, is a flying wing with no conventional center body or fuselage. Both the wing and proposed vertical fins are relatively thick; the wing has a maximum thickness of 12 percent based on the local chord. At high speeds this produces more drag and a lower critical Mach number than a thin wing (Ref 1:2.4). The proposed locations of the stabilizing fins are not the best for stability, especially lateral stability, as the vehicle has a small moment arm between its center of gravity and these vertical fins. The purpose of the design is to provide for low detectability at cruise speed and altitude. This criterion took precedence over designing for good aerodynamic characteristics.

AFFDL has available two different computer programs for predicting lift, drag, and stability coefficients. However, these programs were developed to predict characteristics of conventional aircraft. This aircraft would certainly not be classified as conventional. Thus, the question arises as to how confident one can be in the data obtained

from these analytical methods. Wind tunnel data obtained using a physical model of the Spade should show whether these programs are indeed providing useful information. Wind tunnel data is also very useful at this time since this aircraft is in its conceptual stages of development. Required changes in the Spade's configuration, if determined now, would provide a savings to the Air Force in both time and money.

No test model comparable to the Spade configuration has been tested to date. The main purpose of this study is to determine aerodynamic characteristics of the Spade by means of wind tunnel tests. The cruise flight regime is the area of most concern to AFFDL at this time. This required the wind tunnel tests to be conducted at high subsonic Mach numbers and low angles of attack. If the experimental data thus obtained correlate favorably with the analytically predicted data, the analytical methods can be used to determine what configuration changes in the prototype design may be needed. If the data correlation is not favorable then the experimental model will provide a base of information which can be used in determining the limitations of the prediction methods.

II. Facility and Model Description

Facility Used for Testing

The Spade was tested in the AFFDL Trisonic Gasdynamic Facility (TGF) located at Wright-Patterson Air Force Base. This facility was chosen for several reasons. The TGF is a closed circuit, variable density wind tunnel capable of continuous flow. It may be operated at subsonic, transonic, and supersonic speeds through a range of Mach numbers from 0.23 to 4.76. Test section statistics for subsonic testing are given in Table I. The variable density capability allows for a constant high unit Reynolds number, approximately 2.5 million per foot, as the Mach number is varied. Stagnation temperature is maintained at 100 F with an accuracy of ±1 F. A honeycomb and screen arrangement located in the stagnation section, forward of the test section, serves to minimize turbulence in the test section. This is especially important in that very small side forces and yawing moments are expected. High wind tunnel turbulence would tend to produce large scatter and errors in the recorded data, thus making the data difficult to interpret. The test section has two 28 inch diameter windows which allow an unobstructed view of the model during testing. These windows can be quickly opened to permit access to the model for configuration changes.

They also serve for easy flow visualization and photographing of the model.

Table I

Subsonic Test Section Characteristics

Mach Number Range	0.23-0.86
q PSF (Max.)	1,030
P_o PSF (Max.)	2,850
P_s PSF (Max.)	2,750
R/Ft (Max.)	2.5×10^6
T_o (F)	100
Cross Section (In.)	24x24
Density Alt. (Ft)	57,000

The main model support system for the TGF is a rack mounted fifty-inch radius crescent whose position and angle can be controlled by the operators to an accuracy of 0.01 degree. The center of rotation for the crescent support is the center of the test section viewing window. Its pitch range is negative one to positive nineteen degrees. The roll mechanism attached to the crescent provides for -90 to +180 degrees roll with an accuracy of $\pm$.005 degrees. The combined pitch and roll capability gives a combined pitch and yaw attitude while maintaining flow in the tunnel. This feature provides the capability of testing the model at a wide range of angles of attack and yaw while maintaining the desired Mach number.

The model support system of the TGF allows the use of strain gage force balances to obtain force and moment data. These balances have proven to yield extremely reliable and accurate force and moment information. The balance used in testing the Spade was a Task balance, identification number 6ST80-40-40. This is a six component internal type strain gage balance. It is capable of measuring normal, side, and axial forces of 80,40, and 40 pounds respectively. It allows for roll, pitch, and yaw moments of 60, 120, and 50 inch-pounds to be attained. The over-all measuring accuracy of this type of Task balance is within ±1 percent of the applied load when the load is from 10 percent to 100 percent of full load capacity. The accuracy is within ±0.1 percent of maximum load when the applied load does not exceed 10 percent of full load (Ref 2:16).

The strain gage balance produces electrical signals in milivolts which are fed to self-balancing potentiometers. By use of shaft-to-analog-to-digital converters, the signals are then translated to digital outputs which are printed and card punched. The data in card punched form is reduced to aerodynamic coefficients by a CDC 6600 computer (Ref 3).

The facilities provide very accurate, repeatable test data. By a series of calibration tests, the balance and associated instrumentation was proven to be capable of measuring forces and moments with an accuracy of ±2 percent

of the applied load. Model configuration changes are easily made with a minimum of down time required. With several model changes anticipated, this capability was very important. All these factors taken together provided the basis for the decision to test the Spade in the TGF.

Model Tested

The basic Spade geometry requirements were provided by the Air Force Flight Dynamics Laboratory. The wing geometry tested is shown in Fig 1. Pertinent wing dimensions are given in Table II. The airfoil section to be used in the full-scale aircraft has not been decided on. The section that best matches the currently proposed full-scale airfoil is the NACA 66_1-212 airfoil. This is a 12 percent thick section with the maximum thickness occurring at 0.45 chord. Its 6 percent camber occurs at 0.60 chord. The airfoil has a drag coefficient that is near its minimum value over a range of lift coefficients of 0.1 above and below the design lift coefficient of 0.2 (Ref 4:119-122). The proposed weight and cruise speed of the prototype were used by AFFDL to predict that this is the desired value of the cruise lift coefficient.

With general characteristics such as aspect ratio, planform shape, and tail shape and location provided by AFFDL, the actual dimensions and construction methods had to next be determined. The most pressing decision was that of the wing span dimension. The decision was

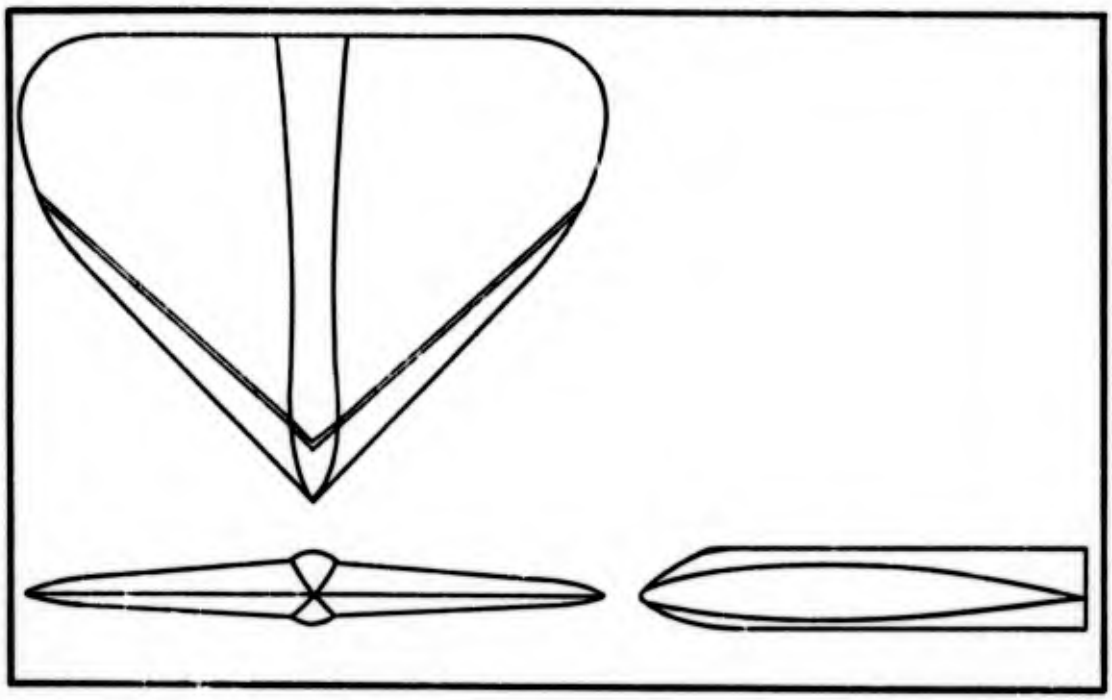

Figure 1. Schematic of Wing with Transition Strip at 12 percent chord.

Table II

Spade Model Wing Geometry

Airfoil Section (constant)	NACA 66_1-212
Planform Area ($in.^2$)	50.0
Frontal Area ($in.^2$)	6.09
Root Chord (in.)	7.63
Wing Span (in.)	10.0
Mean Aerodynamic Chord (in.)	5.39
Sweepback Angle of Leading Edge (deg)	45
Aspect Ratio	2.0
Distance from Nose to Calculated Aerodynamic Center (in.)	3.59
Outside Diameter of Cylinder Used to House Balance (in.)	1.15
Transition Strip Location (% Chord)	12

made to test the model in the subsonic section of the wind tunnel since the prototype will cruise at high subsonic Mach numbers. However, it was decided to make the model compatable with the smaller transonic section due to the possibility of testing the model at transonic speeds at a later date if desired.

The first consideration was to insure the model did not cause the tunnel to be choked at a low Mach number. For high subsonic speeds, the relation between test section and model cross-sectional areas is given by

$$\frac{A_T - A_m}{A_T} = \frac{M_T}{M_m}\left[\frac{1+\frac{\gamma-1}{2}M_T^2}{1+\frac{\gamma-1}{2}M_m^2}\right]^{-\frac{\gamma+1}{2(\gamma-1)}} \qquad (1)$$

where A_T is the test section cross-section area, A_m is the model cross-section area, M_T is the free stream Mach number in the test section, and M_m is the Mach number occurring on the model. γ is the ratio of specific heat of air at constant pressure to that at constant volume and is very nearly a constant 1.4 for Mach numbers below 3.0 (Ref 5:394). As A_m increases, M_T decreases for M_m equal to 1.0.

The prototype is expected to fly at a Mach number of approximately 0.9. Letting M_T equal 0.9 in Eq 1 yields a model cross-section area of 5.06 in.^{2} with the

subsonic test section area of 576 in.^{2} At zero angle of attack this equates to a wing span of approximately 8.8 in. If the span is allowed to be 10.0 in., M_T is lowered slightly to approximately 0.88. This larger size provides more room for a balance cavity with little reduction in free stream maximum Mach number. Also, since the transonic test section is 15 in. square, a 10 in. wing span will allow for possible tests in the transonic section at a later date. With the span b of 10.0 in. and an aspect ratio A of 2.0 as proposed by AFFDL, the planform area S is given by

$$S = \frac{b^2}{A} \qquad (2)$$

This yields a planform area of 50.0 in.^{2}

While the full-scale aircraft will have no fuselage, the model had to provide space for a force balance. The model with a span of 10.0 in. did not allow room for the balance to be completely enclosed within the wing. The decision was made to use a cylindrical body for a balance cavity since a cylindrical body would be the easiest to manufacture and the best geometry input for the prediction methods. The cavity was designed to accomodate a Task balance having a diameter of 0.75 in. The balance cavity is shown in Fig 2.

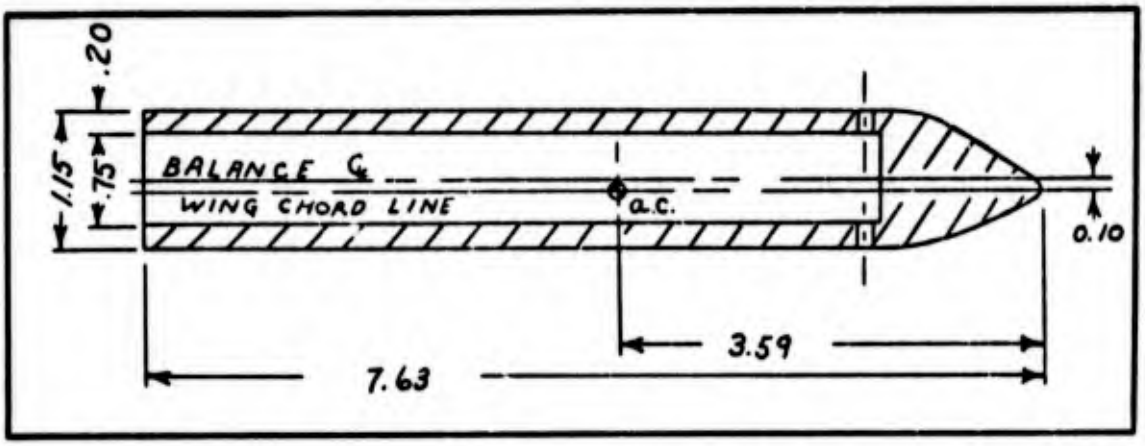

Figure 2. Spade Center Body Section Showing Cavity for Force Balance.

To obtain the maximum force the balance is capable of withstanding, the balance must be located with its load center very near the center of pressure of the Spade. While the c.p. varies with angle of attack, and thus lift coefficient, at lift coefficients on the order of 0.5 and above, the c.p. is found to be at approximately the same location as the aerodynamic center. As C_L is lowered, the c.p. moves toward the trailing edge and tends to infinity behind the wing as C_L approaches zero (Ref 6:78, 79). Since the highest loads occur at the highest C_L encountered, which is estimated in Appendix A to be approximately 0.6, and since at this C_L the center of pressure should approximately coincide with the aerodynamic center, it was decided to mount the balance in the cavity with its load center at the estimated aerodynamic center

location. The a.c. location, calculated in Appendix B, is 3.59 in. from the nose tip of the Spade.

The force balance outer surface is steel with a thermal expansion of approximately 6.3 $\times 10^{-6}$ in./in./F. Brass has a thermal expansion of 11×10^{-6} in./in./F (Ref 7:418). Temperatures normally are higher than ambient in the test section. With brass being used for the balance cavity this difference in thermal expansions would insure the model could be removed from the balance for model changes. Brass is also a high strength material that is easily machined. The decision was thus made to use brass for the balance cavity. A stress analysis for the brass cylinder, required to provide for maximum safety while testing in the TGF, is given in Appendix C.

A stress analysis was performed to determine the feasibility of using epoxy in the wing construction. It was felt that by first making a mold from a wood model and then casting the final wing using the epoxy, a very good tolerance on wing dimensions could be maintained. The maximum stresses that were anticipated are calculated in Appendix D. The maximum stress was expected to be less than 500 psi. The epoxy from which the model was manufactured was rated as having a stress capability of 4500 psi. This epoxy was supplied by the AFIT Training Aids Division. Using this material provided a large margin of safety.

Templates were made at several span locations using the NACA 66_1 -212 coordinates at each location. These

templates were then laminated in wood and the wood worked down to the templates. A mold was then made from the wood model and, with the brass cylinder in place inside the mold, the final wing was cast. As an added measure of safety, an eighth-inch thick brass plate attached to the cylinder was molded into the wing. Its location and size are shown in Fig 3. This procedure produced tolerances on the wing surface to within ±.005 in. of the proposed dimensions.

The tails were made in much the same manner, the exceptions being the horizontal tail, shown in Fig 7, and all outboard fins. These were machined from aluminum to provide more ease in manufacturing and, with aluminum being stronger than epoxy, a better load capability. The tails are mounted with machine screws either through the cylinder or the wing, depending on their location. These mounting holes are visible in Fig 4. All configurations that were tested are shown in Figs 4 through 11. The tails are shown mounted on the Spade in their positions for testing as proposed by AFFDL.

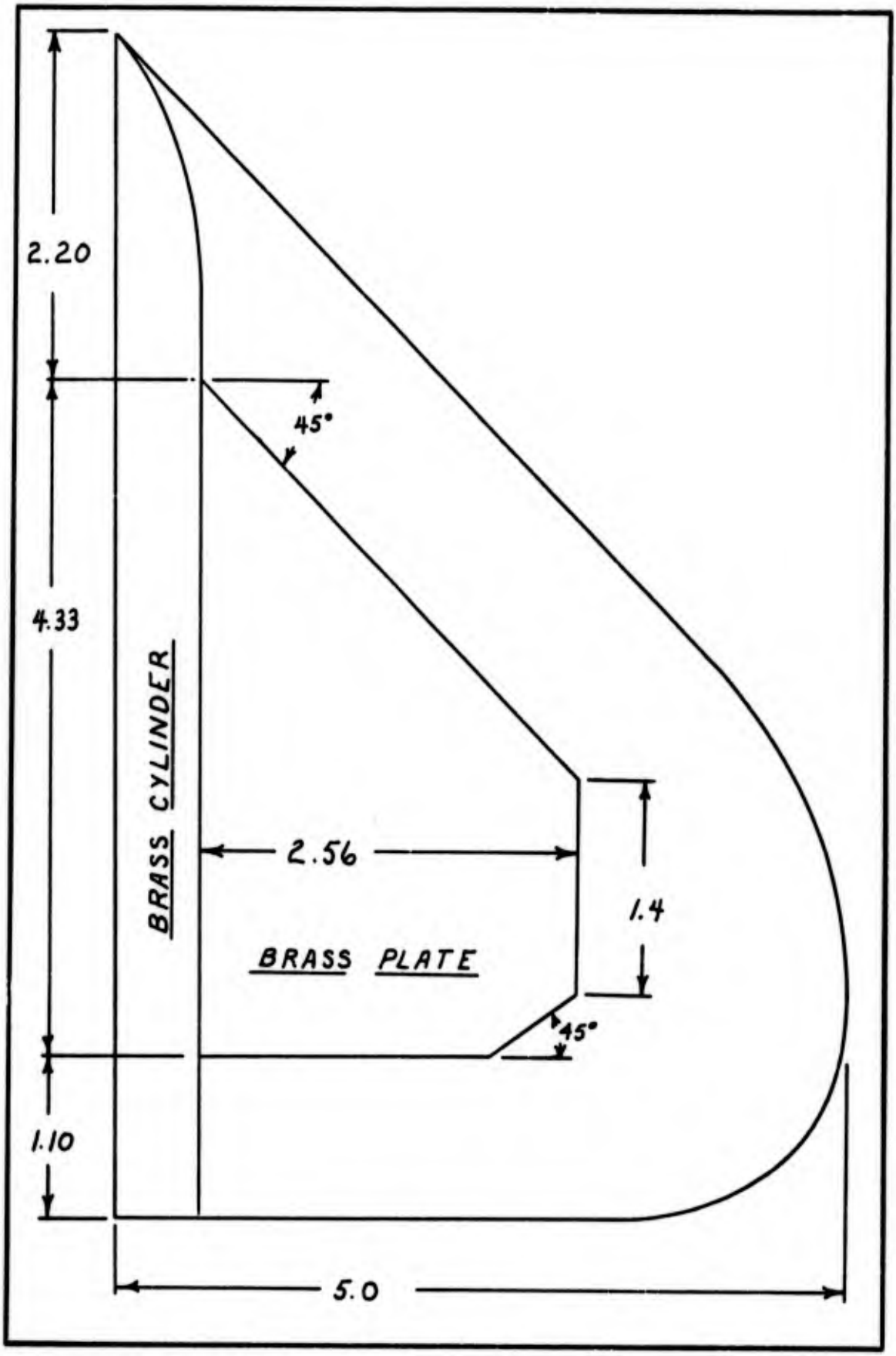

Figure 3. Spade Half-Planform showing Brass Plate Used for Added Strength in Wing.

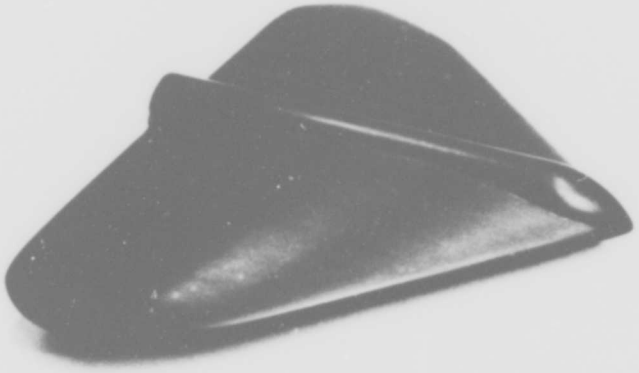

Figure 4. Config. 1.

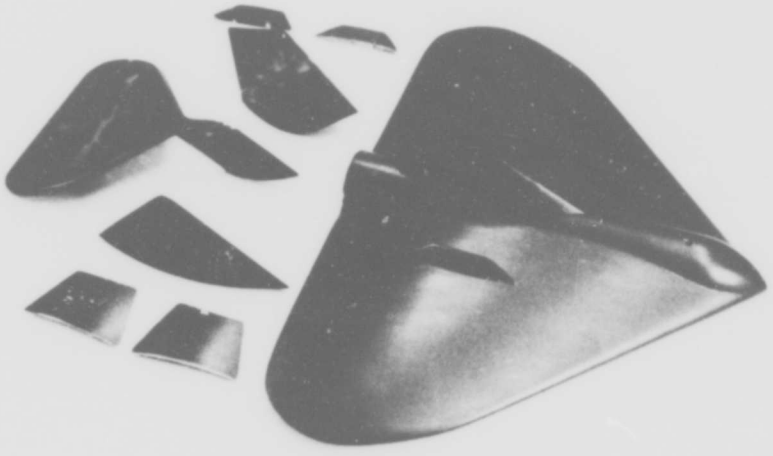

Figure 5. Wing With All Stabilizers Used for the Seven Configs. Tested.

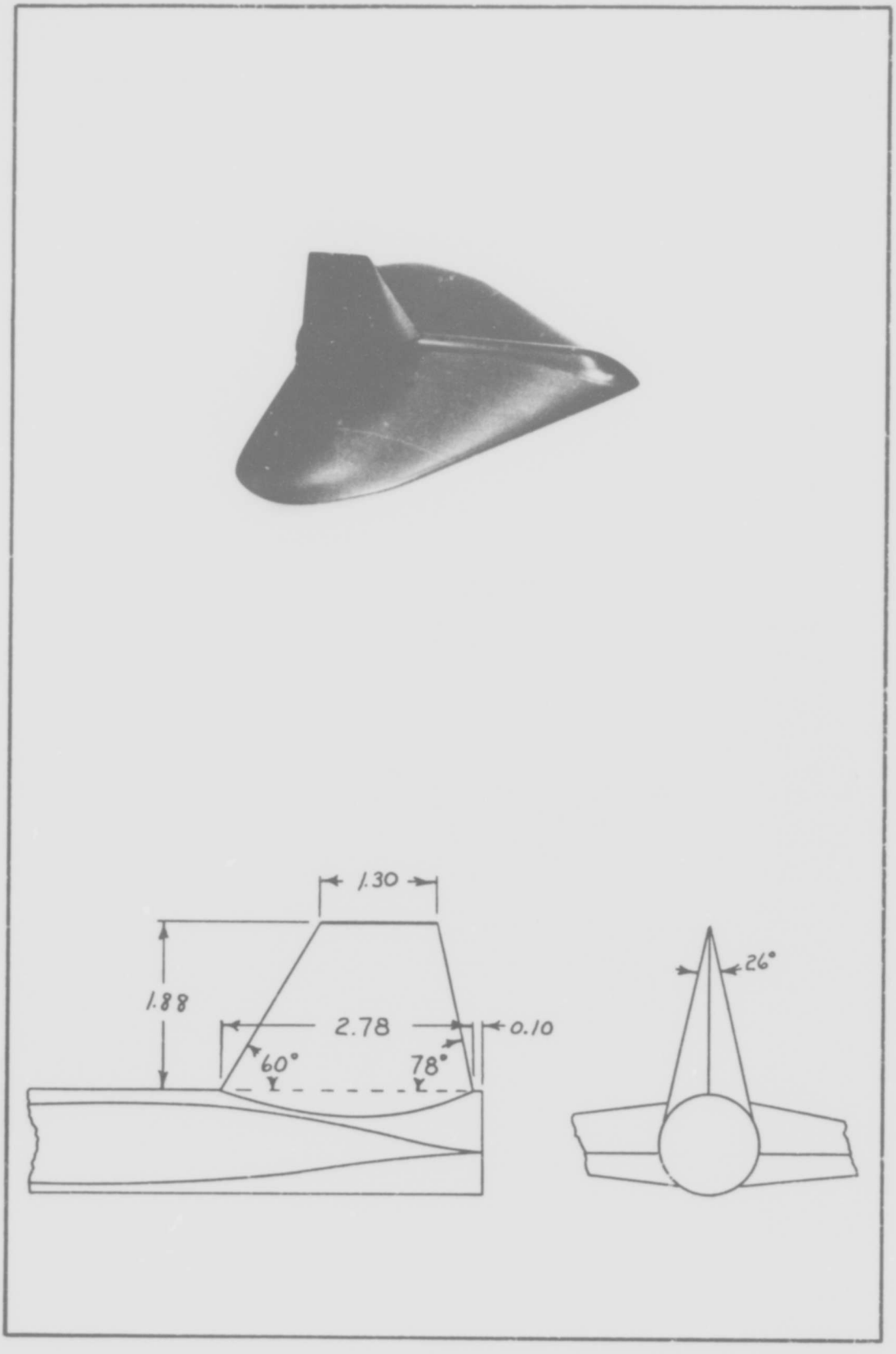

Figure 6. Config. 2.

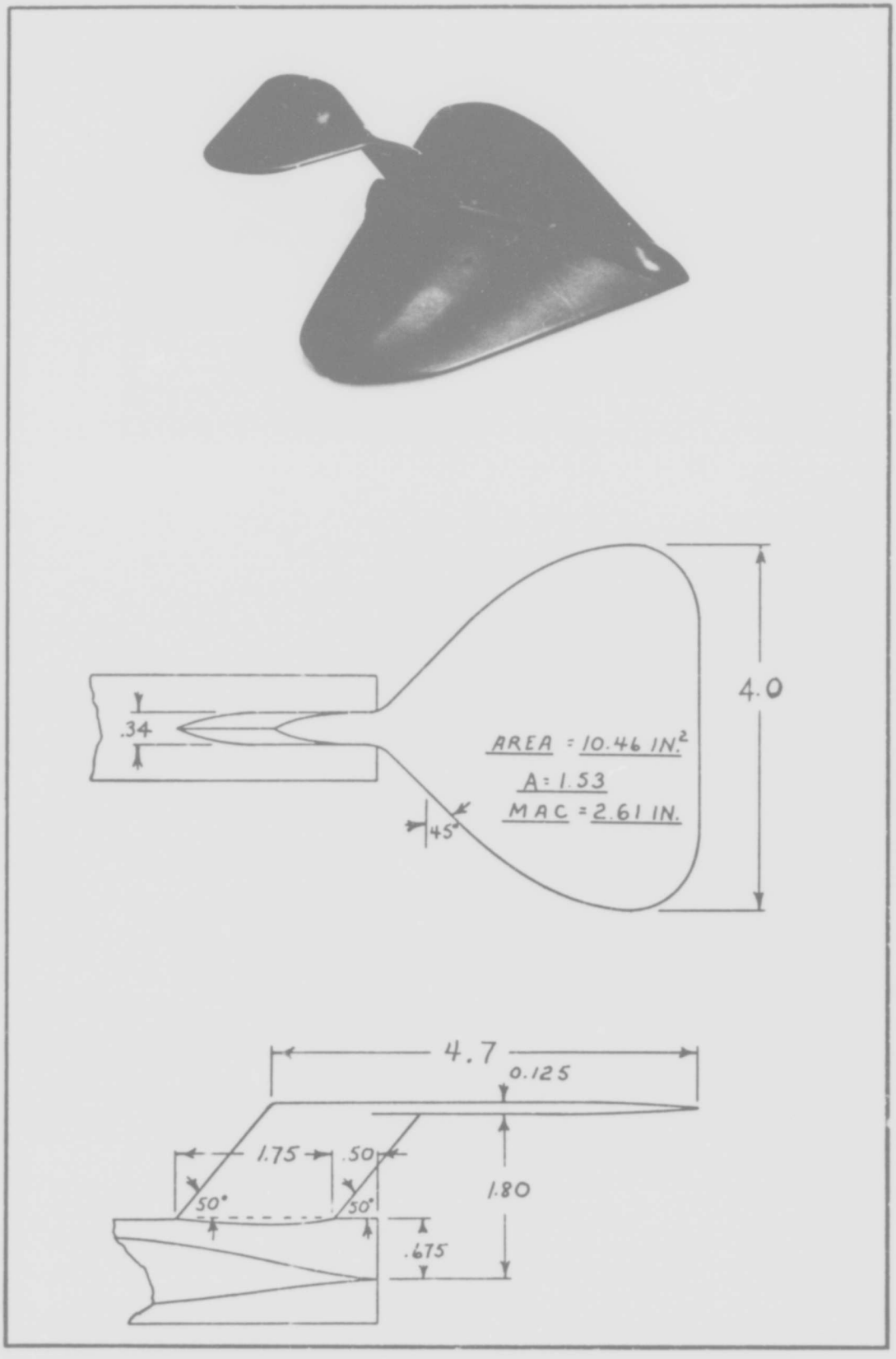

Figure 7. Config. 3.

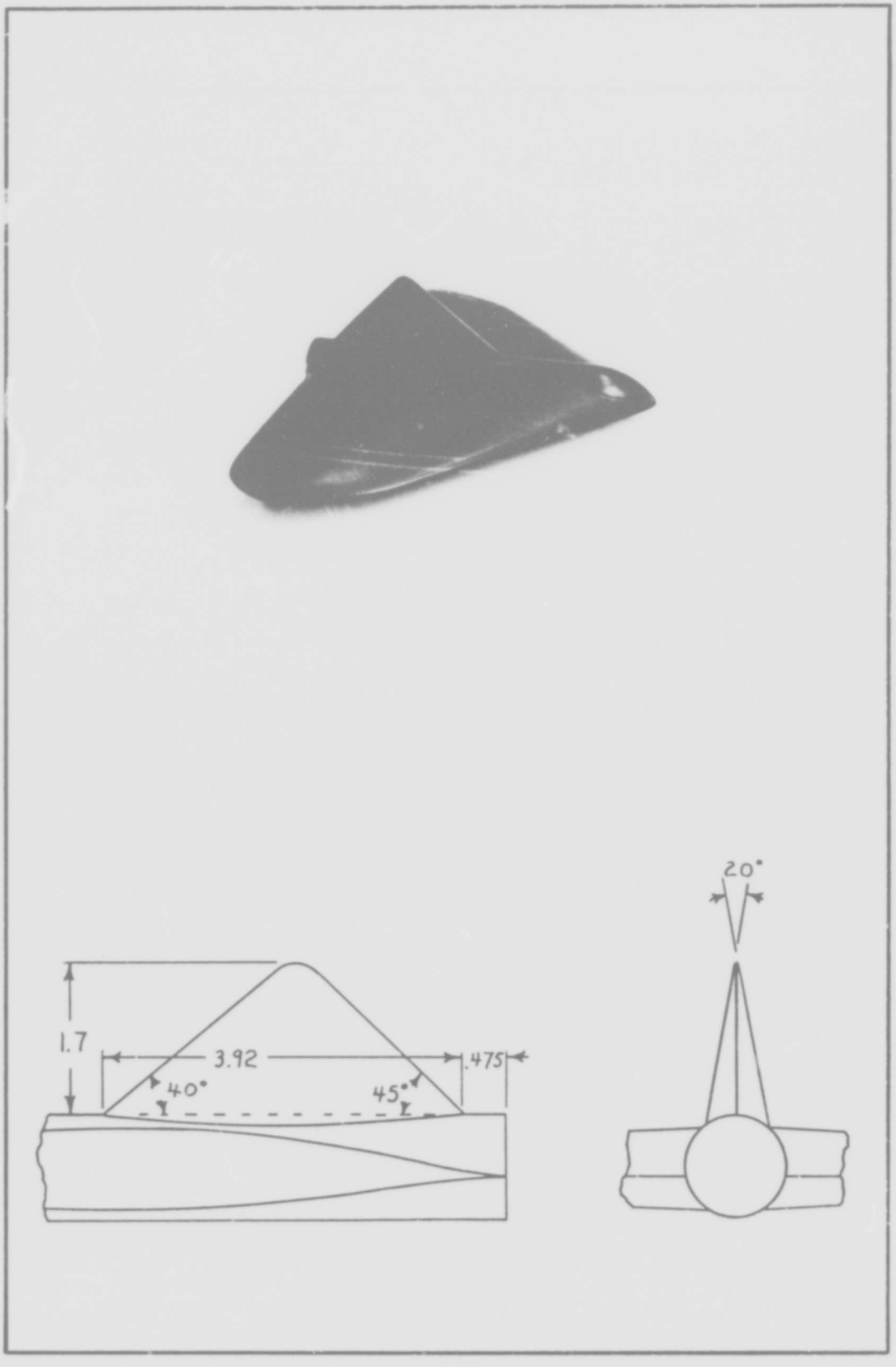

Figure 8. Config. 4.

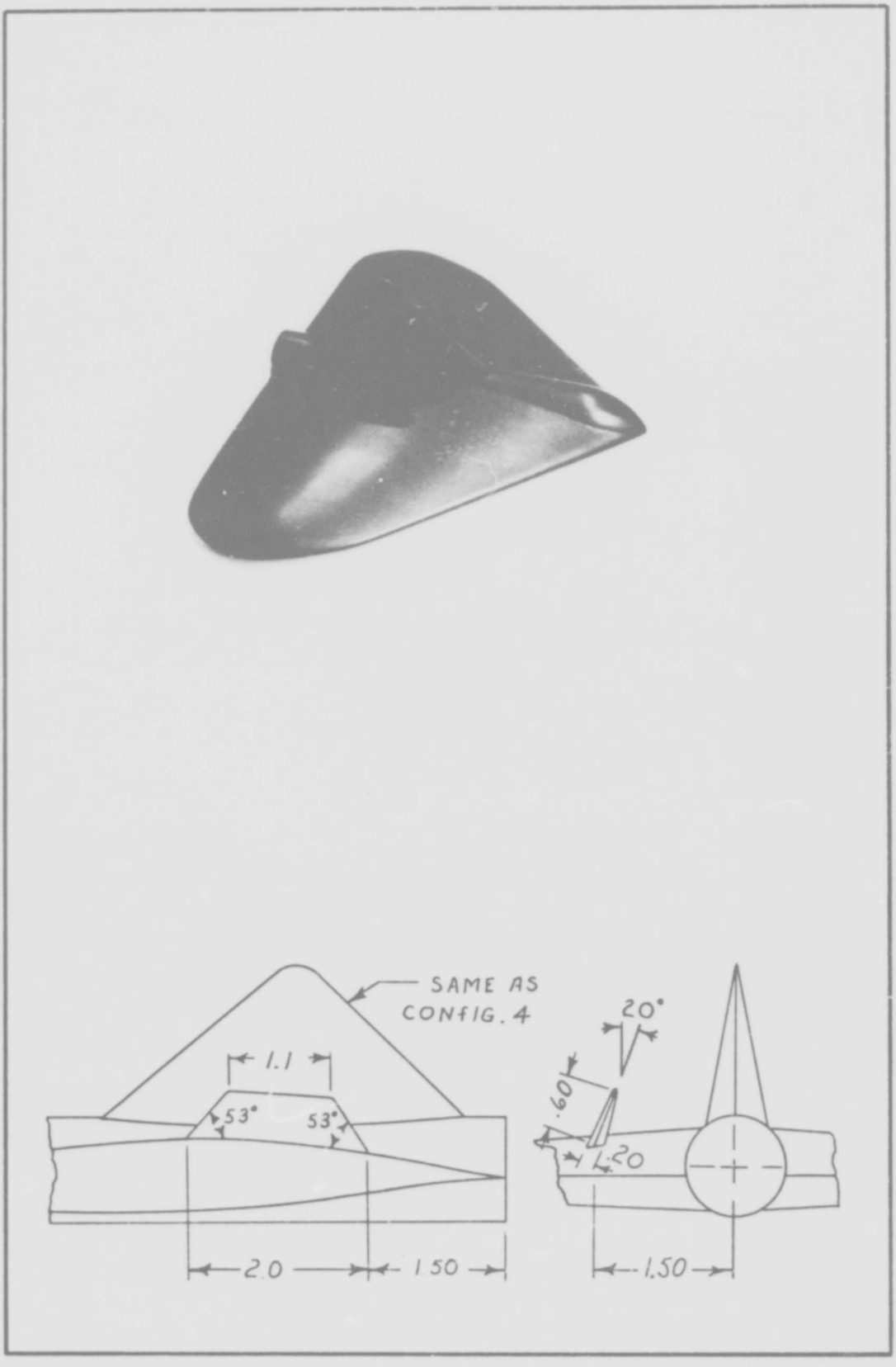

Figure 9. Config. 5.

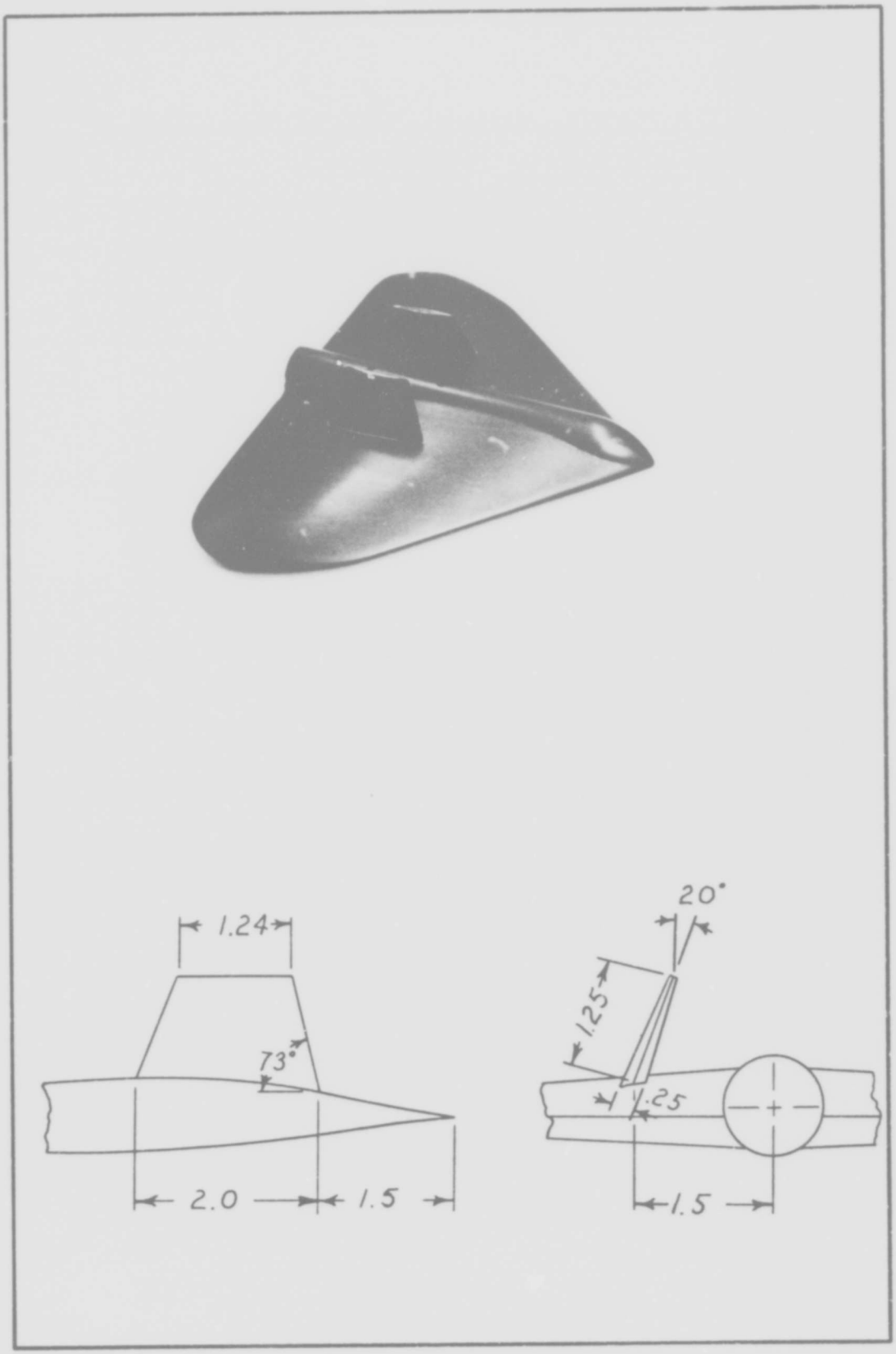

Figure 10. Config. 6.

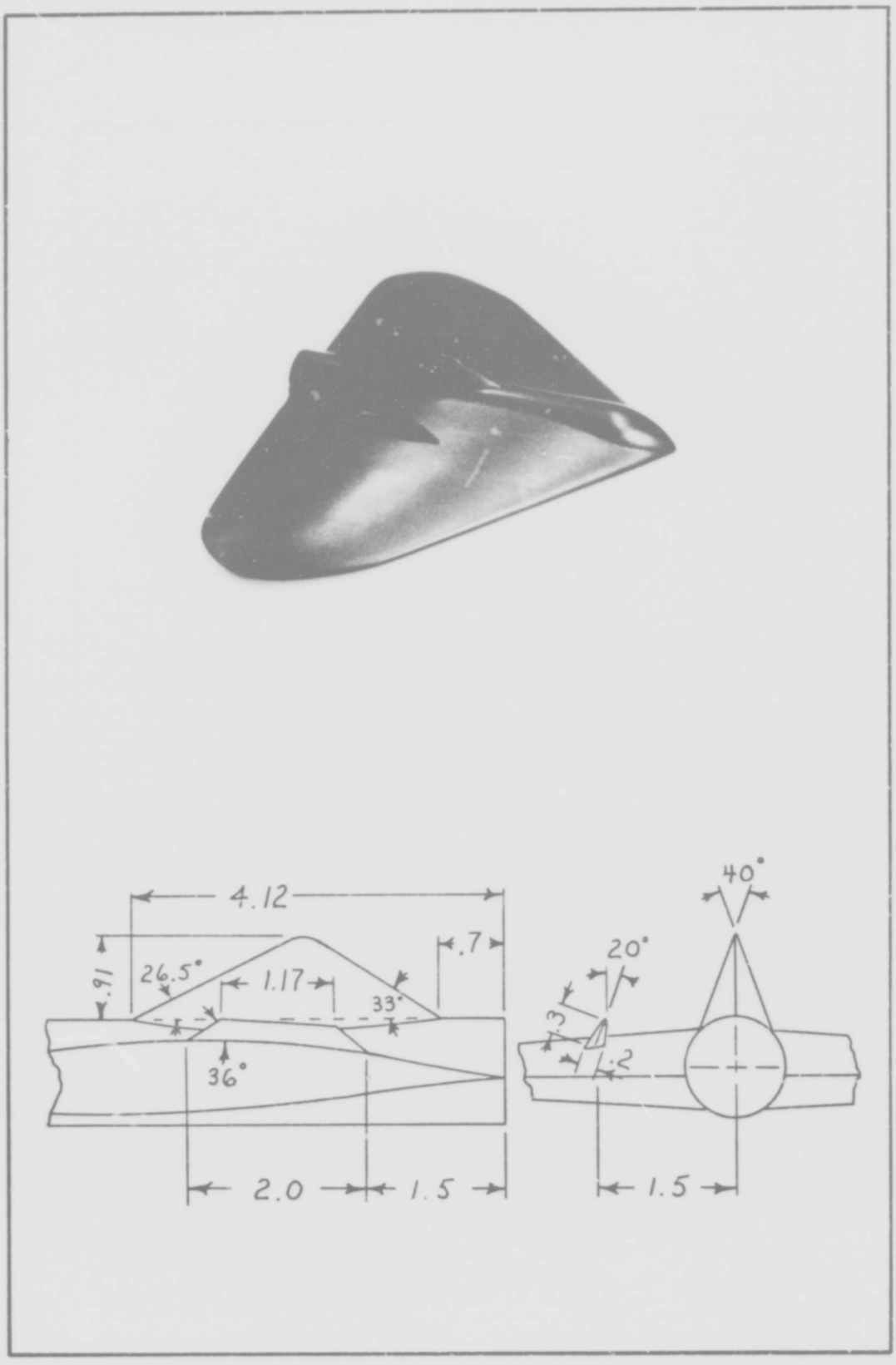

Figure 11. Config. 7.

III. Analytical Predictions

Two computer programs were used to predict aerodynamic characteristics of the Spade. Program TEA-236 predicted lift, induced drag, and pitching moment coefficients for configuration 1 only. The Datcom program predicted lift, drag, and pitching moment coefficients in addition to the lateral stability coefficients C_n, C_l, and C_y for all 7 configurations tested.

Theoretical Program

The computer program known as program TEA-236 was developed by the Boeing Aircraft Company for the purpose of designing and analyzing three-dimensional subsonic wings in the presence of a fuselage. It is based on potential flow theory using a source sheet and a vorticity sheet in the wing plane and sources on the fuselage surface as a flow model to simulate the physical wing-body combination. Small perturbation theory was used in developing the governing integral equations for this program. The flow about the wing was assumed to be ideal, irrotational flow. The Prandtl-Glaurert rule was used to correct for compressibility effects. The program provides lift, induced drag, and pitching moment coefficients in addition to wing section pressure distributions if desired (Ref 8:3).

Empirical Program

The second analytical model comes from a computer program based on empirical methods taken from the *USAF Stability and*

Control Datcom (Ref 9). This is a program used by AFFDL to predict aircraft stability coefficients in addition to lift, drag, and pitching moment coefficients. It allows the determination of the effects of variation in tail size and location on these aerodynamic characteristics. The Datcom program, like program TEA-236, provides other useful features not of interest in this study.

Only straight-tapered and nonstraight-tapered wings can be treated by the program. The Spade planform was therefore approximated as a clipped delta wing as shown in Fig 12. This delta wing has the same root chord length of 7.63 in. and wing area of 50.0 in.^{2} as was used in the wind tunnel model. The delta wing tip chord length is 2.32 in. The computer model thus has the same wing area, leading edge sweep, and aspect ratio as the physical model. The cylindrical center body and the vertical tail geometries of the program model match those of the wind tunnel model.

One of the major possible discrepancies between characteristics predicted by Datcom and those found by wind tunnel investigation is the fact that Datcom does not rigorously treat aerodynamics in the transonic speed range. An extrapolation from subsonic solutions was introduced by AFFDL for free stream Mach numbers in the transonic region of approximately 0.6 and above. Turbulent friction coefficients are employed in the computation of friction drag values (Ref 10).

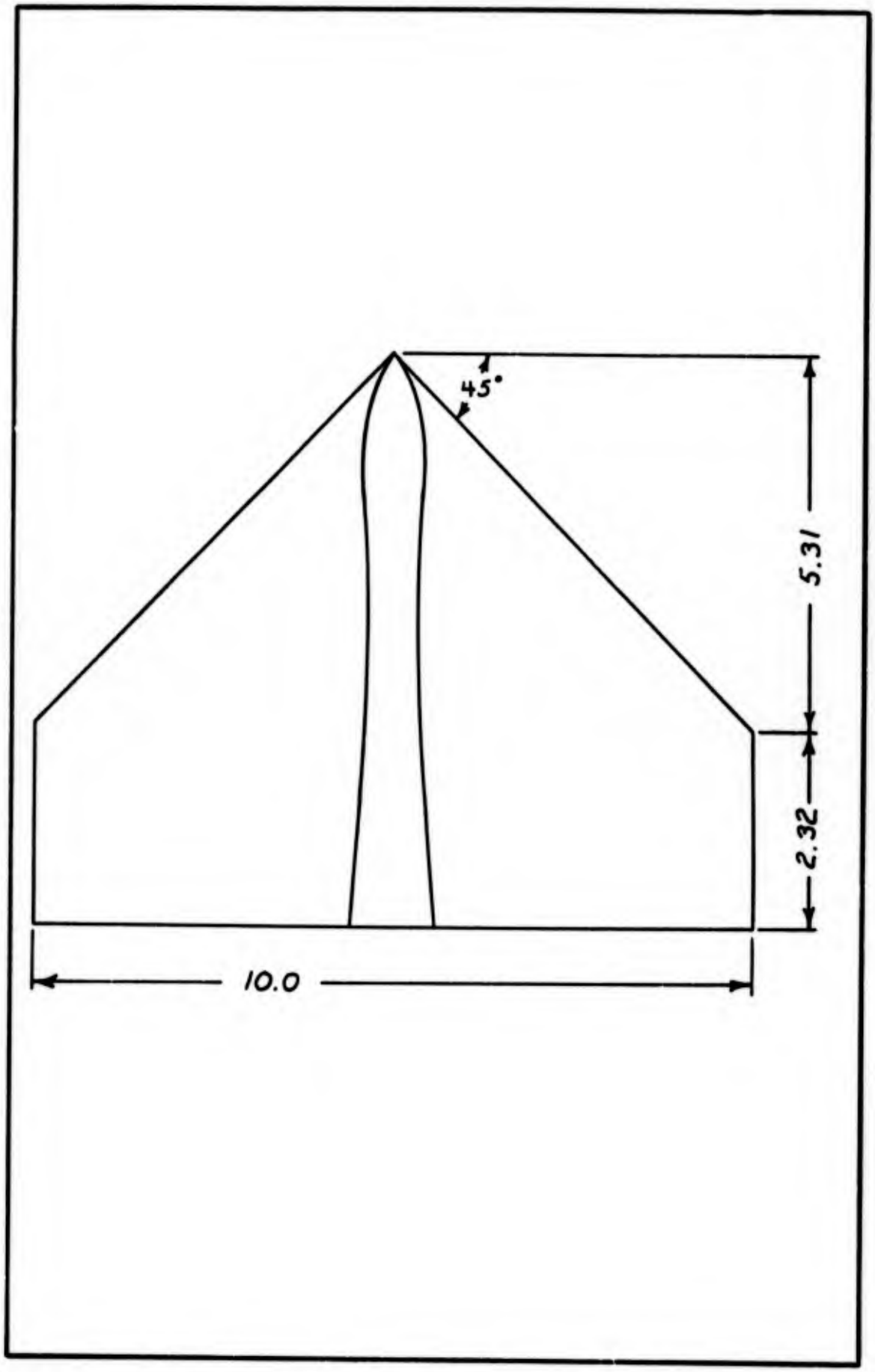

Figure 12. Delta Shape Used as Model for Datcom Prediction Program.

IV. Experimental Procedures

Scale Effects

Data taken from wind tunnel tests may provide very accurate information about the model but provide little useful information about the full-scale aircraft if the aerodynamic coefficients obtained cannot be extrapolated to full-scale flight conditions. Many factors are responsible for this, the most important being geometric and dynamic similarity between the test model and the prototype. Thus it is very desirable to match both Reynolds number and Mach number in the wind tunnel to that encountered in full-scale flight. This, of course, is not always feasible. Most wind tunnels can duplicate the Mach number range of the prototype, but the prohibitive cost of testing at full-scale Reynolds number requires extrapolation of Reynolds number to full-scale values (Ref 11:20). The primary effects of Reynolds number at near sonic and higher Mach numbers are on drag measurements, especially those resulting from skin friction drag. Reynolds number has little effect on lift and stability coefficients at low angles of attack (Ref 12:325). The lift curve slope variation with Reynolds number tends to be small, especially at low angles of attack. The main effect is an increase

of the maximum lift coefficient with increase in Reynolds number (Ref 5:355).

Scale effects on the pitching moment for airfoils which have maximum thickness well rearward, as in the case with the airfoil used here, are difficult to predict at high lift coefficients. However, for lift coefficients less than about 0.6 the effect of Reynolds number on pitching moment is small (Ref 5:359). It was expected that C_L values for the Spade tests would be under 0.6.

The full-scale longitudinal stability characteristics are generally not very different from those obtained in wind tunnel tests. However, experience has shown that the scale effects on directional stability have not been as predictable (Ref 5:360). Hopefully, the seriousness of this possible discrepancy will be lessened by the fact that one of the main objects of this study is to obtain information which can be used as a check on currently used prediction methods.

On a full-scale aircraft with high Reynolds number, the transition point of the boundary layer from laminar to turbulent is usually found on the forward portion of the aircraft surface. A small wind tunnel model, however, will likely have laminar flow over a large but unknown portion of its surface providing considerably lower drag coefficients from those of the full-scale

aircraft. One method often used to reduce this discrepancy is to force transition from laminar to turbulent flow on the model at points corresponding to expected transition points on the prototype (Ref 12:318-322).

This method of forcing transition was used in the investigation. AFFDL expects the transition on the prototype to occur at approximately 12 percent of the local chord on both the upper and lower surfaces. Transition was fixed on the model at 12 percent chord by lightly sprinkling number 80 silicone carbide grit, having a nominal size of 0.0083 in. on an eighth-inch strip of wet lacquer sprayed on the model. The transition strip location is shown in Fig 1. Transition was checked by spraying the model with a petroleum ether compound. Where the boundary layer was turbulent the compound evaporated at a much faster rate than where the boundary layer was laminar. The boundary layer was found to be laminar up to the transition strips and turbulent aft of the strips. Recall that turbulent friction coefficients were used when computing drag values in the Datcom program. Thus, in addition to more realistically simulating full-scale flow, tripping the boundary layer in this manner should provide for a better match between wind tunnel flow conditions and the flow conditions modeled in the Datcom program.

Force Measurements

Data reduction using the Task balance output voltage was performed on a CDC 6600 digital computer (Ref 3:10). Aerodynamic characteristics are presented in the form of coefficients in the wind axis system. Longitudinal moments were computed about the model reference point shown in Fig 2 as the aerodynamic center. The mean aerodynamic chord of 5.39 in., calculated in Appendix B, was used as a reference length. Directional stability coefficients were also computed about the a.c. but used the wing span of 10.0 in. as the reference length. The center of gravity was assumed for test purposes to coincide with the a.c. The effect of c.g. location on both longitudinal and lateral stability was determined for configuration three and four by changing the c.g. location in the data reduction program.

An important consideration in obtaining true scaled axial force measurements in most wind tunnel tests is the treatment of base drag. This drag arises from the pressure acting on the blunt base of the model and inside the balance cavity. The base pressure is influenced considerably by the sting extending from the model base. This influence normally causes the drag values to be smaller than they would be if the model could be tested without the sting and balance in place (Ref 5:413). Therefore, the measurements taken

in testing the Spade were corrected to remove this base pressure effect as follows:

$$F_{ac} = F_a - S_b(P - P_b) \qquad (3)$$

where F_{ac} is the axial force adjusted to zero base drag, F_a is the axial force measured, S_b is the model base area, P is the free stream static pressure, and P_b is the model base pressure (Ref 12:322). The base pressure was measured with a pressure probe located at the base of the model.

Test Procedures

The wind tunnel tests were divided into two main procedures. The first test was for drag rise. If the drag coefficient is plotted against Mach number at a constant angle of attack, the drag coefficient displays a sudden increase at a particular Mach number. This is known as the drag-divergence Mach number. For an aircraft to fly beyond this point, it requires more power with a corresponding increase in fuel consumption. Thus, with a subsonic aircraft one would not normally wish to cruise beyond the drag-divergence Mach number, and it becomes important in the design stage to know what this Mach number is (Ref 13:121).

The method of obtaining drag rise data was to vary the Mach number over a range of 0.50 to approximately 0.86 while maintaining a constant angle of attack. The total pressure was varied with Mach number to maintain a

unit Reynolds number of about two million. This procedure was followed for constant attack angles of -4, 0, 4, and 8 degrees. Other important information obtained from these tests include lift and pitching moment coefficients as functions of angle of attack. The test settings are given in Table III.

Procedures were next set up to obtain characteristics relating to lateral stability of the Spade. A Mach number of 0.70 was chosen for these stability tests to insure the data would be taken at a subcritical Mach number to avoid the effects shocks might have on the stability data. The total pressure was held at 1,156 psf with the total temperature at 100 F. Data was taken at yaw angles ψ of -2, -1, 0, 1, 2, 3, and 4 degrees at angles of attack of 0, 2, 4, 6, and 8 degrees. Configuration 4 was tested in this manner at additional Mach numbers of 0.50 and 0.80 to determine any effects Mach number might have on directional stability.

After force measurements on all configurations were completed, a brief flow visualization study was made. A white tinted oil was brushed on the model. Flight conditions typical of those tested were then investigated. The oil flow permitted visualization of the interactions of streamlines. Shock locations and regions of flow separation are normally detectable using this method of flow visualization.

Table III

Drag Rise Test Conditions

T_o = 100 F

Data taken at each Mach number for alpha = -4^o, 0^o, 4^o, 8^o

P_o varied to maintain R = 2×10^6 per ft

M	P_o (psf)
.50	1,462
.60	1,280
.70	1,156
.74	1,112
.76	1,108
.78	1,078
.80	1,071
.82	1,063
.84	1,043
.86	1,040

V. Results

The wind tunnel investigation of the Spade resulted in a series of aerodynamic coefficients for each configuration tested. The coefficients presented for configurations 1 through 7 included lift, drag, and pitching moment coefficients in addition to the lateral stability coefficients C_n, C_l, and C_y. The coefficients are presented in the wind axis as shown in Fig 13. The results for each configuration are presented in graphical form in Appendix E.

Lift

The lift coefficients for the Spade are shown in Figs 14 and 15 for configurations 1, 3, and 4. These values are typical of those obtained on all configurations. The slope of the lift curve is approximately .052 to .060 per degree, depending on angle of attack, for all configurations except configuration 3. The horizontal tail in configuration 3 increases the lift curve slope slightly to a range of about 0.055 to 0.065 per degree. The angle of zero lift for all configurations is approximately -0.65 degrees.

Drag

A typical set of drag coefficients is plotted in Fig 16 as a function of lift coefficient. The drag

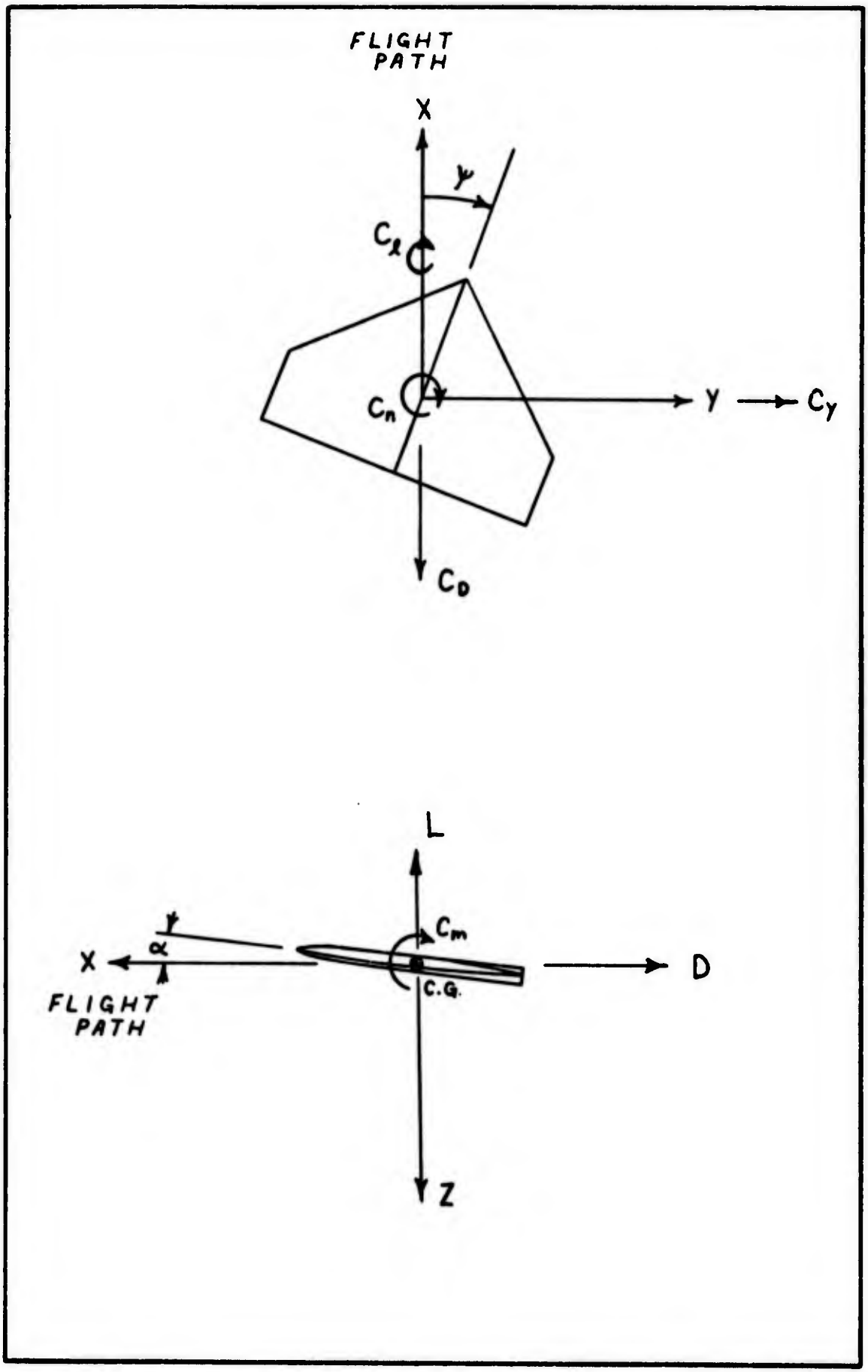

Figure 13. Coordinate and Sign Convention Used for Aerodynamic Coefficients

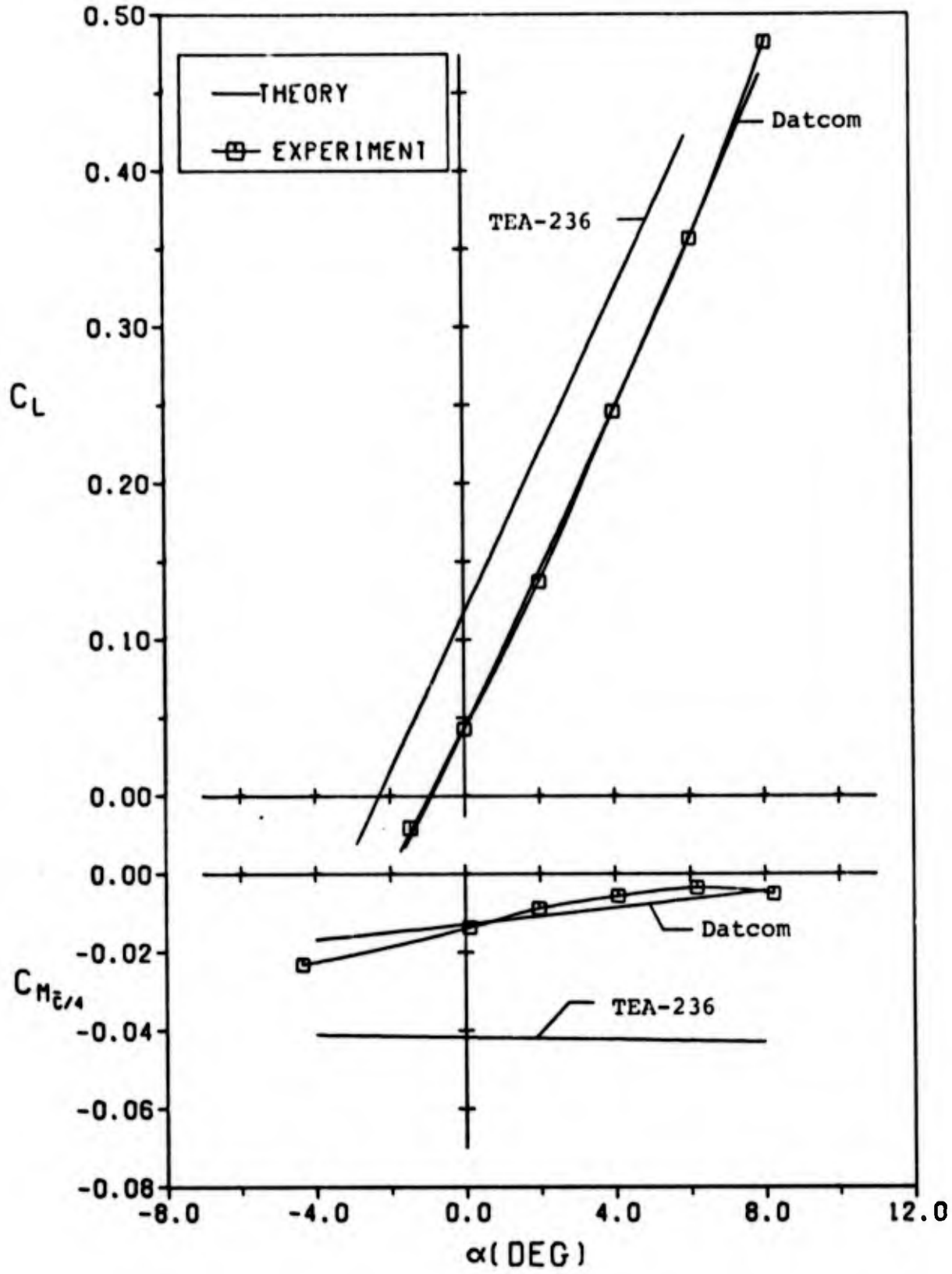

Figure 14. C_L and C_M vs Angle of Attack for Config. 1.

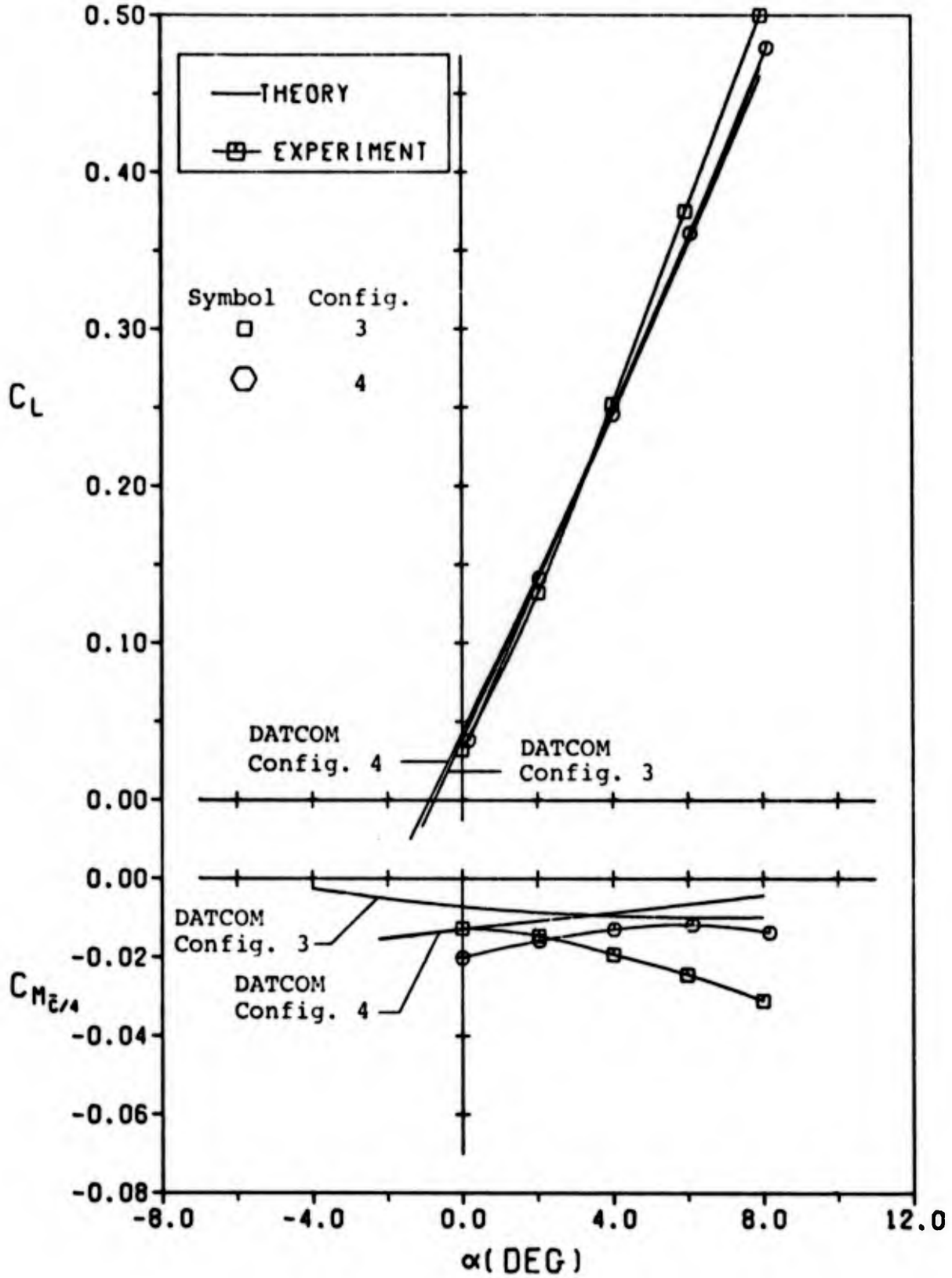

Figure 15. C_L and C_M vs Angle of Attack for Configs. 3 and 4.

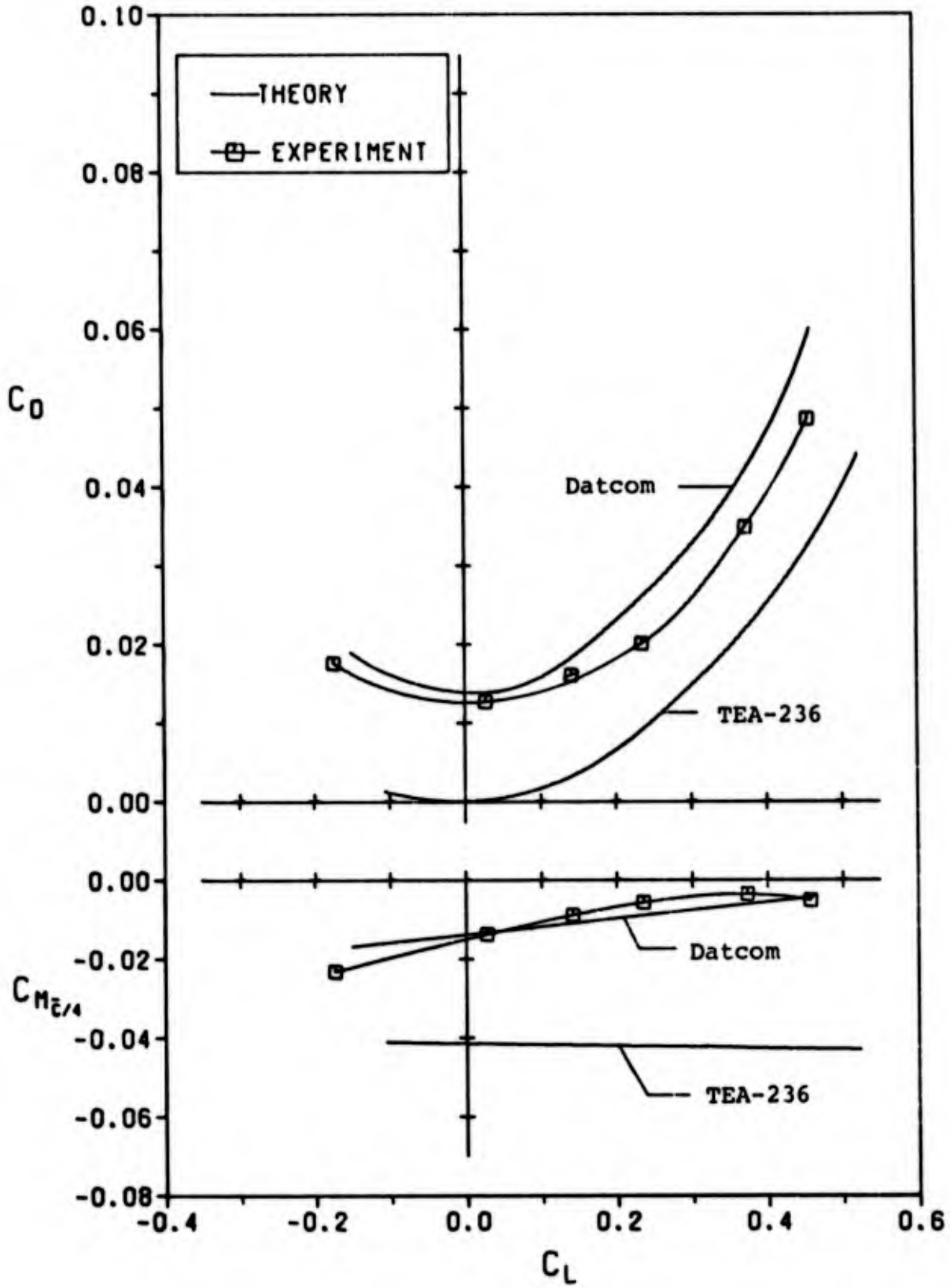

Figure 16. C_D and C_M vs C_L for Config. 1.

coefficient for configuration 1, which had no stabilizing fin, varies from 0.013 at zero angle of attack to 0.049 at an angle of attack of eight degrees. The drag values typical of the other configurations with stabilizers are 0.015 to 0.018 at zero degrees alpha and 0.051 to 0.054 at eight degrees alpha.

The maximum lift to drag ratio may be determined by drawing the tangent to the C_D vs. C_L curve from the origin (Ref 12:330). This yields an $L/D|_{max}$ for configuration 1 of 11.74 at a C_L of 0.27. This corresponds to an angle of attack of 4.6 degrees. For the other configurations it is observed that an $L/D|_{max}$ of 10.82 is achieved at C_L equal to 0.33 with alpha equal to 5.5 degrees.

Figure 17 shows the effects of Mach number on the drag coefficient. Two points on the curve that are sometimes used for references are the Mach critical drag M_{CR_D} and the drag divergence Mach number M_{DD}. The M_{CR_D} may be defined as the Mach number at which C_D increases by 0.002 above the low speed C_D. The M_{DD} is the Mach number at which dC_D/dM is equal to 0.10 (Ref 1:2-3). The M_{CR_D} for the Spade is approximately 0.76 at an alpha of 4 degrees and varies little with configuration changes. M_{CR_D} decreases with an increase in angle of attack and is lower than 0.50 at alpha equal to eight degrees.

The M_{DD} also decreases with increase in alpha. It is above 0.80 for alpha equal to four degrees and less. It

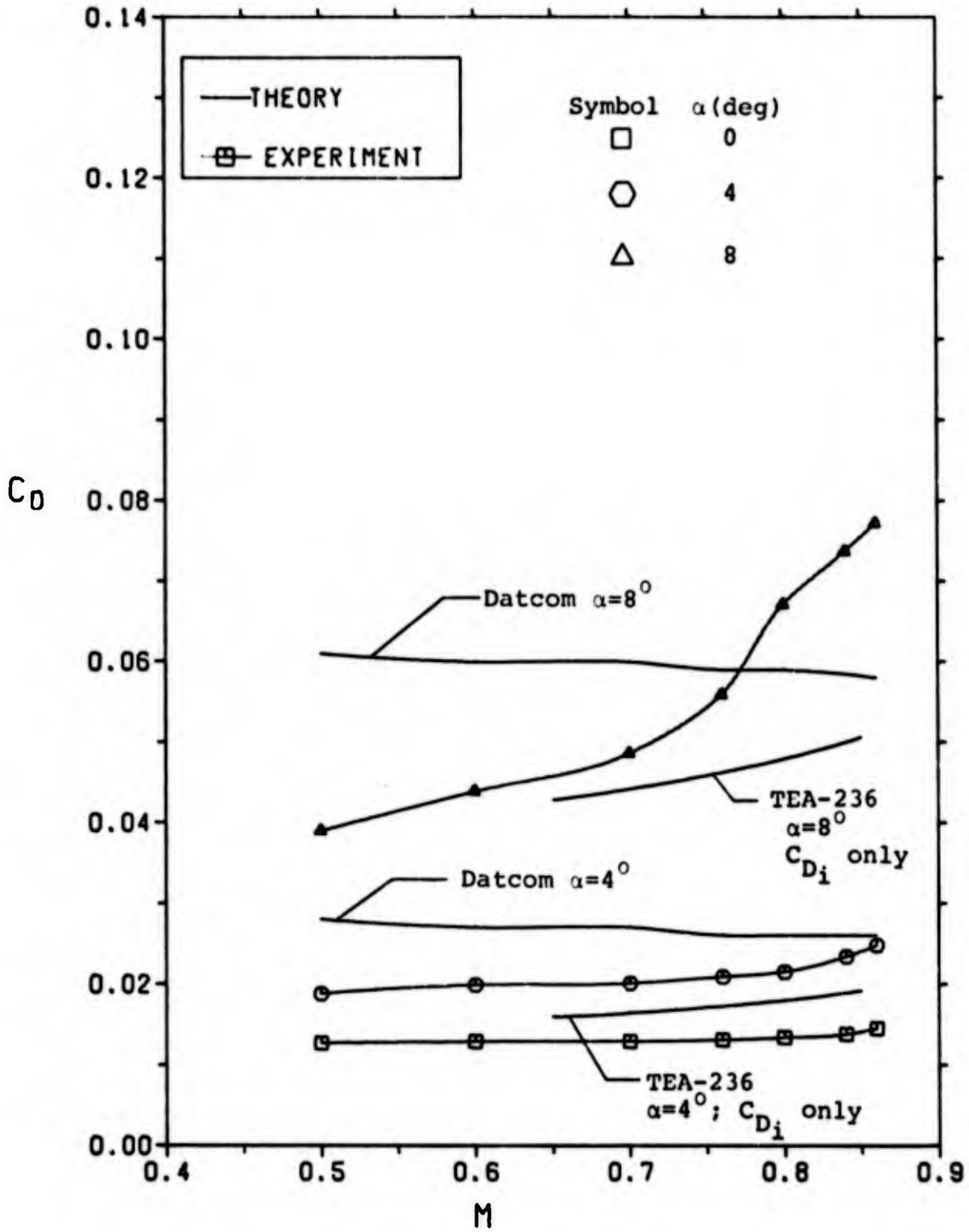

Figure 17. C_D vs M for Config. 1.

is approximately 0.74 at alpha equal to eight degrees. These values are consistent for all configurations.

Pitching Moment

The pitching moment about the aerodynamic center is shown in Figs 14 and 15. The slope of this curve varies little between configurations except for configuration 3. At alpha of four degrees the slope of the pitching moment curve is approximately -.002 per degree for configuration 3 and +.001 per degree for other configurations.

Figure 18 shows the effect of center of gravity location on C_M taken about the c.g. The change in slope is typical of all configurations. It is seen that the slope decreases at alpha of four degrees by .0031 per degree for each .05 MAC movement forward. The slope and changes are, of course, dependent on the angle of attack.

Yawing Moment

The yawing moment is the moment about the z axis as shown in Fig 13. The yawing moment coefficient derivative C_{n_ψ} is given for all configurations in Table IV for $\alpha=2^\circ$ and 4° and $\psi=0^\circ$. It should be noted that this derivative varies considerably with angle of attack and yaw angle for each configuration. This can be seen in Fig 19 in which C_n vs. ψ is shown for each configuration tested. Note that for static stability C_{n_ψ} should be negative, the more negative values denoting a more stable condition (Ref 11:318).

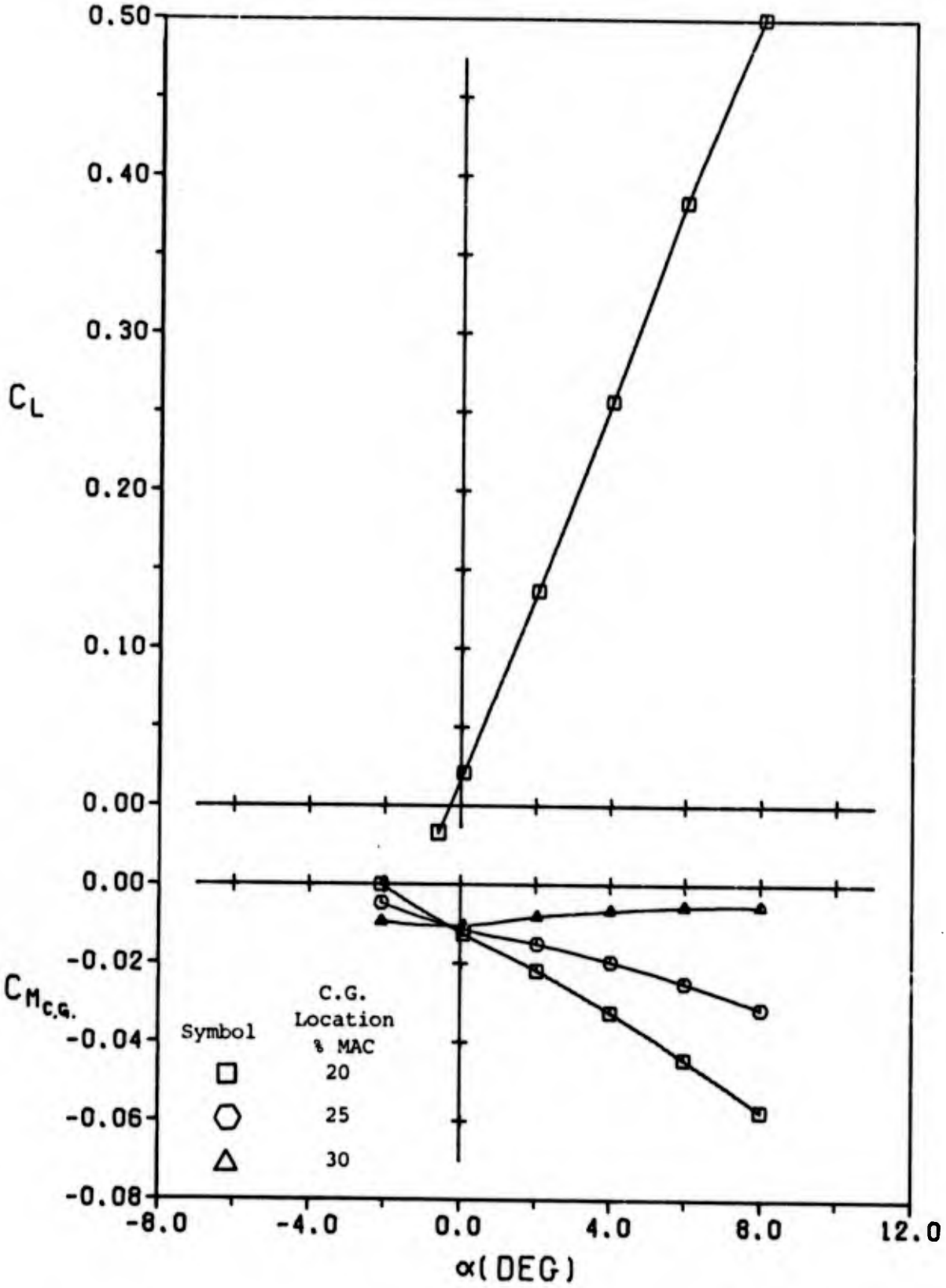

Figure 18. Effect of C.G. Location on C_m vs α for Config. 3.

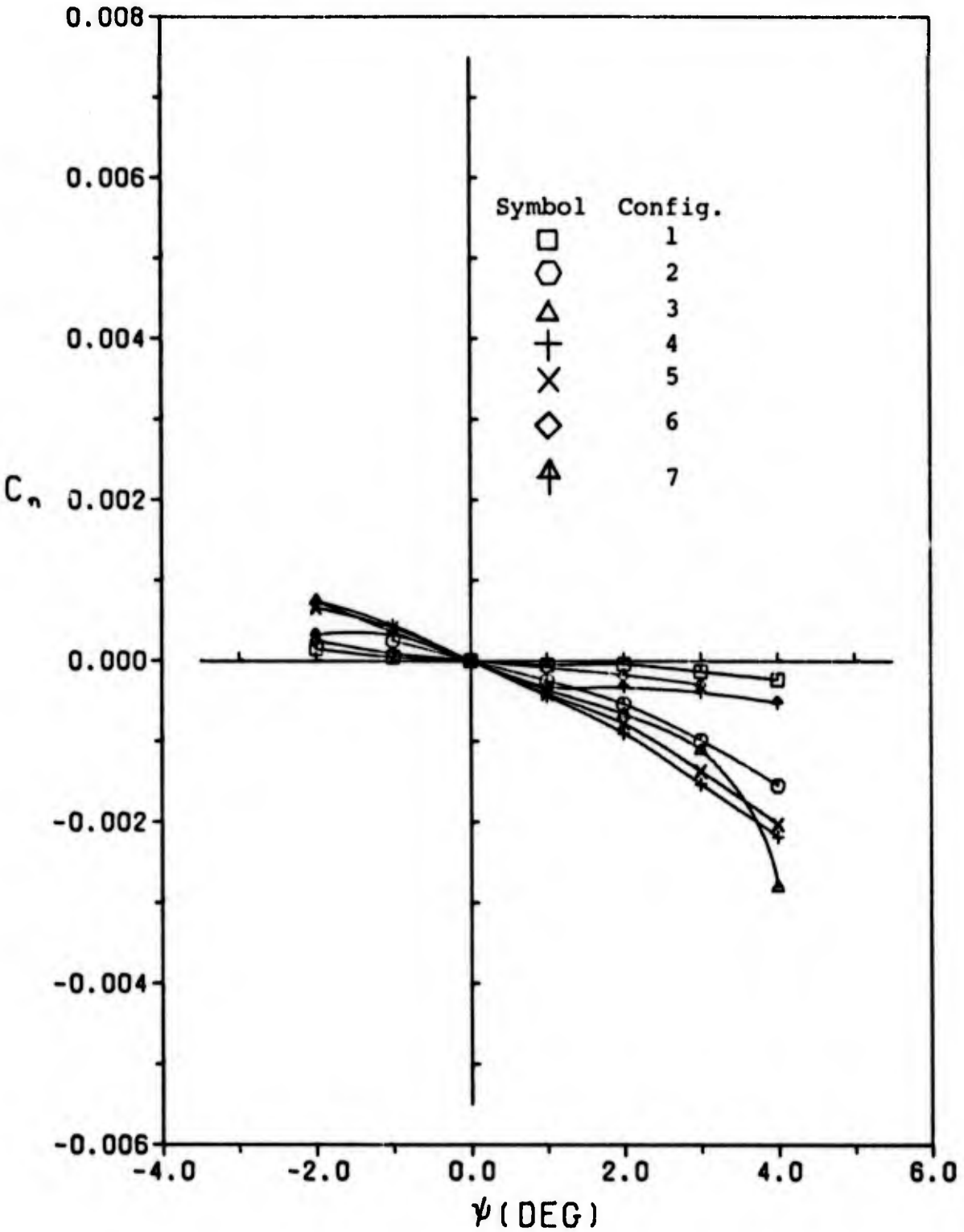

Figure 19. Yaw Moment Coefficient C_n vs Yaw Angle for All Configs. α=4 deg

The effects of c.g. location on C_n can be seen in Figs 20 and 21. The change in C_n at $\alpha=2^o$, $\psi=0^o$ is given in Table V. As the c.g. is moved 5 percent of the MAC forward, C_{n_ψ} becomes approximately .00008 per degree more negative for configuration 3 and .00015 per degree more negative for configuration 4. Again, the amount of change in C_{n_ψ} depends on α, ψ, and configuration.

Rolling Moment

The rolling moment is the moment about the x axis and is caused primarily by a difference in the lift between the right and left sides of the wing as the aircraft is yawed. The rolling moment coefficient C_l is plotted against yaw angle ψ in Fig 22 for all configurations. The values of C_{l_ψ} are given in Table IV for $\alpha=2$ and 4 degrees with $\psi=0$. Effects of c.g. location on C_l are shown in Figs 23 and 24. Typical changes in C_{l_ψ} with c.g. locations are given in Table V. It is seen that C_{l_ψ} becomes approximately .00006 per degree more positive for configuration 3 and .00005 per degree more positive for configuration 4 as the c.g. is moved .05 MAC forward. Note that the more positive C_{l_ψ} reflects a more stable condition (Ref 11:342).

Side Force

The side force coefficient C_Y as defined in Fig 13 is shown for all configurations in Fig 25 at $\alpha=4$ degrees. The derivative C_{Y_ψ} is given in Table IV. For static stability C_{Y_ψ} should be positive, the more positive values denoting a more stable aircraft.

Table IV

Comparison of Lateral Stability Derivatives (per deg)

$\alpha=2^{\circ}$ $\psi=0^{\circ}$ C.G. at A.C.	Experimental			Predicted by Datcom		
Config.	C_{n_ψ}	C_{l_ψ}	C_{Y_ψ}	C_{n_ψ}	C_{l_ψ}	C_{Y_ψ}
1	.00014	.00057	.00030	.00021	.00074	.00017
2	.00006	.00048	.00275	-.00047	.00108	.00353
3	-.00013	.00050	.00275	-.00009	.00084	.00146
4	-.00019	.00015	.00505	-.00011	.00095	.00290
5	-.00034	.00008	.00625	-.00019	.00038	.00364
6	.00003	.00034	.00260	-.00008	.00093	.00265
7	-.00020	.00007	.00375	.00009	.00082	.00174
$\alpha=4^{\circ}$ $\psi=0^{\circ}$	Experimental			Predicted by Datcom		
1	-.00006	.00103	.00025	.00021	.00119	.00017
2	-.00025	.00093	.00255	-.00047	.00153	.00353
3	-.00036	.00099	.00270	-.00009	.00130	.00146
4	-.00044	.00052	.00525	-.00011	.00141	.00290
5	-.00041	.00066	.00510	-.00019	.00144	.00364
6	-.00009	.00081	.00180	-.00008	.00136	.00265
7	-.00032	.00049	.00350	.00009	.00127	.00174

Table V

Effect of C.G. Location on Lateral Derivatives C_{n_ψ} and C_{l_ψ}

$\alpha=2^\circ$, $\psi=0^\circ$, M=0.7				
Config.	Coef. per deg	C.G. at .20 MAC	C.G. at .25 MAC	C.G. at .30 MAC
3	C_{n_ψ}	-.00021	-.00013	-.00004
3	C_{l_ψ}	.00056	.00050	.00043
4	C_{n_ψ}	-.00034	-.00019	-.00005
4	C_{l_ψ}	.00020	.00015	.00009

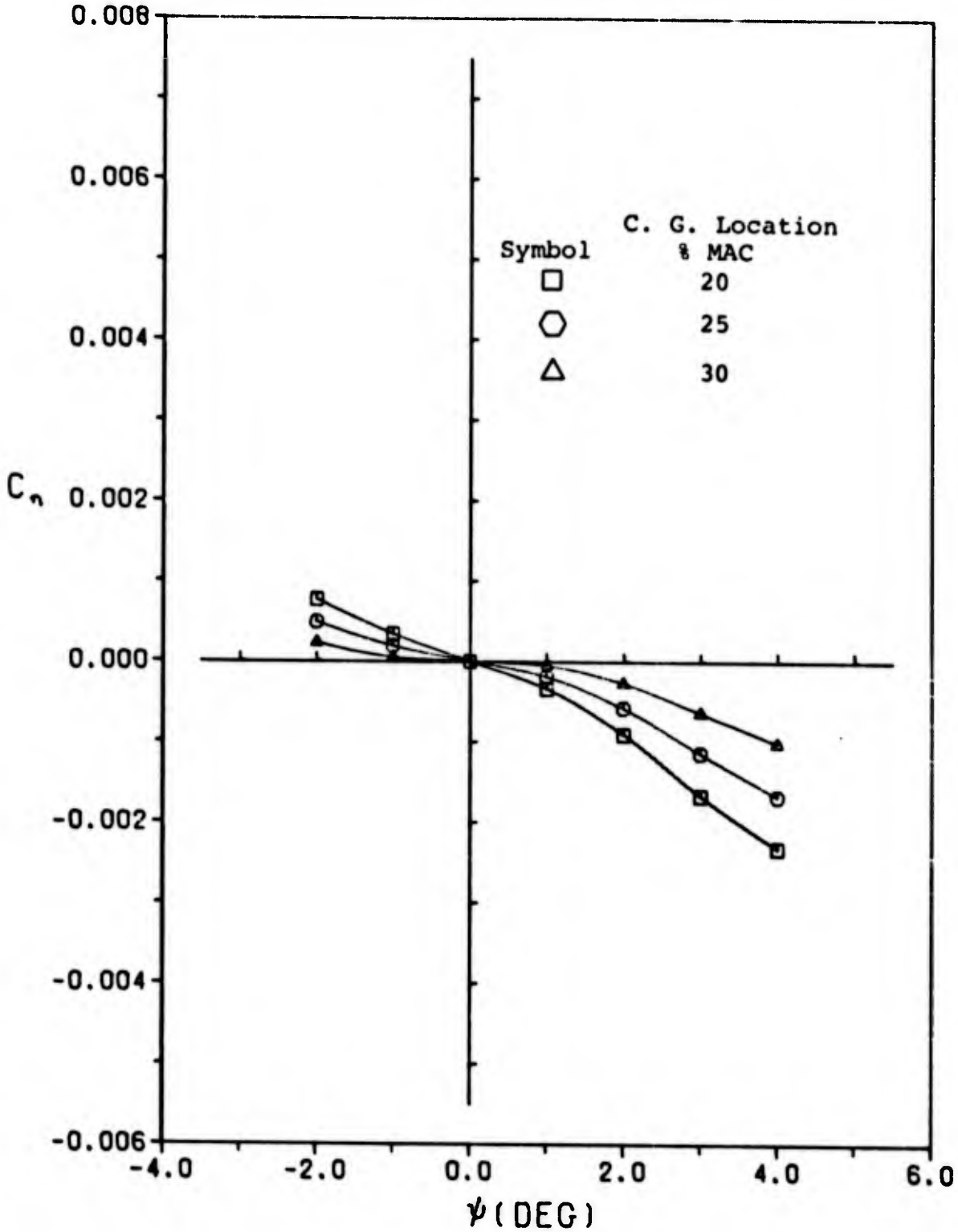

Figure 20. Effect of C.G. Location on C_n vs ψ for Config. 4. α=2 deg

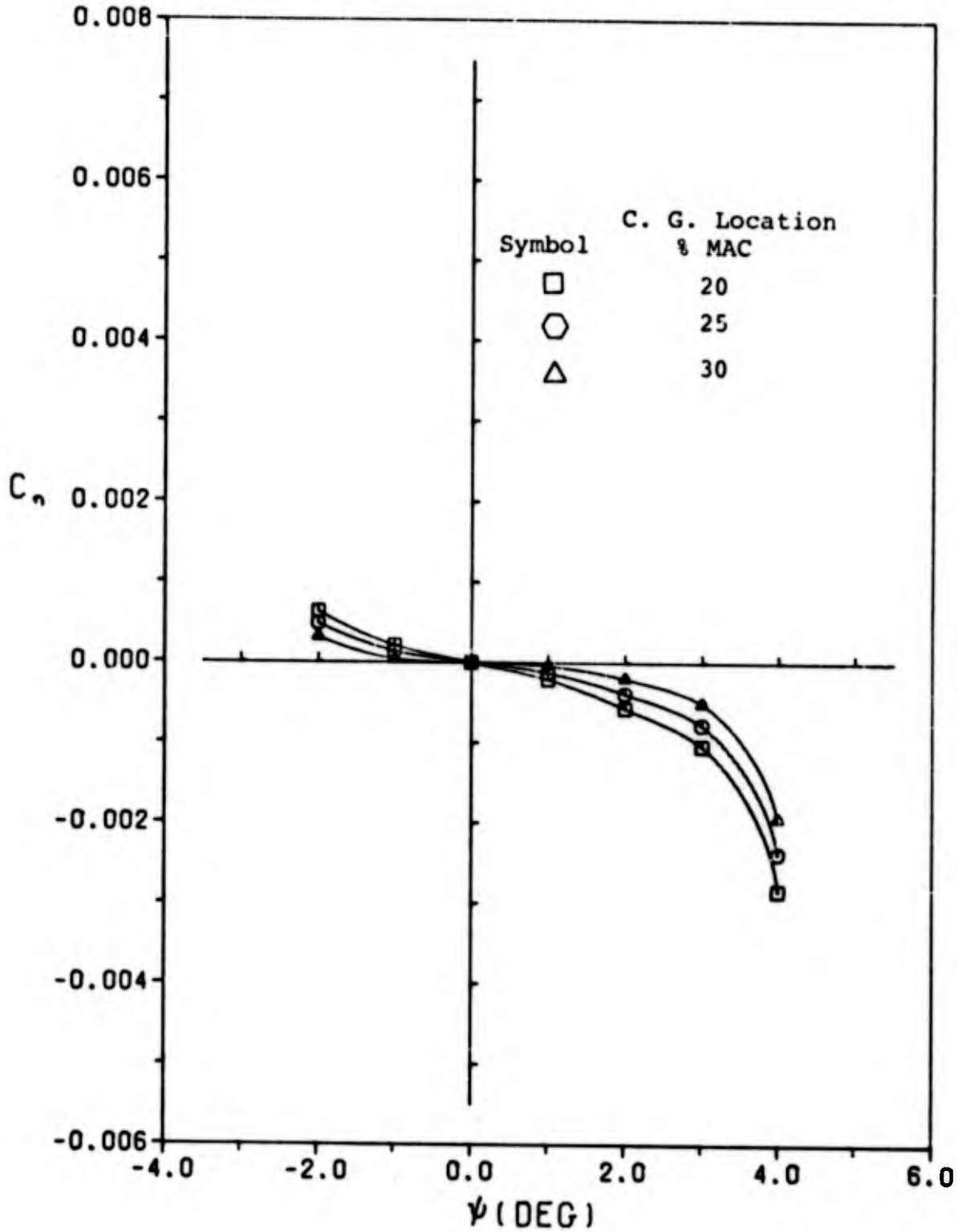

Figure 21. Effect of C.G. Location on C_n vs ψ for Config. 3. α=2 deg

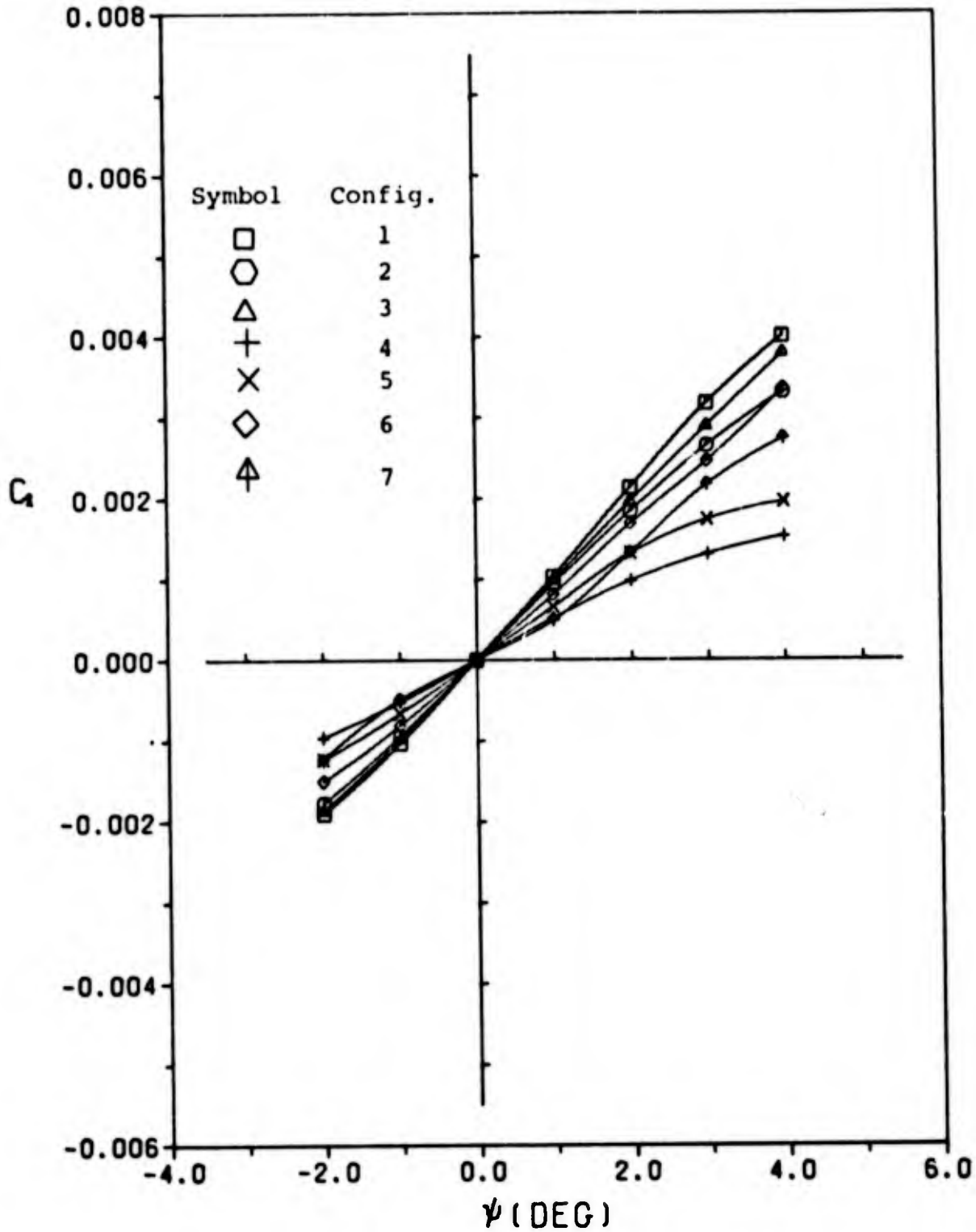

Figure 22. Roll Moment Coefficient C_l vs Yaw Angle for All Configs. α=4 deg

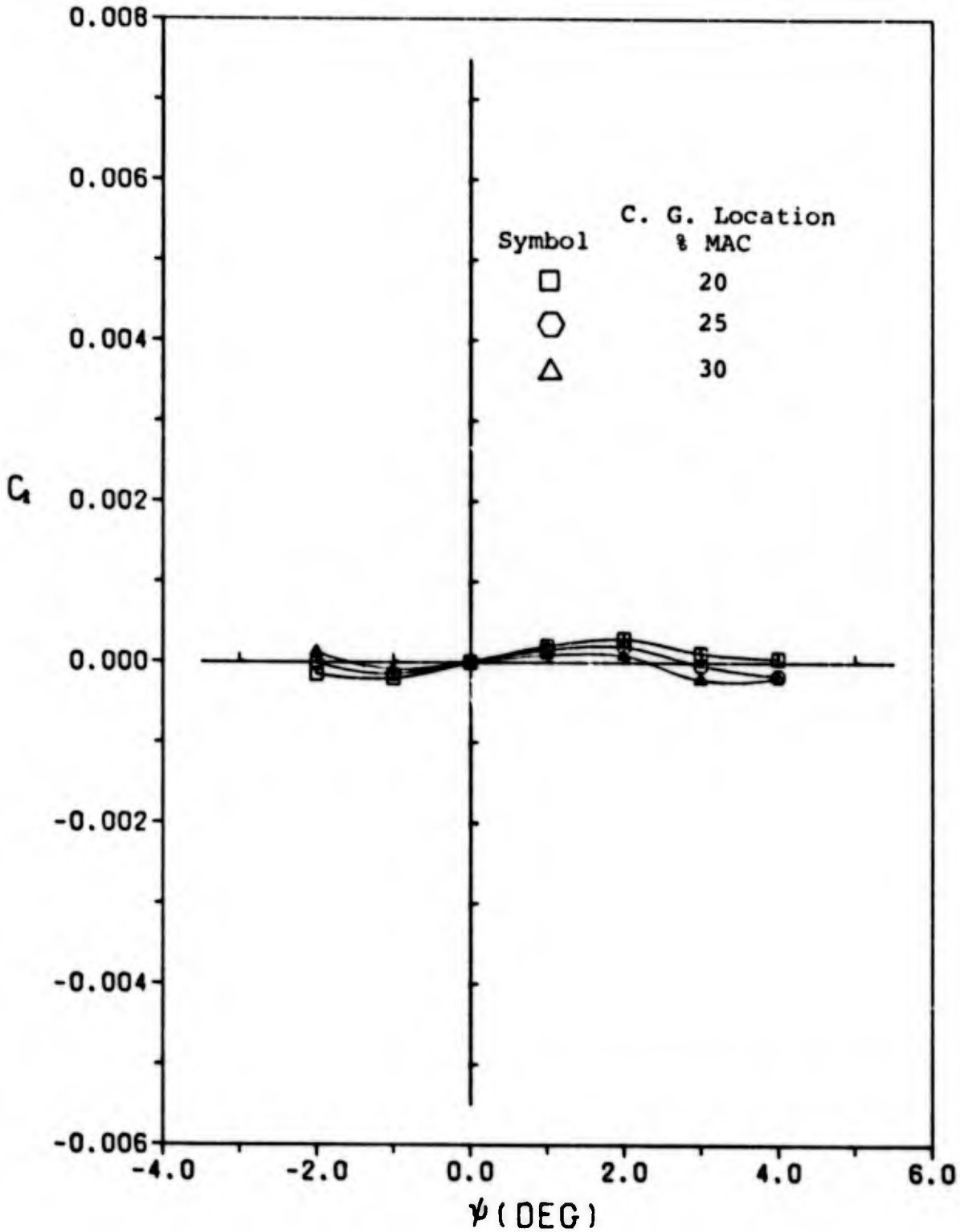

Figure 23. Effect of C.G. Location on C_l vs ψ for Config. 4. α= 2 deg

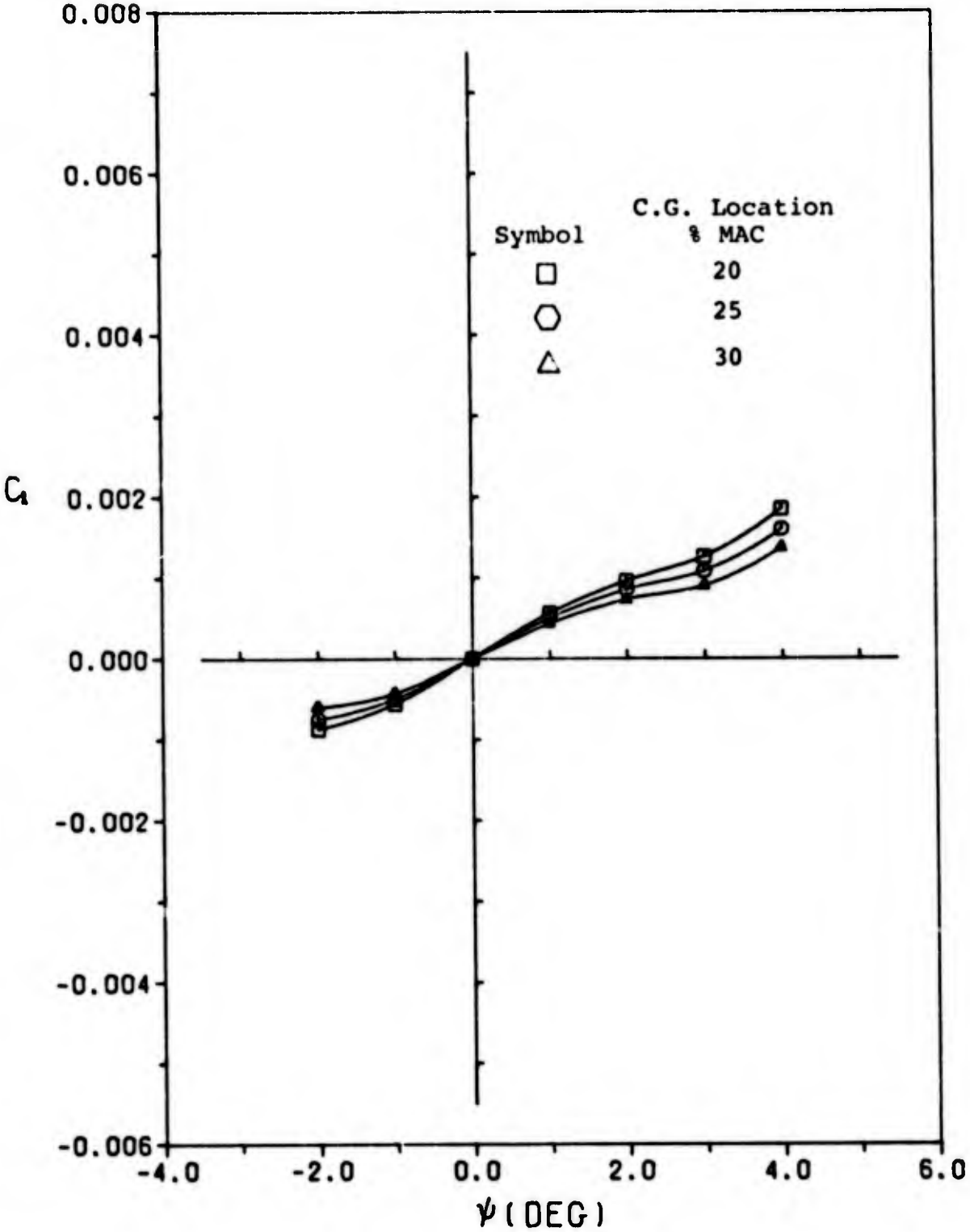

Figure 24. Effect of C.G. Location on C_l vs ψ for Config. 3. α=2 deg

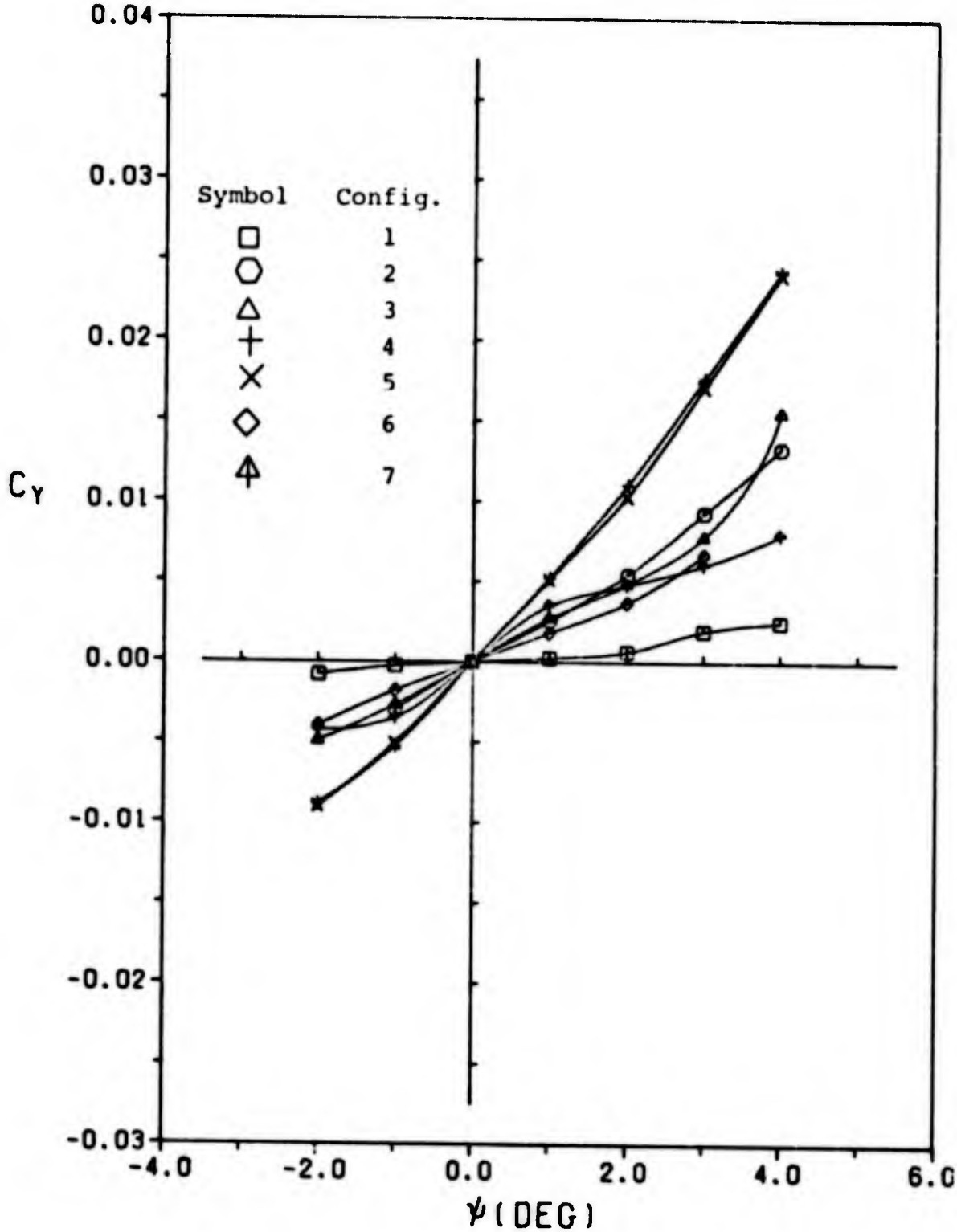

Figure 25. Side Force Coefficient C_y vs Yaw Angle for All Configs. α=4 deg

Predictions

The lift and pitching moment curves for both the TEA-236 and the Datcom prediction methods are shown for comparison in Fig 14 for configuration 1. Comparison of the Datcom predictions with experimental results for configurations 3 and 4 is given in Fig 15. Drag comparisons are shown in Figs 16 and 17. Note that TEA-236 only predicts induced drag and does not predict any coefficients for configurations 2 through 7.

The values for C_{n_ψ}, C_{l_ψ} and C_{y_ψ} predicted by Datcom are given in Table IV. The actual curves can be found in Appendix E.

Recall that configuration 4 was tested at Mach number equal to 0.50 and 0.80 to determine Mach effects on lateral stability. The results of this test were that there was a very small increase in stability associated with yawing moment and side force with an equally small decrease in roll stability. The Datcom program predicted this trend although the actual values of the coefficients were different from those predicted.

Oil Visualization

Results of the oil flow study can be seen in Figs 26, 27, and 28. Figure 26 shows the Spade at α=0, ψ=0, M=0.70. It is apparent that the wing tips have stalled even at zero angle of attack. There is also a region of separation that starts at approximately the 60 percent chord location along

Figure 26. Oil Flow at M=0.70, α=0, ψ=0.

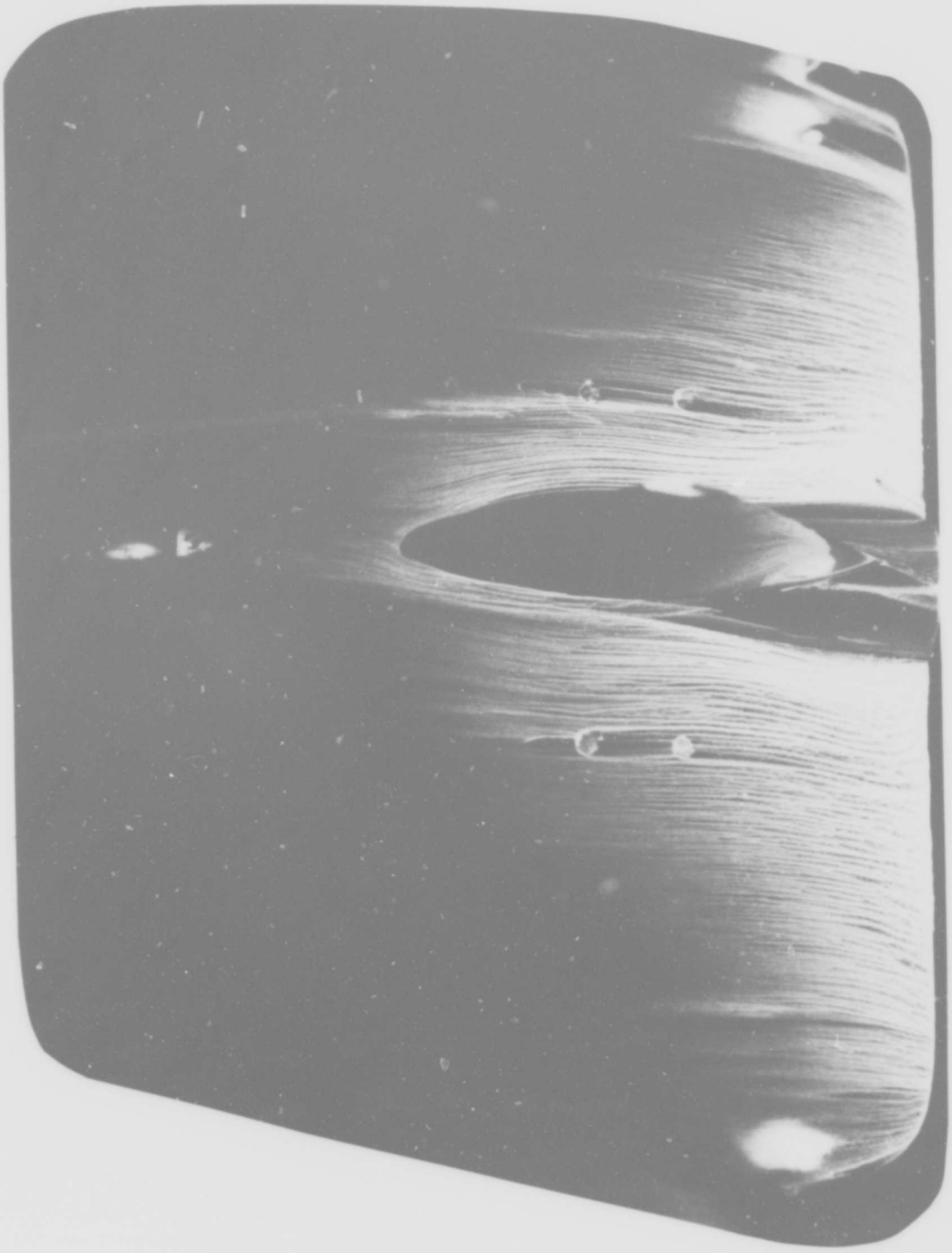

Figure 27. Oil Flow at M=0.70, α=0, ψ=-2.

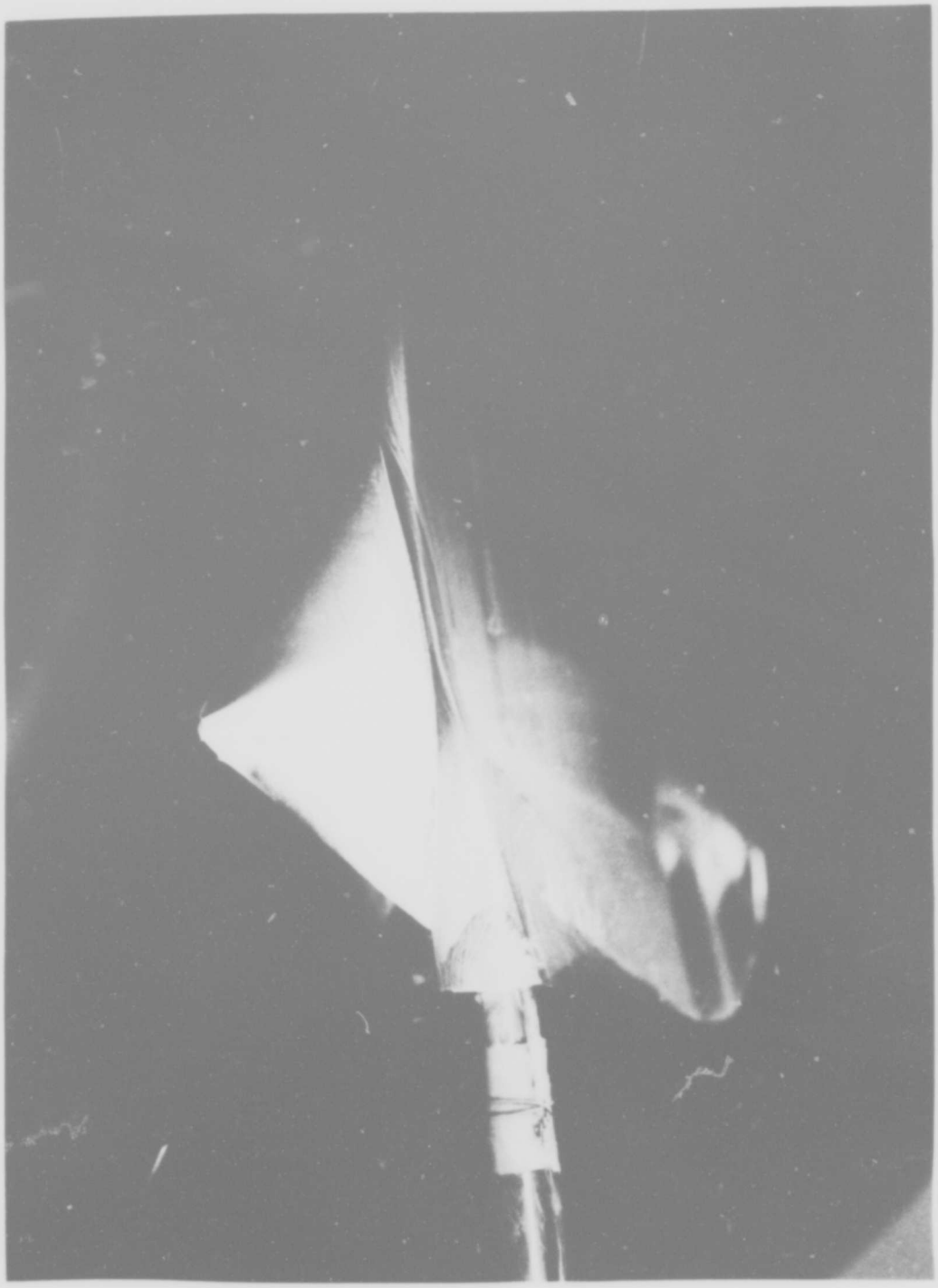

Figure 28. Oil Flow at M=0.86, α=6, ψ=0.

the span. This is just aft of the thickest part of the wing at each span station. The vertical fin has separation occurring on it also just past its thickest point. Note that the two circles on each wing appearing about a third of the way out from the body are mounting holes for the outboard fins and are not aerodynamic phenomena.

Figure 27 presents the same alpha of zero and Mach number equal to 0.70, but now the yaw angle is -2°. The flow has not changed dramatically as this is a small angle of yaw. Note however that the flow inward along the trailing edge of the right wing is more pronounced than before.

Figure 28 shows the Spade at angle of attack of 8 degrees with 0 degrees yaw. The free stream Mach number here is 0.86. Close observation will reveal a standing shock wave at about 30 percent chord from the trailing edge and extending up the fin at about its mid-point. Behind the shock the flow is completely separated with backflow occurring on both the wing and fin.

Aerodynamic Center

The slope of the pitching moment curve in Fig 14 indicates that the prediction for the aerodynamic center location is very accurate. The a.c. of course varies slightly with angle of attack and more so with configuration changes. The center of pressure, which is given as part of the data reduction program, is located for configuration 1 at 3.65 in. from the nose for C_L=0.458. Recall that at lift

coefficients of approximately 0.5 and above, the c.p. location approaches that of the a.c. The data showed a forward moving c.p. with increase in C_L. The most forward position recorded was 3.65 in. The a.c. is estimated in Appendix B to be located 3.59 in. from the nose. This places the error of prediction at less than 2 percent if 3.65 in. is assumed to be the a.c. location. However, the c.p. actually never quite reaches the a.c. (Ref 6:78). Therefore, it is justified to accept the a.c. location as that computed. This places the a.c. at 0.47 of the root chord from the nose of the Spade for configuration 1.

VI. Conclusions and Recommendations

Conclusions

The Spade appears to be laterally stable for all configurations at angles of attack of 4 to 8 degrees. Below 4 degrees some configurations become either neutrally stable or unstable. Stability in yaw and roll tends to increase with angle of attack while side force stability decreases. The increase in yaw stability with angle of attack probably is due to the increased induced drag on the wing whose leading edge is brought more perpendicular to the wind. This induced drag would create a moment causing the aircraft to rotate back to its equilibrium position. The increase in roll stability would also be explained by an increase in lift differential between the two sides of the wing as the aircraft is yawed at a higher angle of attack.

For a given yaw angle the side force, resulting mostly from the force on the vertical fin, tends to decrease. This is probably due to the fin being blanked out more by the wing flow separation at increased angles of attack.

Stability in yaw can be increased by 60 to 80 percent by moving the c.g. .05 MAC forward of the aerodynamic center. Stability in roll can be increased by 10 to 30 percent with this movement. With the exception of configuration 3 the c.g. must be moved forward to provide a negative

pitching moment coefficient slope if longitudinal stability is to be achieved.

The Datcom predicted values for lift appear to be in excellent agreement with those obtained experimentally. The drag values agree closely for low values of C_L. As C_L increases the predicted values begin to diverge from the true values. The Datcom methods introduce more error in drag predictions as the Mach number increases. Figure 17 shows that Datcom fails entirely to predict drag rise.

The TEA-236 program predicts the slope of the lift curve well but is in disagreement with the angle of zero lift. It also predicts much more negative pitching moments than those obtained experimentally. No direct comparison of the drag predicted by TEA-236 can be made since it only predicts induced drag.

The trends in stability predicted by Datcom are in close agreement with the experimental values, though the actual values differ considerably in many cases. The differences may stem from the fact that Datcom assumes C_{n_ψ} and C_{y_ψ} to be independent of angle of attack and yaw. This is obviously not true. It also assumes C_{l_ψ} to be independent of yaw angle. Again, this is not the case. The Datcom program can be used to predict lift values for this shape aircraft with a high degree of accuracy. It appears to predict drag values somewhat higher than those actually achieved. More error is introduced in the predictions at higher lift coefficients. It can be used to

predict general trends in the lateral stability coefficients keeping in mind that the actual values may vary considerably from those predicted. The program may indicate correctly that the aircraft is stable, but the degree of stability may be quite different from that predicted.

Recommendations

Four recommendations follow from the results of the Spade tests.

1. The DATCOM program correctly predicts the trends in the lateral stability coefficients of the various configurations. It is recommended that DATCOM be used to predict the effects of small design changes and these predictions be used to adjust the wind tunnel data.

2. Due to small stability margins and small values of stability derivatives exhibited by the Spade, experimental investigation of control effectiveness is required. Design of ailerons, elevons, and rudder(s) will require sufficient experimental data to determine size, shape, and location effects of control surfaces.

3. The location and design of the propulsion system inlets and nozzles could have significant effects on the stability characteristics of the Spade. Due to the small stability margins exhibited by the Spade, experimental data will be required to determine the magnitude of these effects.

4. The oil flow study indicates that a large portion of the vertical fins lose their stabilizing effectiveness due to flow separation. A study should be made to determine the effectiveness of adding a fairing aft of these fins in the area of adverse pressure gradient. A fairing might delay separation and thus provide better stability characteristics for the Spade configurations having thick stabilizers.

BIBLIOGRAPHY

1. Corning, G. Supersonic and Subsonic Airplane Design. Ann Arbor, Michigan: Braun-Brumfield, Inc., 1970.

2. Ward, H.E. Proposal to Aeronautical Systems Division Wright-Patterson Air Force Base for Two .50" Diameter Six Component Floating Frame Wind Tunnel Balances. Document number T-548(1842). Anaheim, California: Task Corporation, 1962.

3. White, H. L. Trisonic Gasdynamic Facility User Manual. Task number 14760401. Wright-Patterson Air Force Base, Ohio: Air Force Flight Dynamics Laboratory, June 1973.

4. Abbott, I. H. and A. E. Von Doenhoff. Theory of Wing Sections. New York: Dover Publications, Inc., 1959.

5. Pope, A. Wind-Tunnel Testing. New York: John Wiley and Sons, Inc., 1961.

6. Houghton, E. L. and A. E. Brock. Aerodynamics for Engineering Students. London: Edward Arnold Ltd., 1970.

7. Van Vlack, L. H. Elements of Materials Science. Reading, Massachusetts: Addison-Wesley Publishing Company, Inc., 1964.

8. Geller, E. W. An Approximate Method for Incompressible Wing Design and Analysis. Document Number D6-15036. Renton, Washington: The Boeing Company, 1968.

9. Finck, R. D. et al. USAF Stability and Control Datcom. Project Number 8219, Task Number 821901. McDonnell Douglas Corporation, October 1960.

10. Murray, S. C. et al. The USAF Stability and Control Digital Datcom Users Manual. AFFDL-TR-74-68. Wright-Patterson Air Force Base, Ohio: Air Force Flight Dynamics Laboratory, February 1975.

11. Perkins, C. D. and R. E. Hage. Airplane Performance Stability and Control. New York: John Wiley and Sons, Inc., 1965.

12. Pope, A. and K. L. Goin. High Speed Wind Tunnel Testing. New York: John Wiley and Sons, Inc., 1965.

13. Dommasch, D. O. et al. Airplane Aerodynamics. New York: Pitman Publishing Corporation, 1951.

14. Ketter, Robert L. and S. P. Prawel, Jr. Modern Methods of Engineering Computation. New York: McGraw-Hill Book Company, 1968.

15. Miller, F. E. and H. A. Doeringsfield. Mechanics of Materials. Scranton, Pennsylvania: International Textbook Company, 1965.

APPENDIX A

PRELIMINARY LIFT COEFFICIENT ESTIMATIONS

APPENDIX A

Preliminary Lift Coefficient Estimates

Lift coefficients were needed for the Spade model to estimate the loads that might be expected during the testing procedures. These were calculated in the following manner.

The three-dimensional lift curve slope a, per degree, is given by

$$a = f\frac{\bar{a}_0}{1+(57.3\bar{a}_0/\pi A)} \qquad (4)$$

where A is the aspect ratio and $\bar{a}_0$ is the mean section slope of the lift curve between root and tip section. For the Spade, which has a constant airfoil section, this is the slope of the NACA 66_1-212 airfoil and is equal to 0.1025 per degree. The factor f is a constant allowing for variation from elliptical lift distribution and is a function of wing aspect ratio and taper ratio. It may be determined from Fig 2-55 of Reference 11. For the Spade, f is equal to 0.998. Then from Eq 4

$$a = .0529/\text{deg}$$

The lift coefficient may be given as

$$C_L = a(\alpha-\alpha_0)$$

where α_0 is the angle of attack for zero lift and α is the angle of attack corresponding to C_L. For the NACA 66_1 -212 airfoil the two-dimensional α_0 is approximately -1.5 degrees. The Spade angle of attack in the wind tunnel was not expected to exceed 10 degrees. Then if α equals 10 degrees and α_0 is assumed to be -1.5 degrees, the maximum lift coefficient expected is 0.608. The lift of the wing is given by

$$L = C_L qS \qquad (5)$$

where q is the dynamic pressure and S is the reference area, in this case equal to the wing area of 50.0 in.^{2} The maximum q attainable in the TGF in the subsonic test section is 1,030 psf. The maximum possible lift calculated from Eq 5 would be approximately 217 pounds.

The Task force balance used for the Spade investigation has a lift force limit of 80 pounds, this being attainable only if the balance load center is located at exactly the center of pressure. For safety reasons, therefore, it was decided to limit the tunnel q to a maximum of 300 psf. This yields a maximum lift of 63.3 pounds, well below the balance limit.

APPENDIX B

MEAN AERODYNAMIC CHORD AND AERODYNAMIC CENTER ESTIMATIONS

APPENDIX B

Mean Aerodynamic Chord and Aerodynamic Center Estimations

The Task balance maximum normal force is limited to 80 pounds if it is located with its load center at the center of pressure of the wing. To obtain the widest load range possible it was desired to determine the center of pressure location. The c.p. location varies with angle of attack and lift coefficient. At lift coefficients of about 0.5 and above, however, the c.p. is normally found at approximately the same location as the aerodynamic center (Ref 6:78,79). The a.c. can be located at approximately the quarter chord point of the mean aerodynamic chord. The following method of calculating the MAC is taken from Reference 12.

The mean aerodynamic chord $\bar{c}$ is defined as

$$\bar{c} = \frac{2}{S}\int_0^{b/2} c^2 dy \qquad (6)$$

where S is the wing planform area, b is the wing span from tip to tip, c is the local chord of the wing, and y is the spanwise distance from the aircraft axis to the local chord of interest. In this case b is 10.0 in. and S is 50 in.^{2} By dividing the planform into a finite number

of sections and using Simpson's one-third rule for numerical integration, the mean aerodynamic chord length was found to be equal to 5.39 in. (Ref 14:231). By locating the MAC on the planform, and taking the aerodynamic center to be located at the 25 percent point of the MAC, the aerodynamic center was estimated to be located 3.59 inches from the Spade nose tip. For lift coefficients of 0.5 and above this was also assumed to be the location of the center of pressure. The load center of the Task force balance was thus located at this point.

APPENDIX C

CYLINDER STRESS ANALYSIS

APPENDIX C

Cylinder Stress Analysis

To assure safe operation in the wind tunnel, a stress analysis of the brass cylinder used for a balance cavity was required.

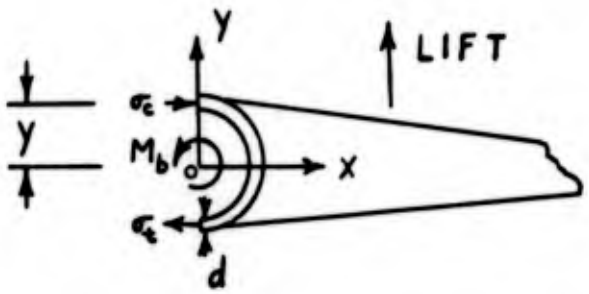

Figure 29. Moments and Bending Stresses Acting on Cylindrical Center Body.

With reference to Fig 29, the stresses in the cylinder σ_c and σ_t were assumed to be constant and equal over d. Summing moments about 0,

$$M_b = 2\sigma dly$$

where l is the cylinder length. Rearranging this equation yields

$$\sigma = \frac{M_b}{2dly}$$

Substituting for y gives

$$\sigma = \frac{M_b}{2dl\left(\frac{d}{2} + 0.375\right)} \qquad (8)$$

The maximum bending moment, M_b, expected is 60 inch pounds since the Task balance is limited to this. For an approximation, and as an added safety precaution, let M_b equal 120 inch pounds. A d of .20 in. was selected to allow clearance for mounting the vertical stabilizers with machine screws running through the cylinder wall. With l equal to the root chord of 7.63 in. this yields a stress, σ, of 82.8 psi. Since brass has an average modulus of elasticity of 16×10^6 psi, using brass with the given dimensions for the balance cavity would yield a very hefty margin of safety even if the estimated stresses were exceeded several times over (Ref 7:418).

APPENDIX D

WING STRESS ANALYSIS

APPENDIX D

Wing Stress Analysis

Pressure Distributions

A wing stress analysis was required for the Spade to insure that it could withstand the expected loads while being tested in the wind tunnel. In performing the analysis it was assumed that the spanwise and chordwise load distributions could be approximated to be linear distributions. This is a good approximation for low aspect ratio wings since the wing tips tend to carry very little load. The center of pressure was assumed to be located at the 25 percent point of the local chord. These distributions are illustrated in Figs 30 and 31. From Fig 30, for

$$x \leq \frac{c}{4}$$

$$P = \frac{4P_i}{c} x \qquad (9)$$

and for

$$x \geq \frac{c}{4}$$

$$P = \frac{4P_i}{3c}(c-x) \qquad (10)$$

where P_i is the pressure at $\frac{c}{4}$ and P is the pressure at any point along the chord.

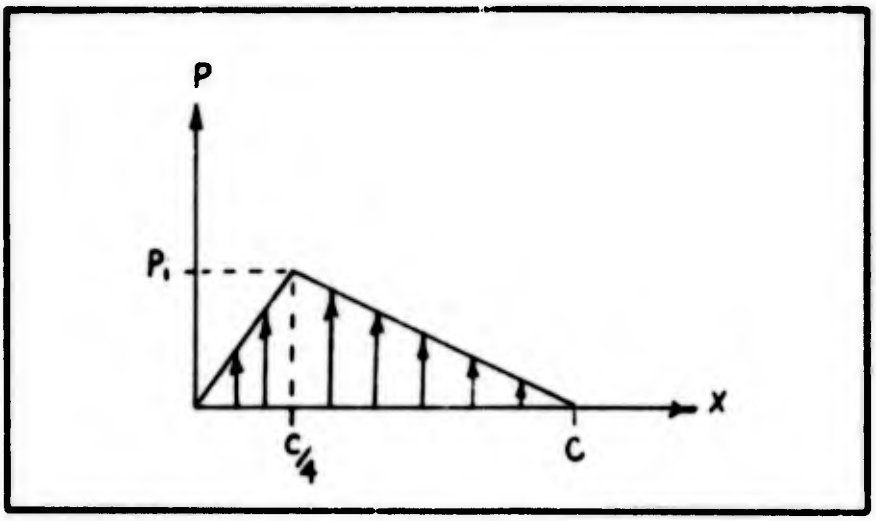

Figure 30. Wing Chordwise Load Distribution.

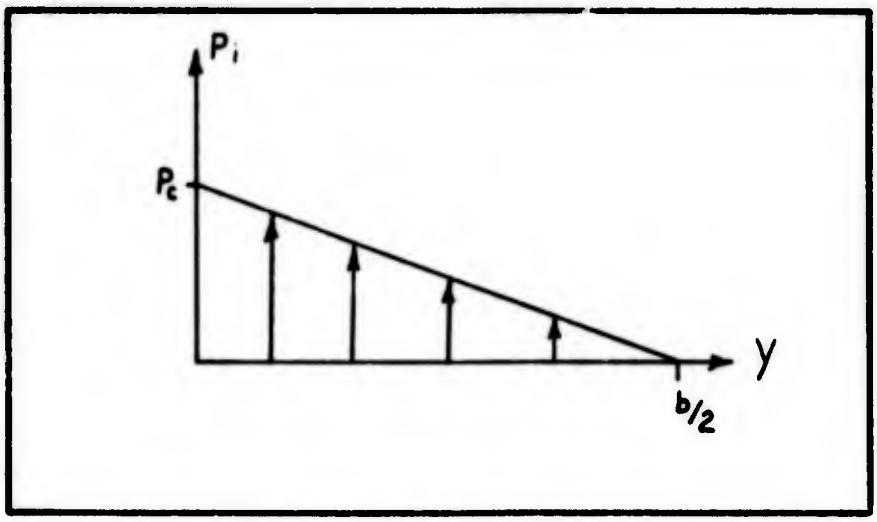

Figure 31. Wing Spanwise Load Distribution.

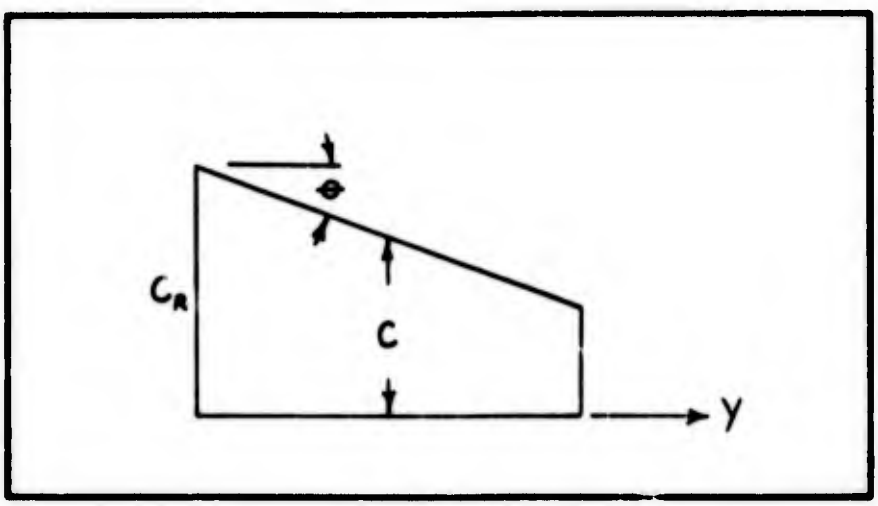

Figure 32. Wing Half Planform.

From Fig 31

$$P_i = \frac{2P_c}{b}\left(\frac{b}{2} - y\right) \qquad (11)$$

where P_c is the maximum pressure occurring on the wing. By substituting Eq 11 into Eqs 9 and 10 for

$$x \leq \frac{c}{4}$$

$$P = \frac{8P_c}{bc}\left(\frac{b}{2} - y\right)x \qquad (12)$$

and for

$$x \geq \frac{c}{4}$$

$$P = \frac{8P_c}{3bc}\left(\frac{b}{2} - y\right)\left(c - x\right) \qquad (13)$$

The local chord length c, as shown in Fig 32, is given by

$$c = C_R - y \tan \theta \qquad (14)$$

where C_R is the root chord of the wing. Substituting Eq 14 into Eqs 12 and 13 yields for

$$x \leq \frac{c}{4}$$

$$P = \frac{8P_c}{b}\left(\frac{b}{2} - y\right)\frac{x}{(C_R - y \tan \theta)} \qquad (15)$$

and for

$$x \geq \frac{c}{4}$$

$$P = \frac{8}{3}\frac{P_c}{b}\left(\frac{b}{2} - y\right)\left(1 - \frac{x}{C_R - y \tan \theta}\right) \qquad (16)$$

By integrating Eqs 15 and 16 over the wing one obtains the lift L:

$$L = 2\left[\int_0^{b/2}\int_0^{c/4} \frac{8P_c}{b}\left(\frac{b}{2} - y\right)\frac{x}{(C_R - y \tan \theta)}\, dxdy\right. \qquad (17)$$

$$\left. + \int_0^{b/2}\int_{c/4}^{c} \frac{8P_c}{3b}\left(\frac{b}{2} - y\right)\left(1 - \frac{x}{C_R - y \tan \theta}\right) dxdy\right]$$

Eq 17 integrates to give

$$L = \frac{P_c}{24}(6bC_R - b^2 \tan \theta)$$

Solving for P_c yields

$$P_c = \frac{24L}{(6bC_R - b^2 \tan \theta)} \qquad (18)$$

The maximum permissible load using the Task balance is 80 pounds. Substituting this value for L and using the Spade dimensions in Eq 18 yields a maximum expected pressure of

$$P_c = 5.37 \text{ psi}$$

Bending Moments

The bending moments at the root chord are next considered. As seen in Fig 33 the moment about the origin, in this case the root chord of the wing, may be found by integrating the products of the pressures acting on differential areas and their respective moment arms:

$$M = 2\int_0^{b/2}\int_0^{c} yp\,dx\,dy \qquad (19)$$

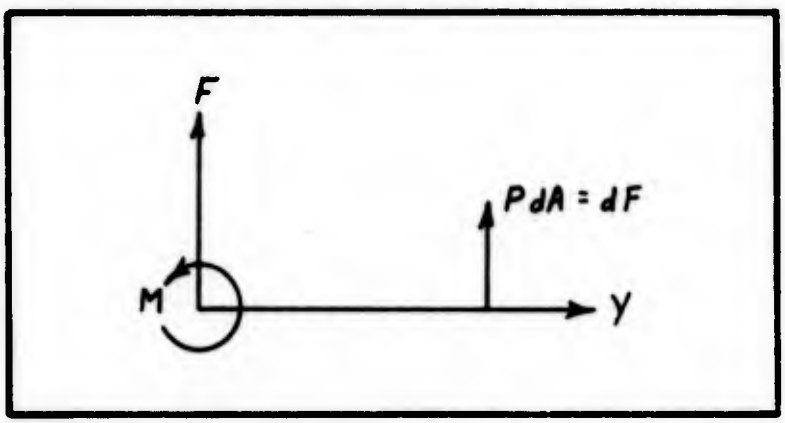

Figure 33. Moments About Wing Root Chord.

Substituting Eqs 15 and 16 this yields

$$M = 2\,P_c\left(\frac{b^2C_R}{48} - \frac{b^3\tan\theta}{192}\right)$$

Using the expression in Eq 18 for P_c and simplifying, the moment about the root chord is

$$M = \frac{L\left(4bC_R - b^2\tan\theta\right)}{\left(24C_R - 4b\tan\theta\right)} \qquad (20)$$

With the Spade geometry and L equal to 80 pounds this gives the maximum expected bending moment of

$$M = 115 \text{ in. lb}$$

Bending Stresses

The maximum bending stress in the Spade is assumed to occur at the root chord of the wing. This was calculated by modeling the wing as a thin beam as shown in Fig 34.

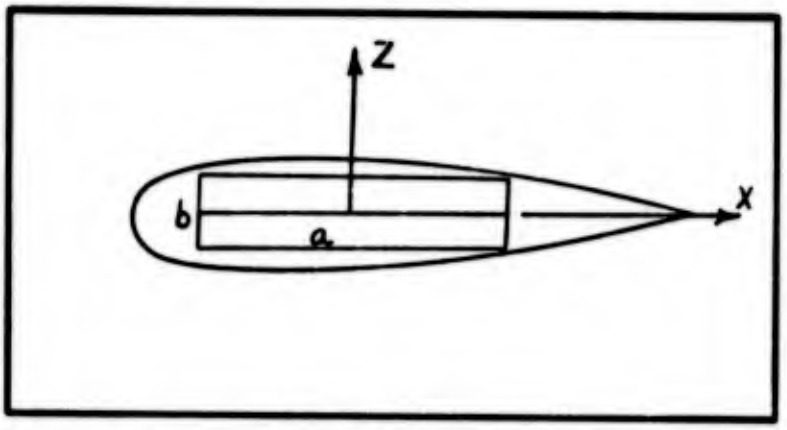

Figure 34. Wing Root Chord Modeled as A Thin Beam.

From beam theory (Ref 15:134)

$$I_x = \frac{ab^3}{12} \qquad (21)$$

where I_x is the moment of inertia about the x axis. Then bending stress σ in the section is given by

$$\sigma = \frac{M_x}{I_x} z$$

The maximum bending stress would occur at the surface. Therefore, with z equal to $b/2$

$$\sigma_{max} = \frac{M_x b}{2I_x}$$

and with Eq 21

$$\sigma_{max} = \frac{6M_x}{ab^2} \qquad (22)$$

The maximum thickness of the root chord is approximately 0.92 in. To be conservative the beam dimension b was assumed as 0.50 in. with a equal to 6.00 in. This gives a stress of

$$\sigma_{max} = 460 \text{ psi}$$

with M_x equal to 115 in. lb. With the epoxy used for the wing having a tensile stress capability exceeding 4,500 psi the factor of safety F.S. is

$$\text{F.S.} = \frac{4,500}{460} = 9.78$$

As an added safety factor an 1/8 in. thick brass plate was molded into the wing. With the stress capability of the brass plate being much higher than that of the epoxy, the safety factor would be much higher than calculated here.

A stress analysis similar to that performed on the wing indicated that for various tails, with the maximum loads expected from the anticipated operating conditions, the factor of safety for each tail would exceed 100.

APPENDIX E

AERODYNAMIC CHARACTERISTICS ARE PRESENTED
IN GRAPHICAL FORM FOR CONFIGS.
1 THROUGH 7

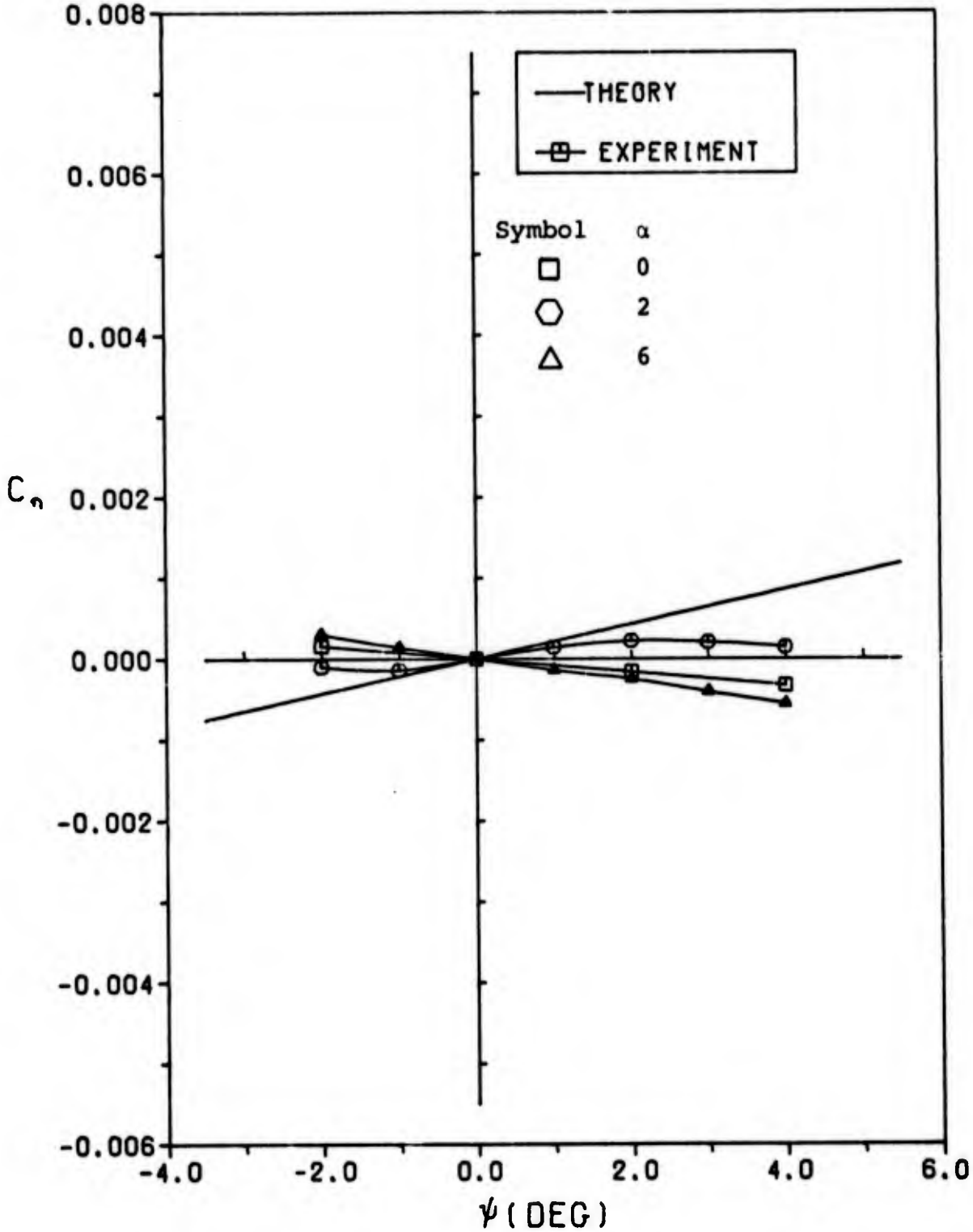

Figure 35. Yaw Moment Coefficient C_n vs Yaw Angle for Config. 1.

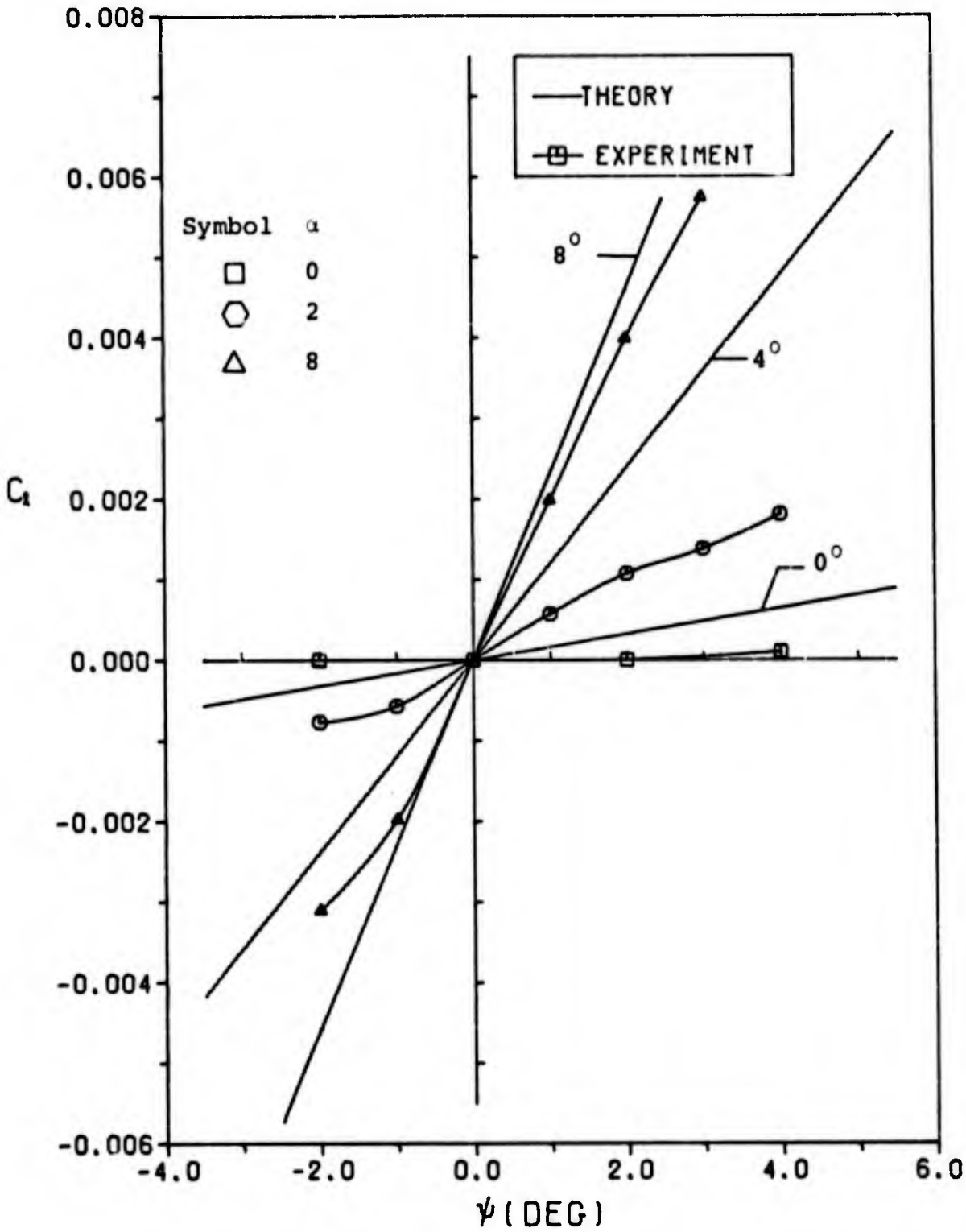

Figure 36. Roll Moment Coefficient C_l vs Yaw Angle for Config. 1.

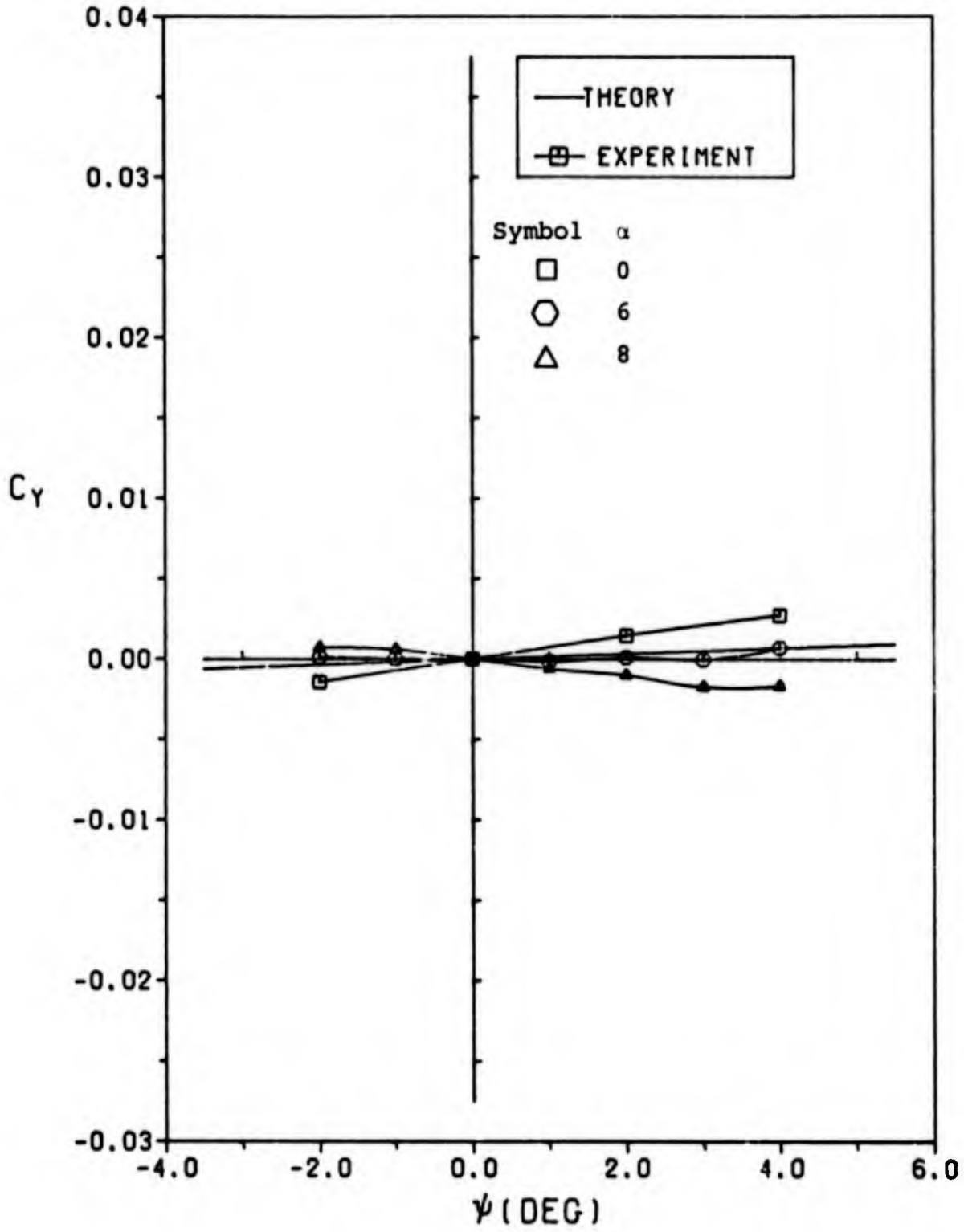

Figure 37. Side Force Coefficient C_y vs Yaw Angle for Config. 1.

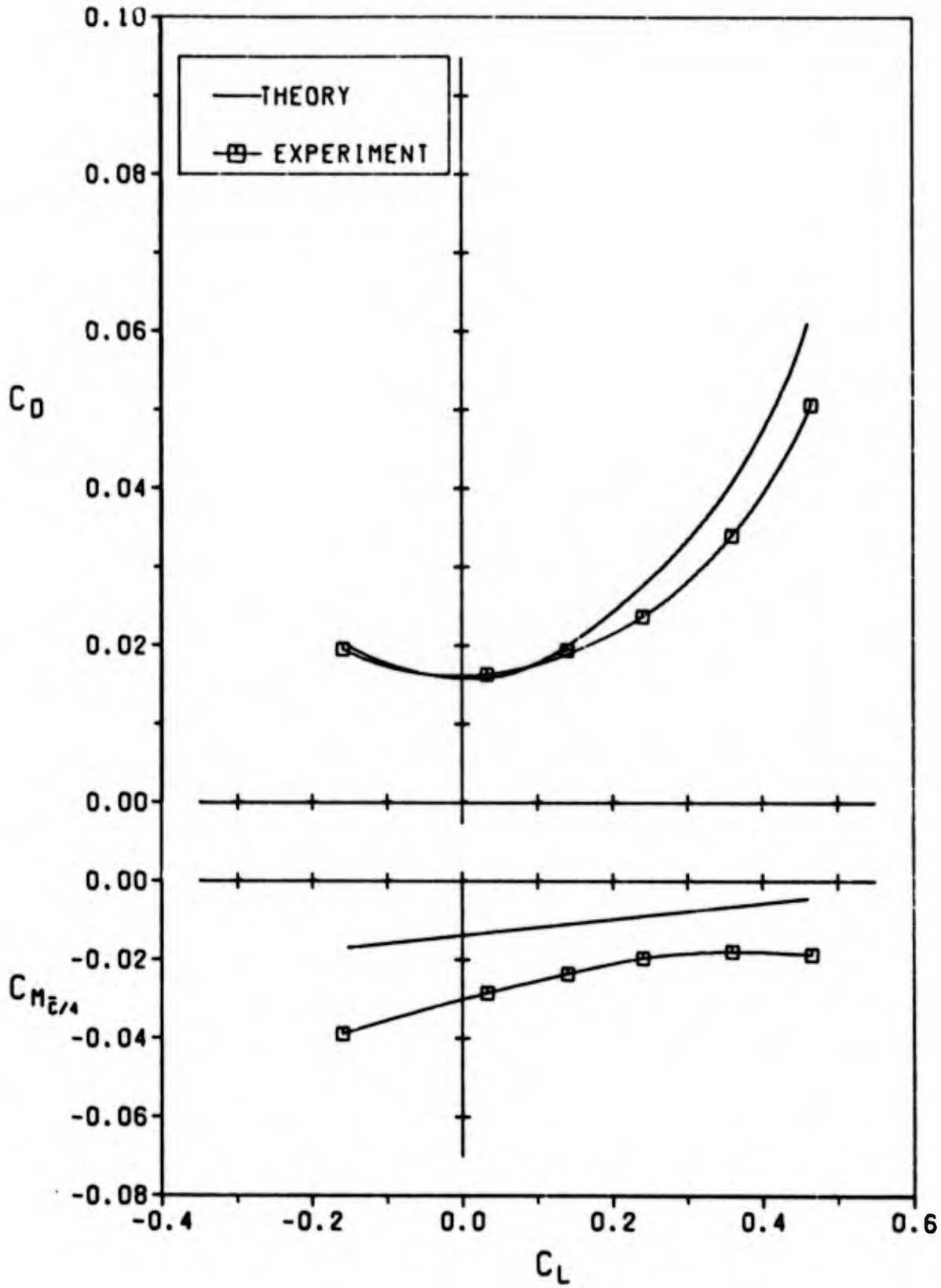

Figure 38. C_D and C_M vs C_L for Config. 2.

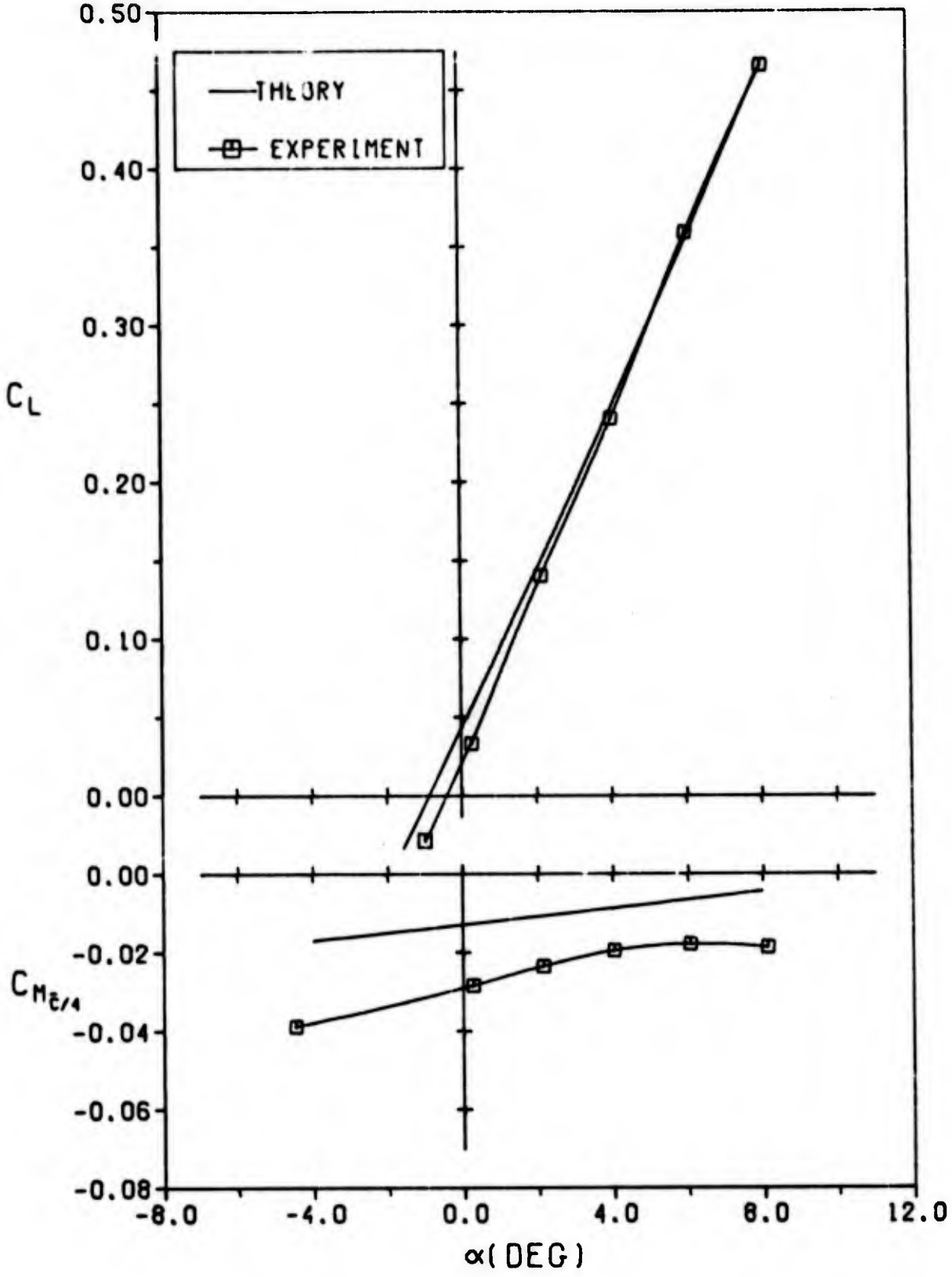

Figure 39. C_L and C_M vs Angle of Attack for Config. 2.

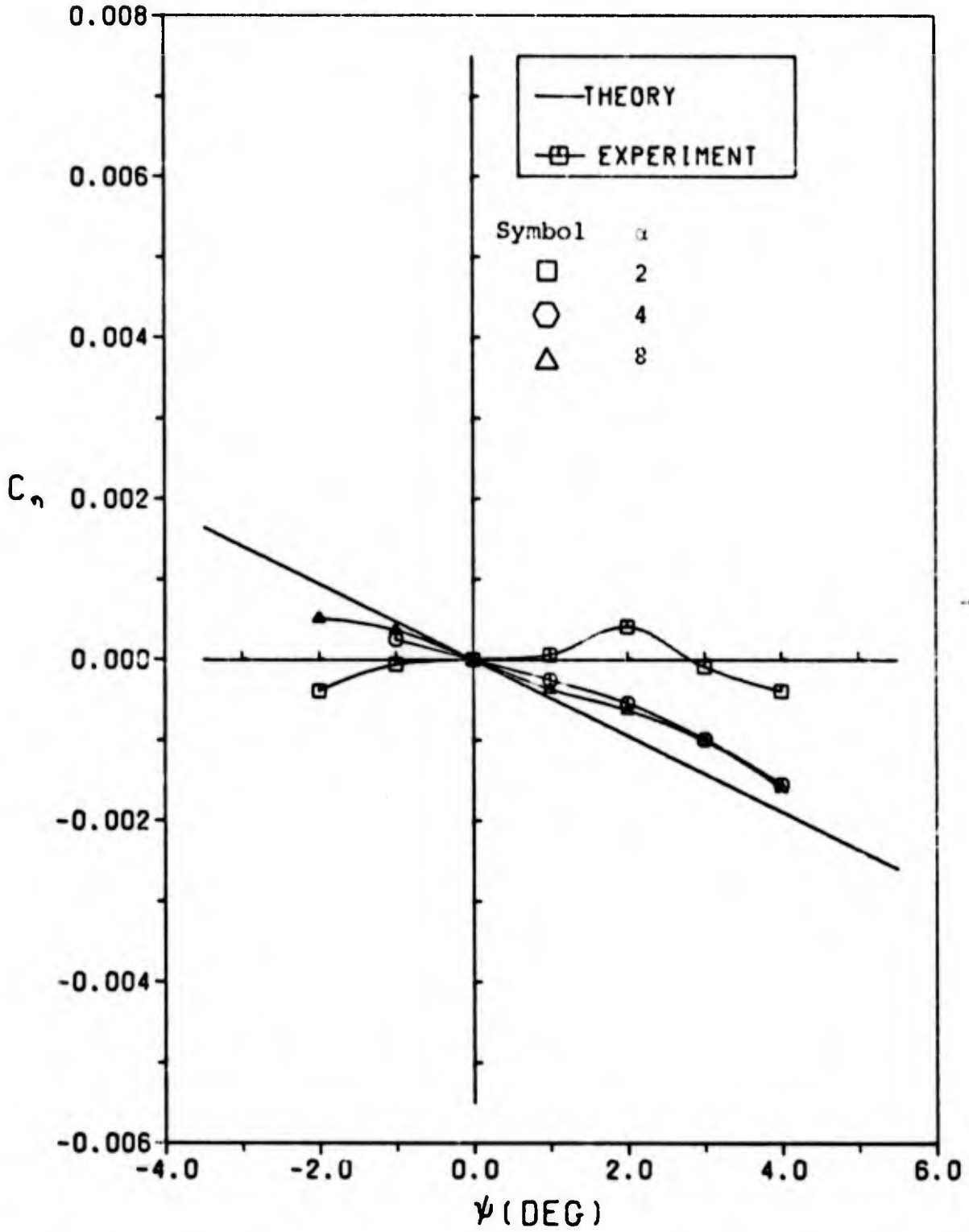

Figure 40. Yaw Moment Coefficient C_n vs Yaw Angle for Config. 2.

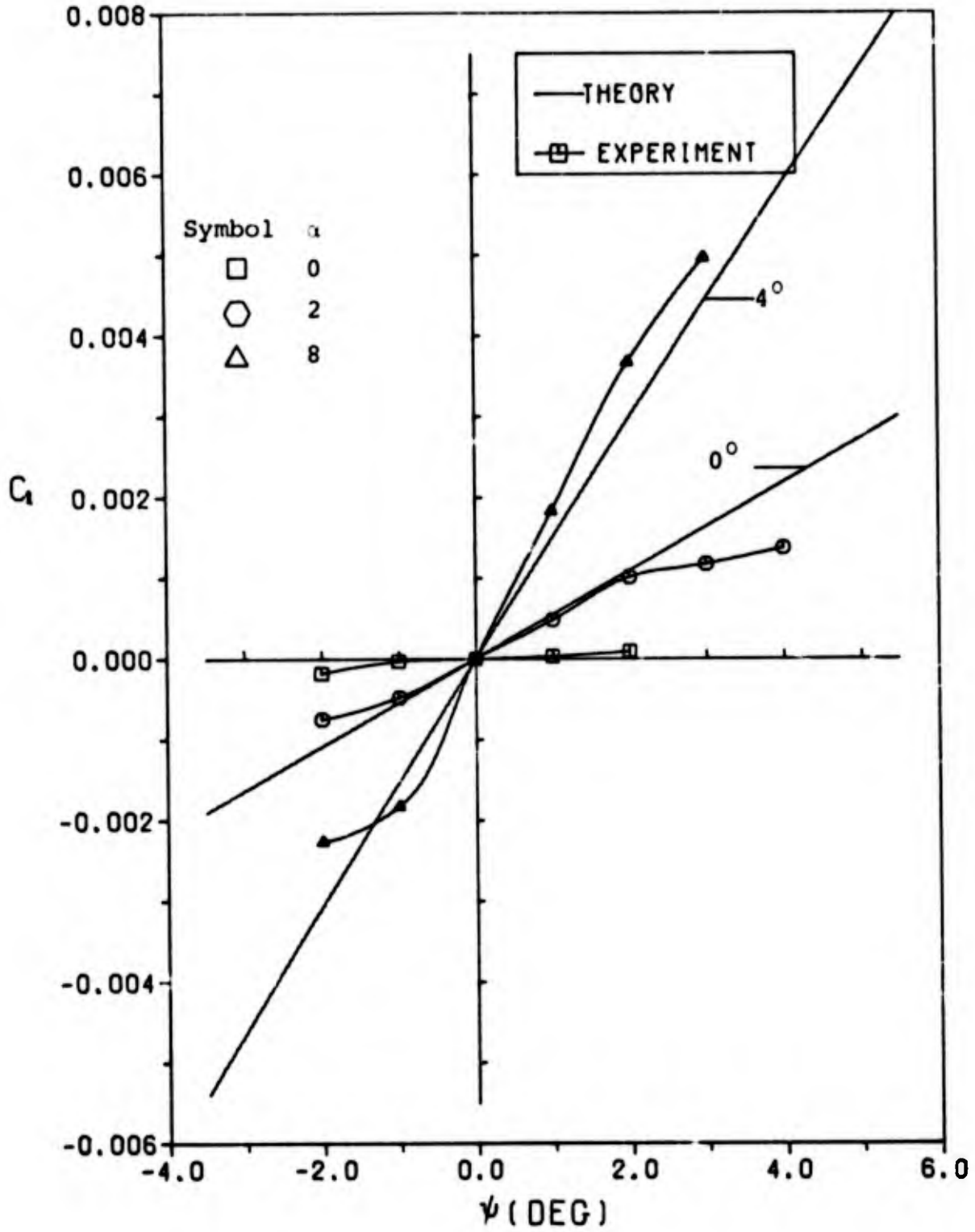

Figure 41. Roll Moment Coefficient C_l vs Yaw Angle for Config. 2.

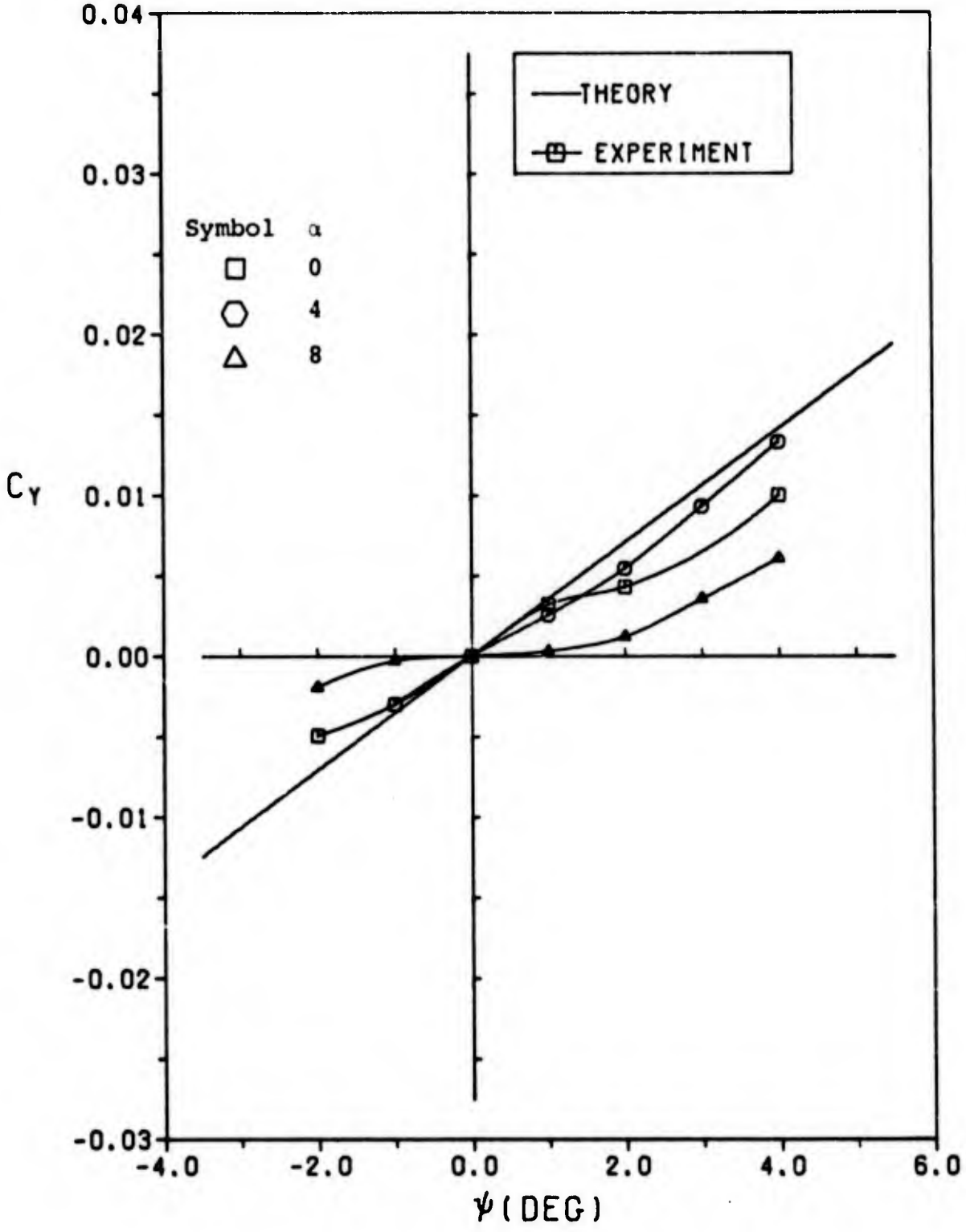

Figure 42. Side Force Coefficient C_Y vs Yaw Angle for Config. 2.

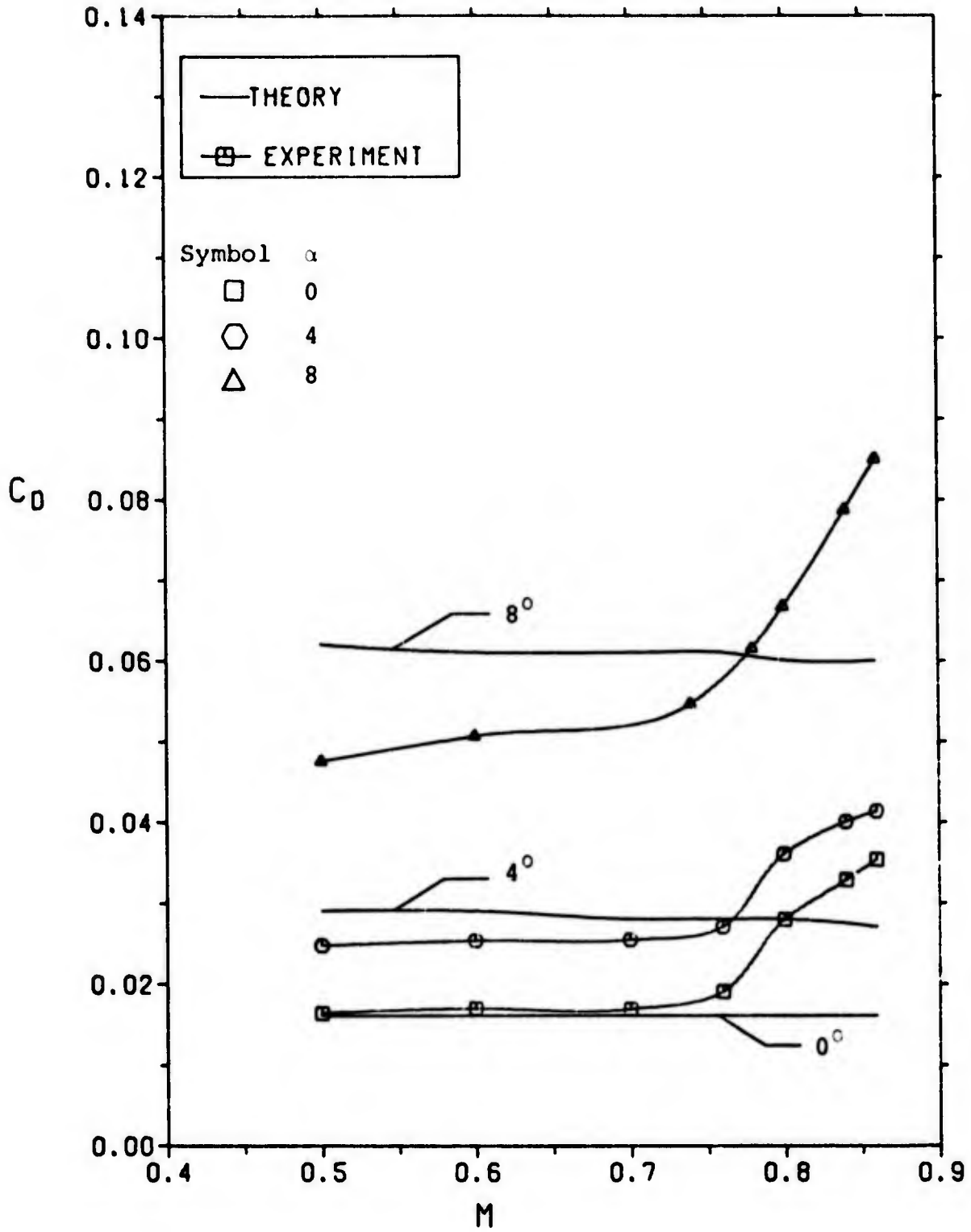

Figure 43. C_D vs M for Config. 2.

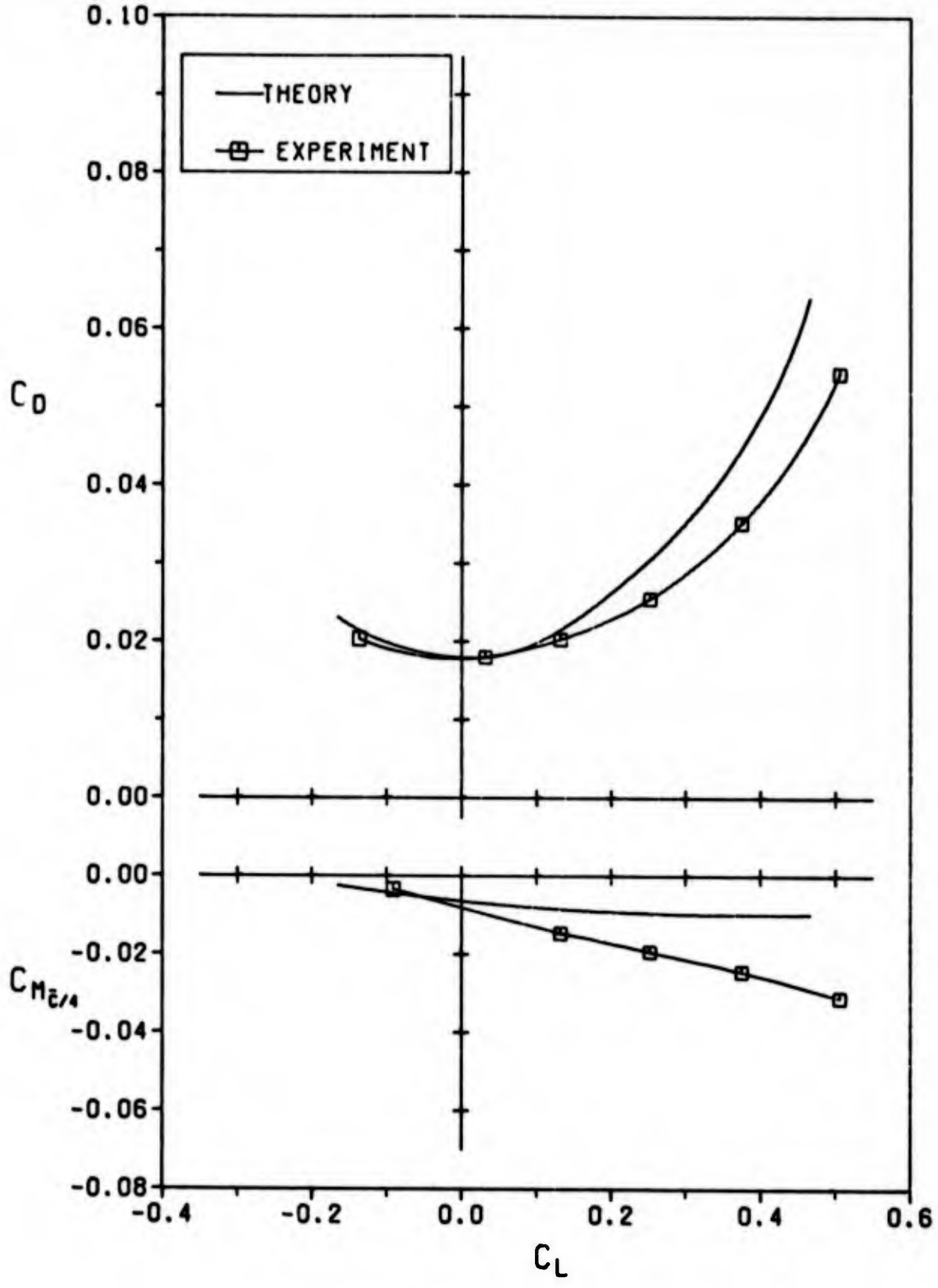

Figure 44. C_D and C_M vs C_L for Config. 3.

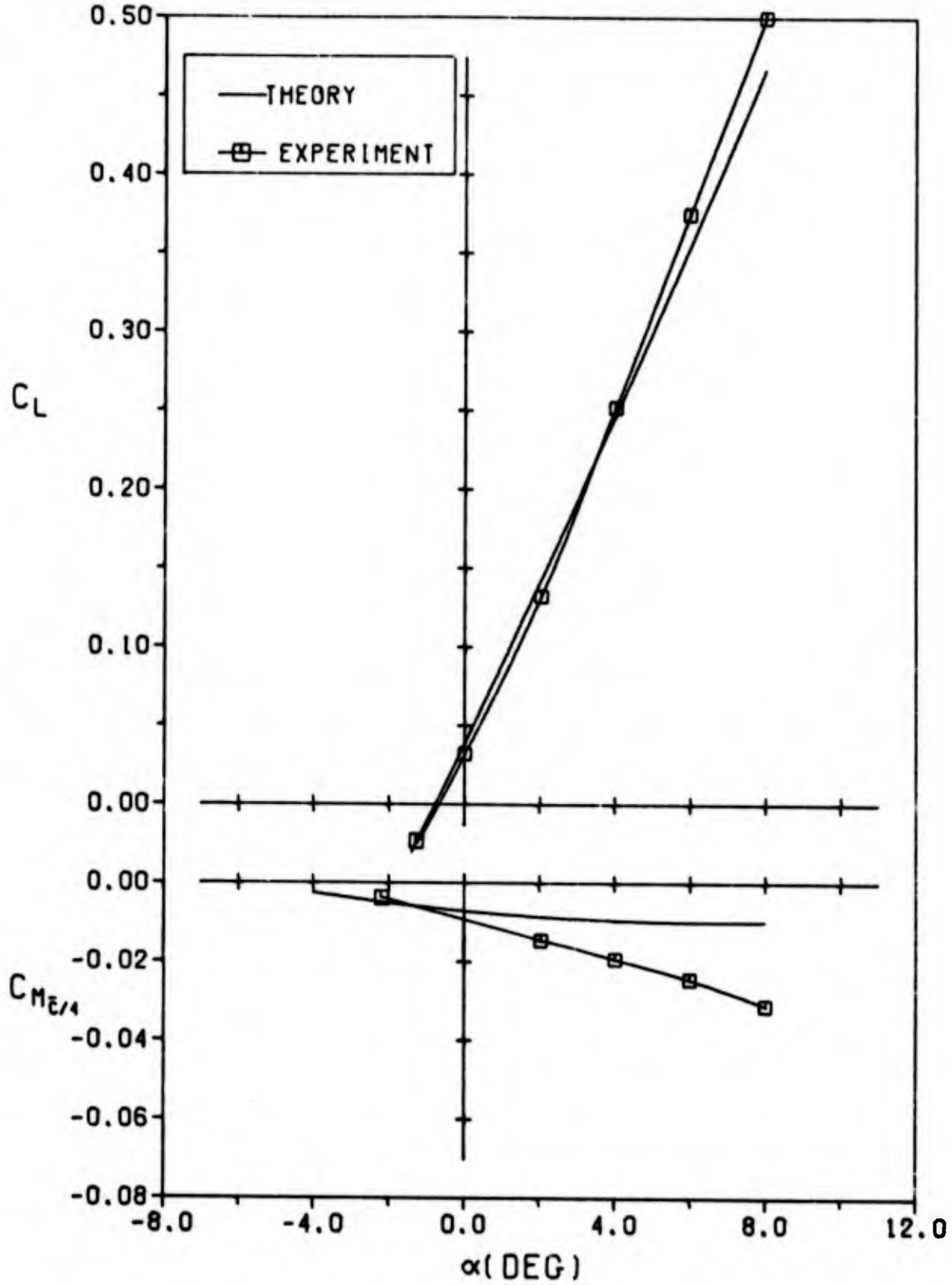

Figure 45. C_L and C_M vs. Angle of Attack for Config. 3.

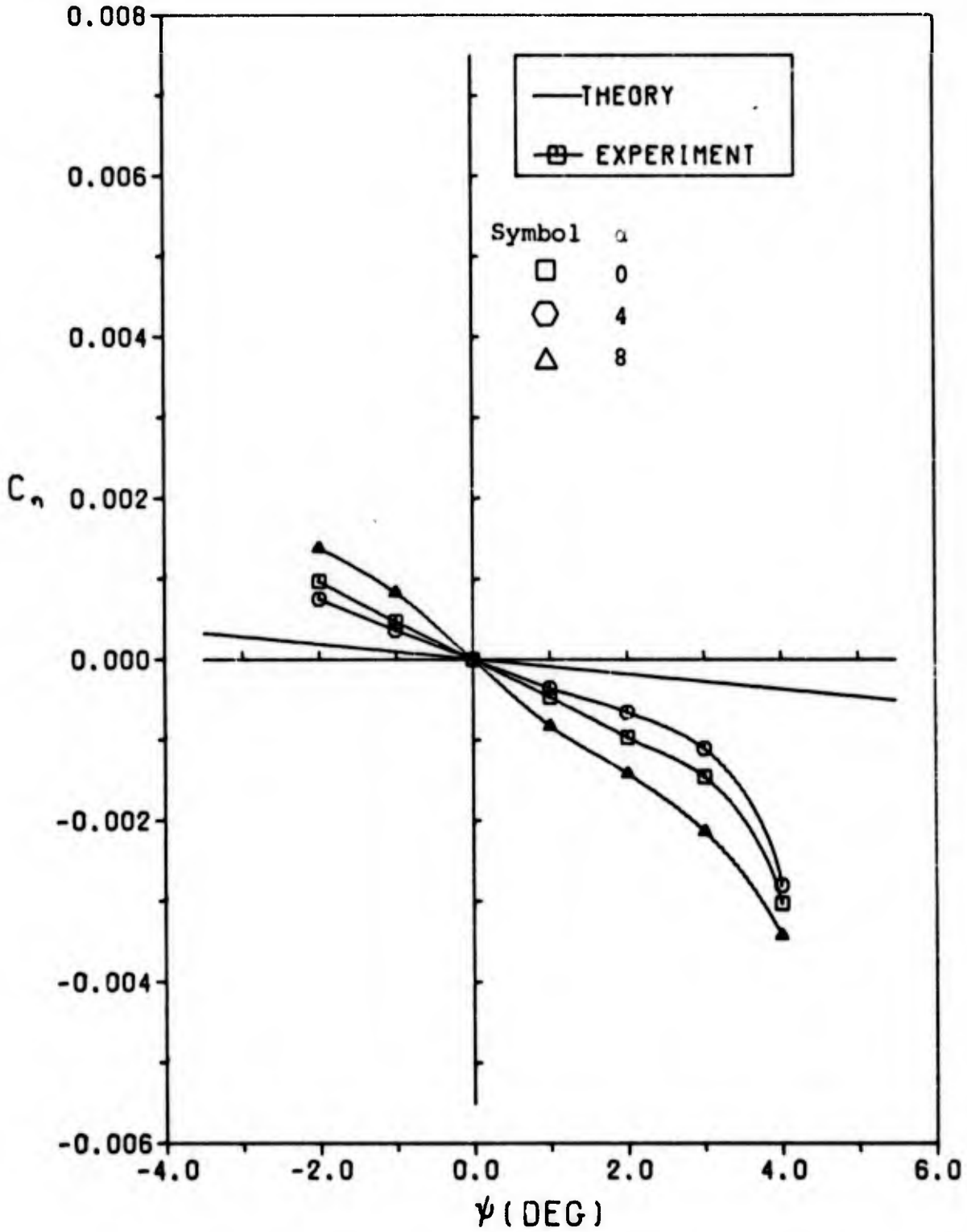

Figure 46. Yaw Moment Coefficient C_n vs. Yaw Angle for Config. 3.

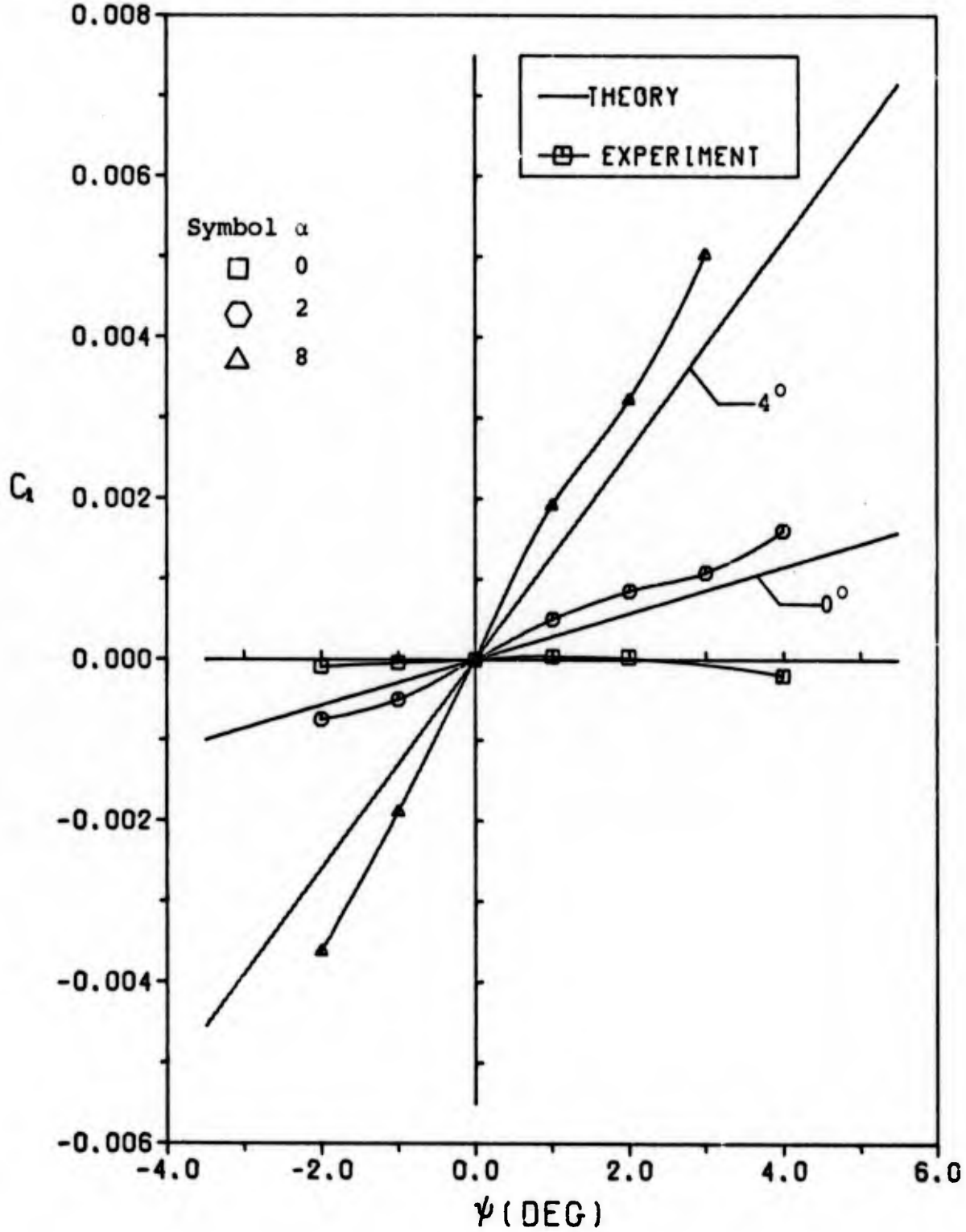

Figure 47. Roll Moment Coefficient C_1 vs Yaw Angle for Config. 3.

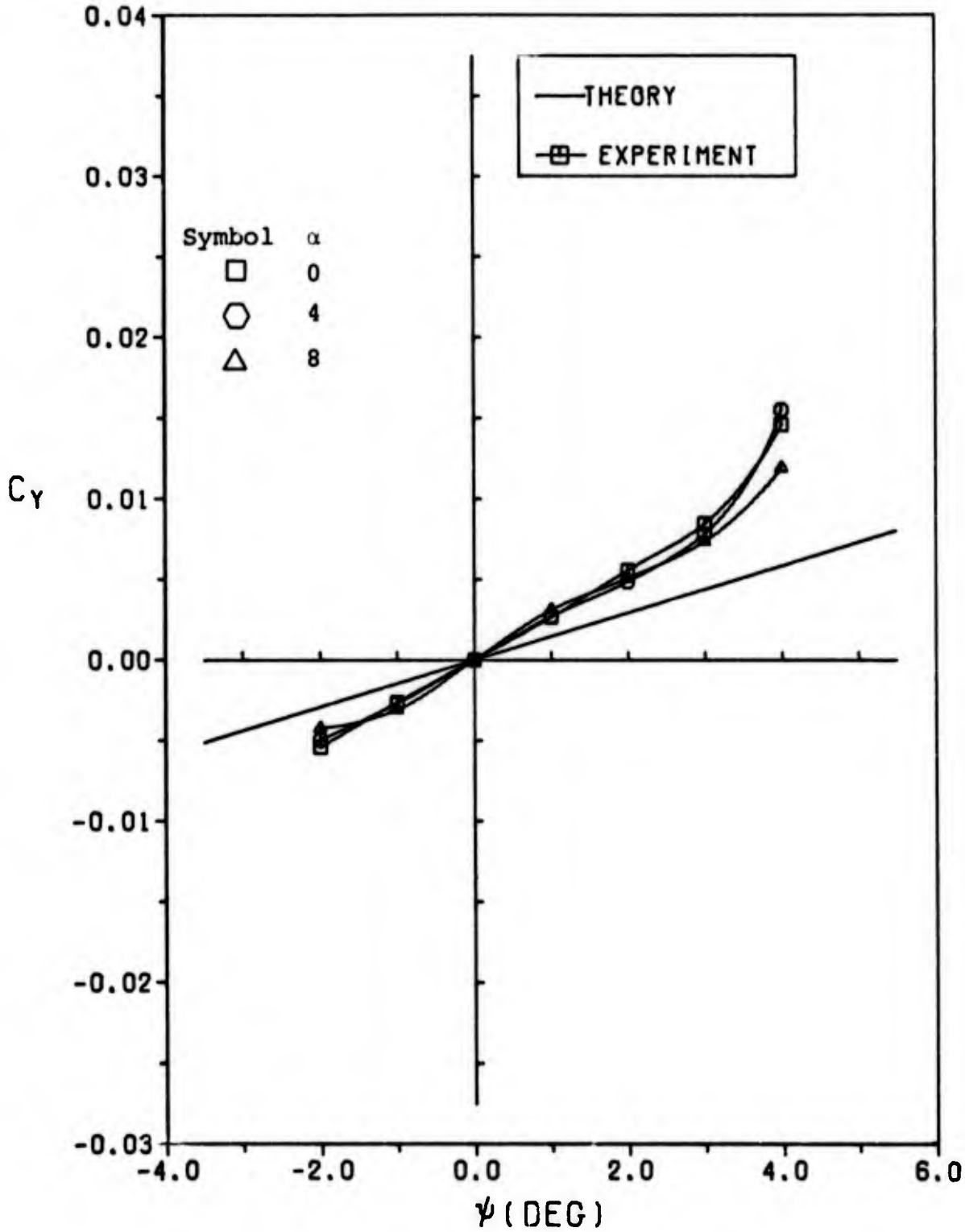

Figure 48. Side Force Coefficient C_Y vs Yaw Angle for Config. 3.

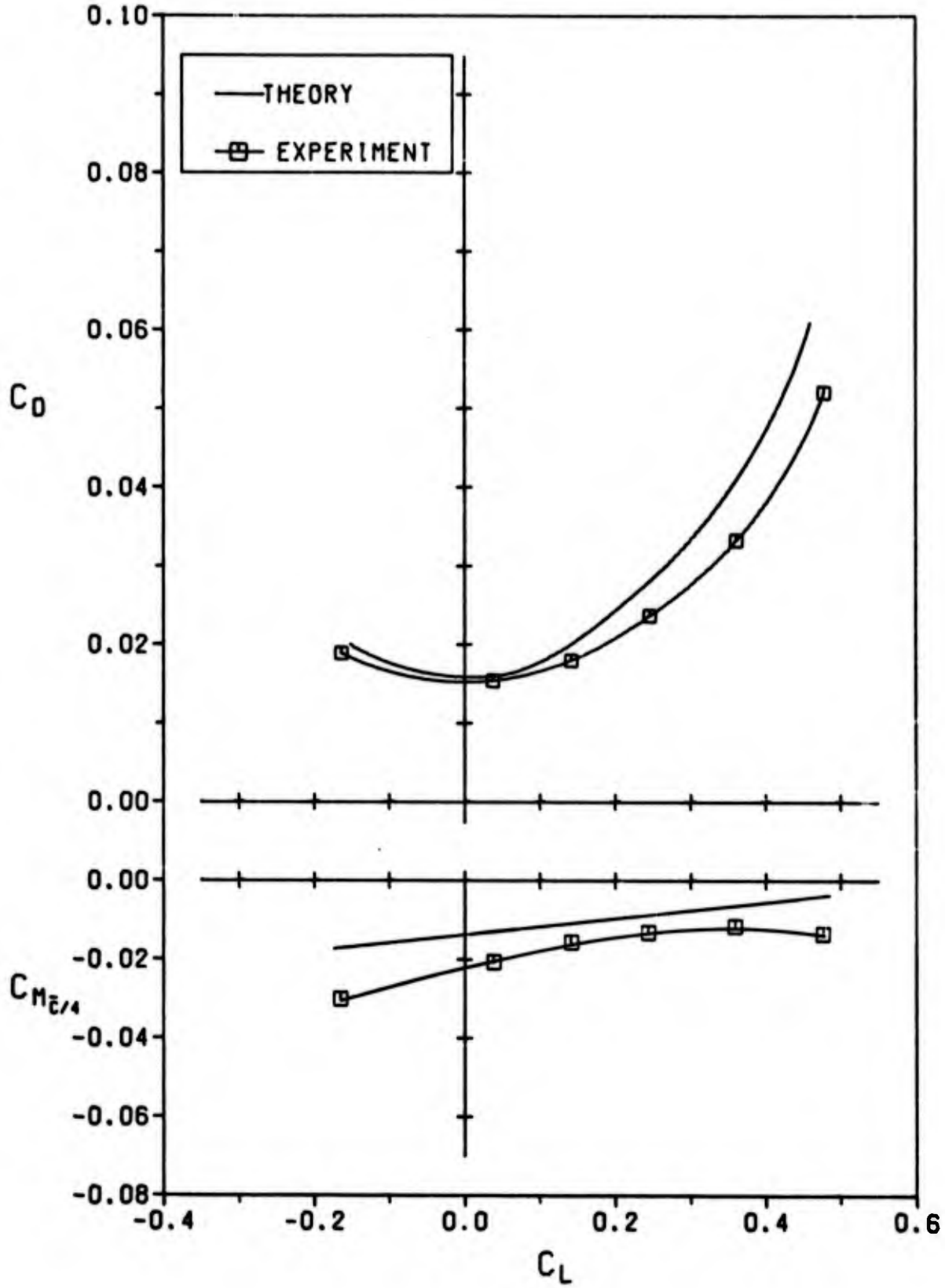

Figure 49. C_D and C_M vs C_L for Config. 4.

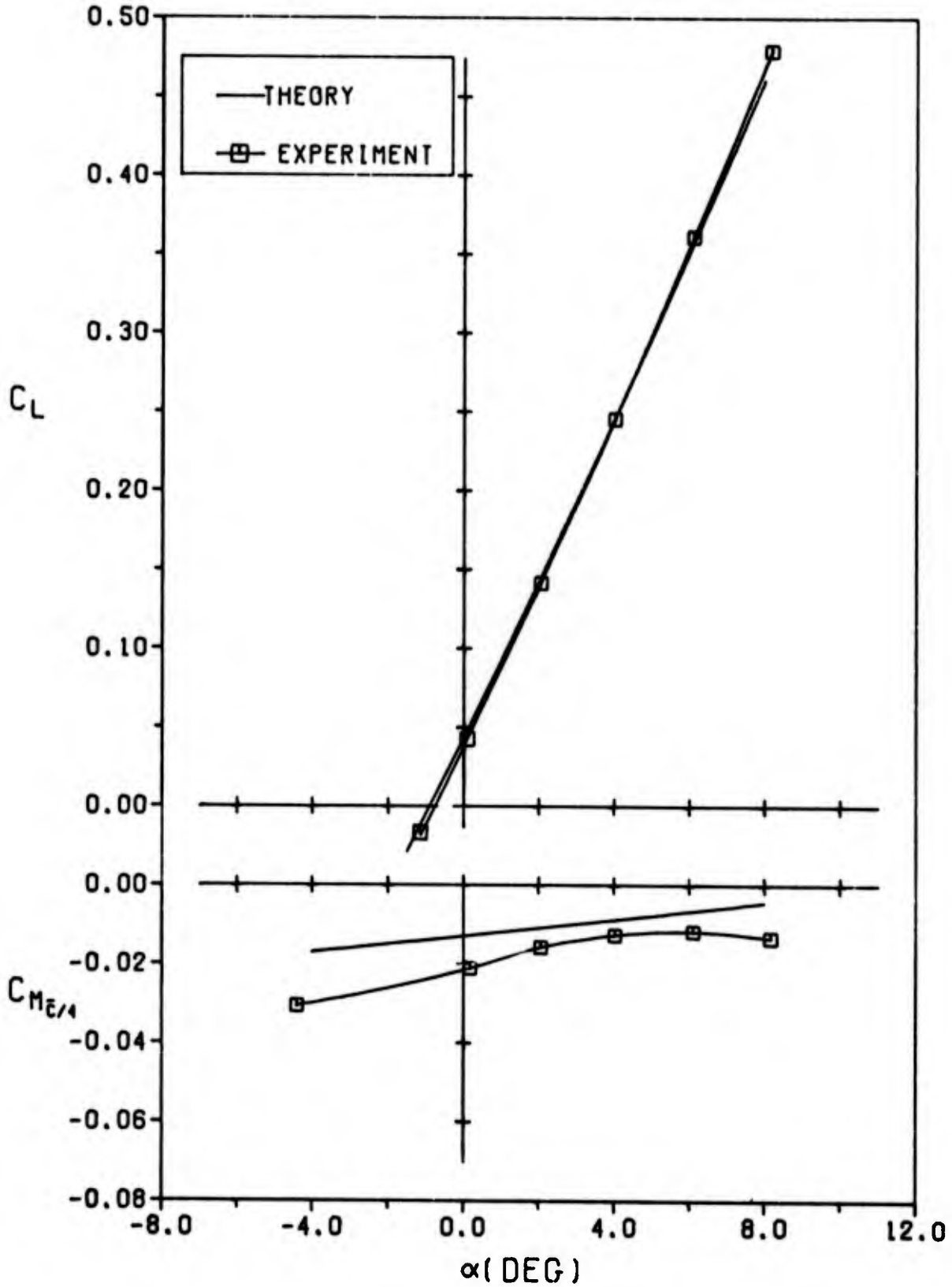

Figure 50. C_L and C_M vs Angle of Attack for Config. 4.

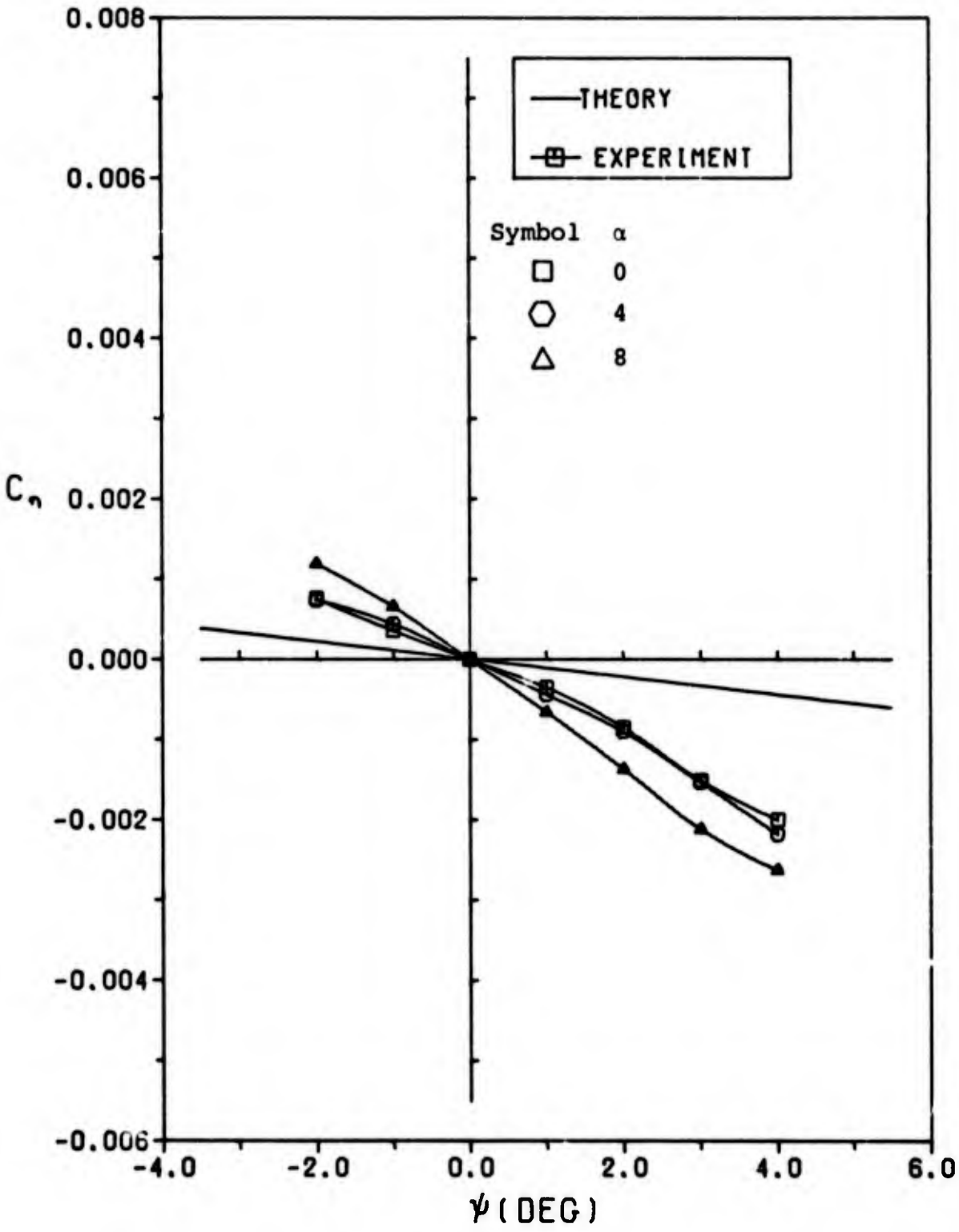

Figure 51. Yaw Moment Coefficient C_n vs Yaw Angle for Config. 4.

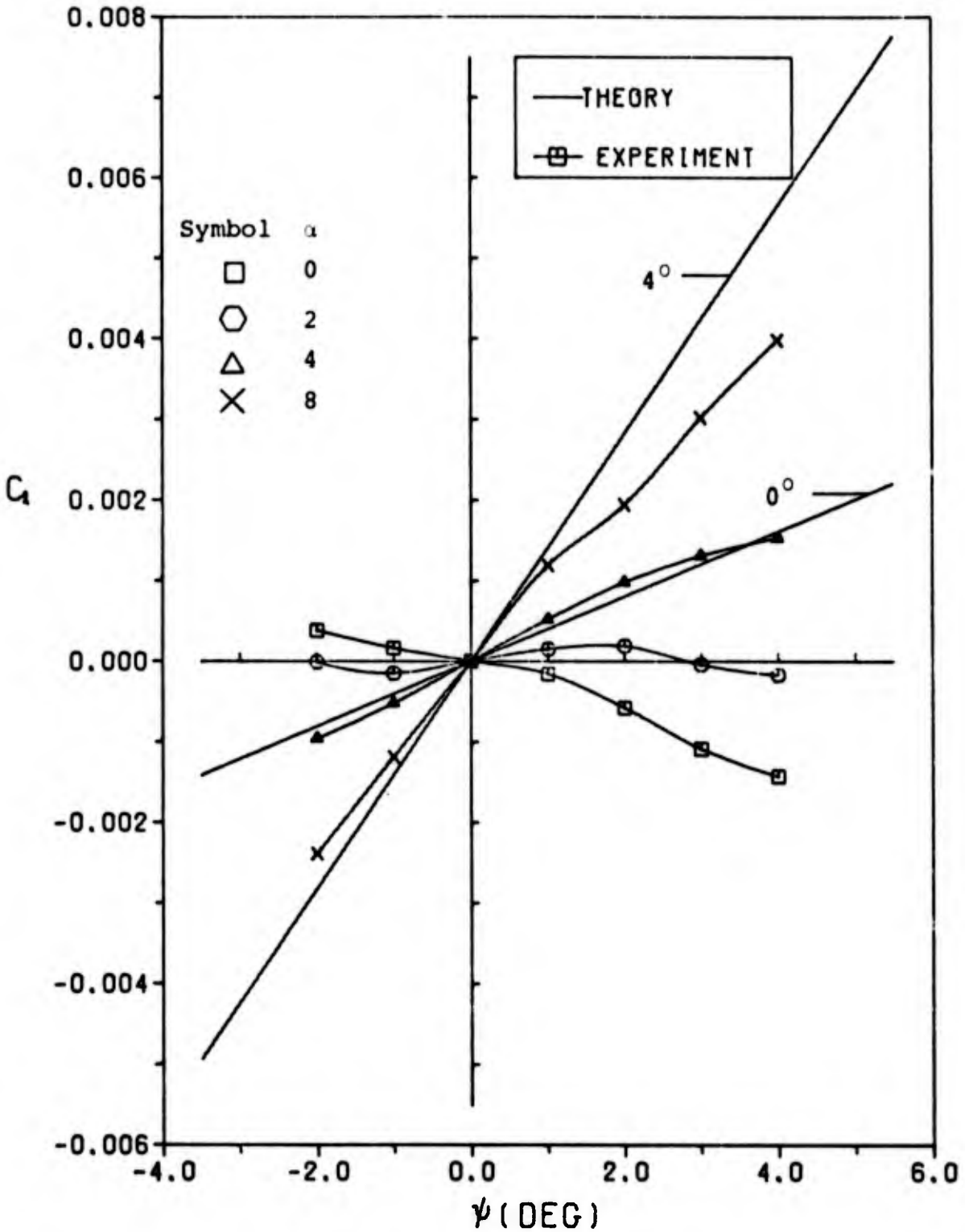

Figure 52. Roll Moment Coefficient C_l vs Yaw Angle for Config. 4.

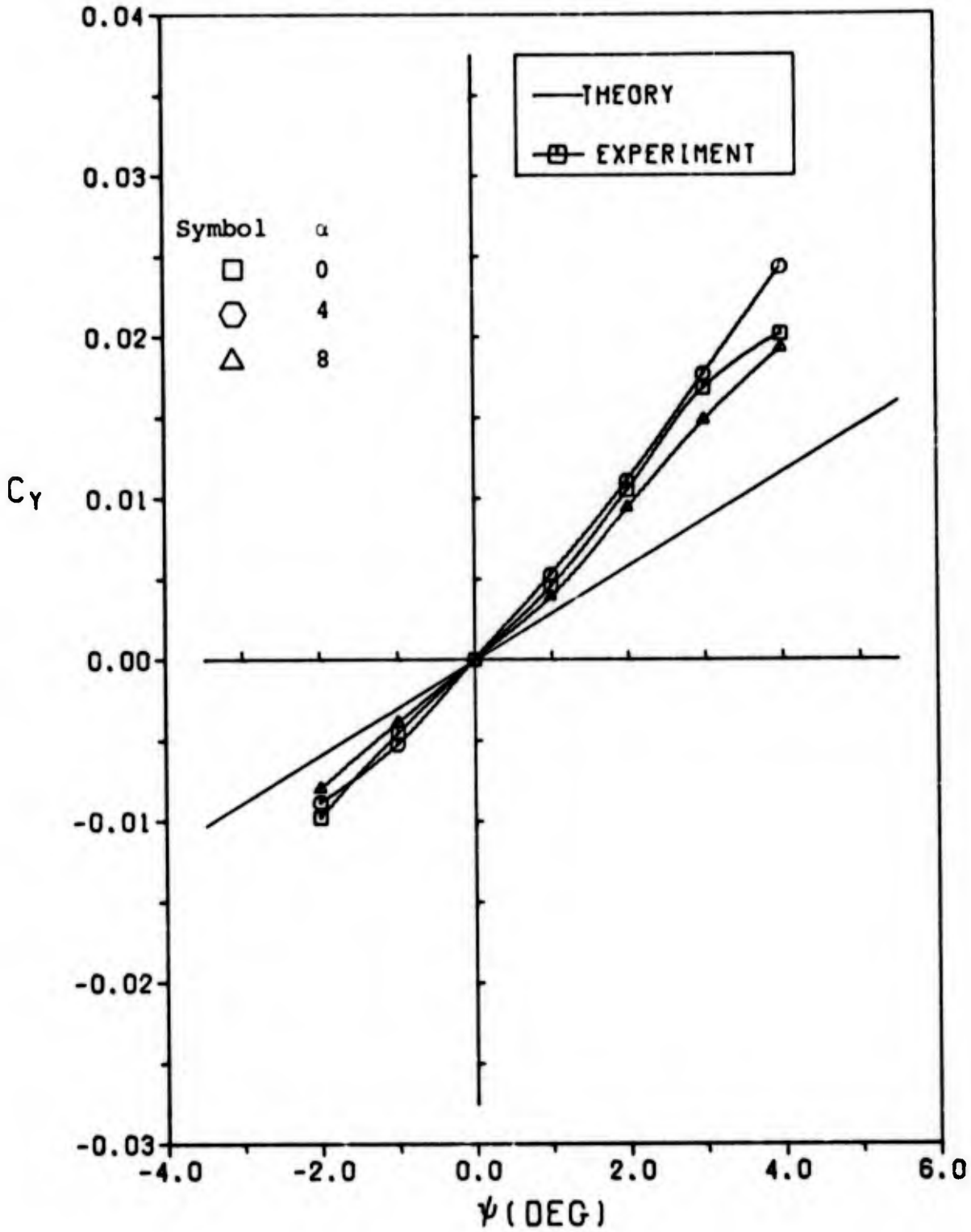

Figure 53. Side Force Coefficient C_Y vs Yaw Angle for Config. 4.

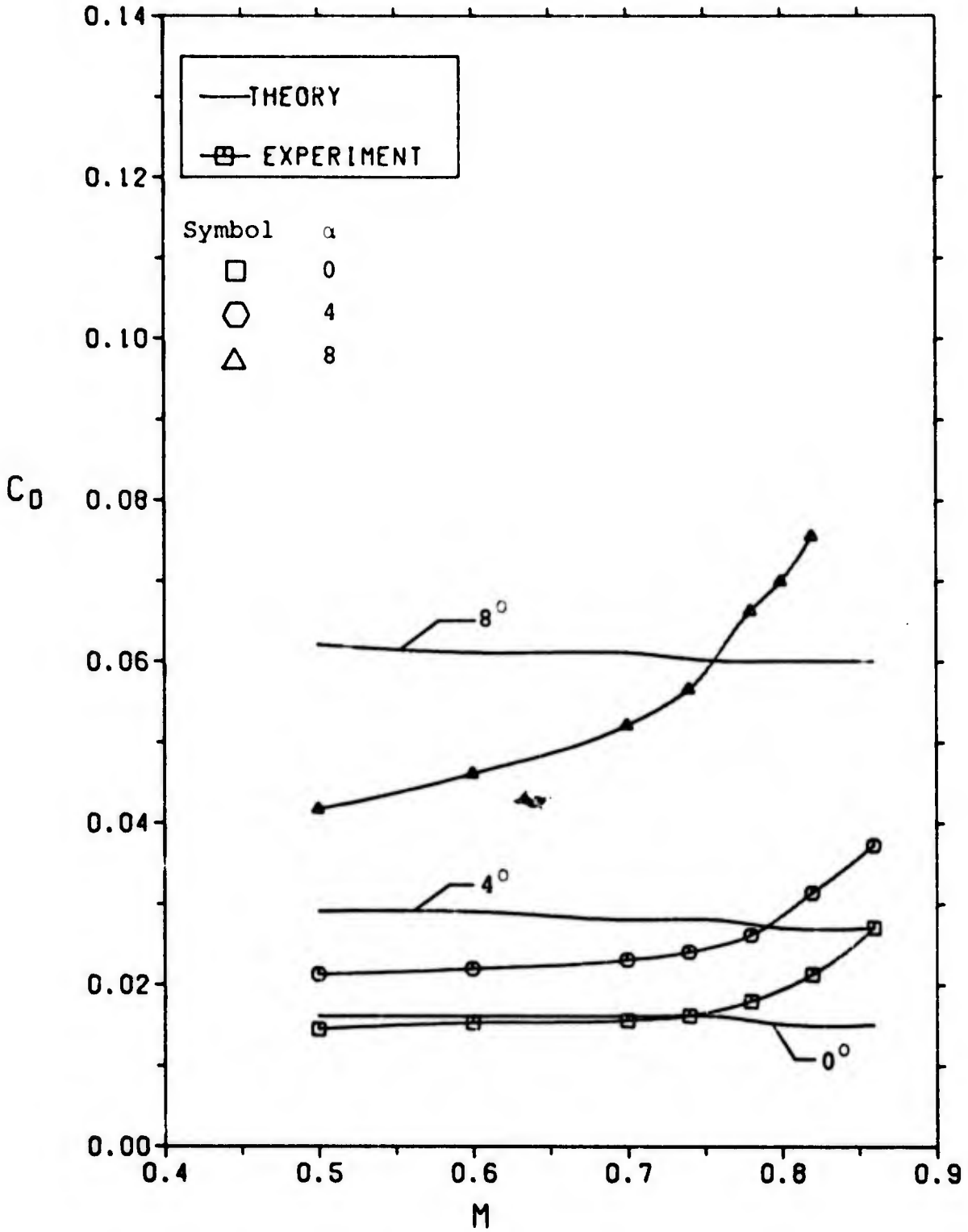

Figure 54. C_D vs M for Config. 4.

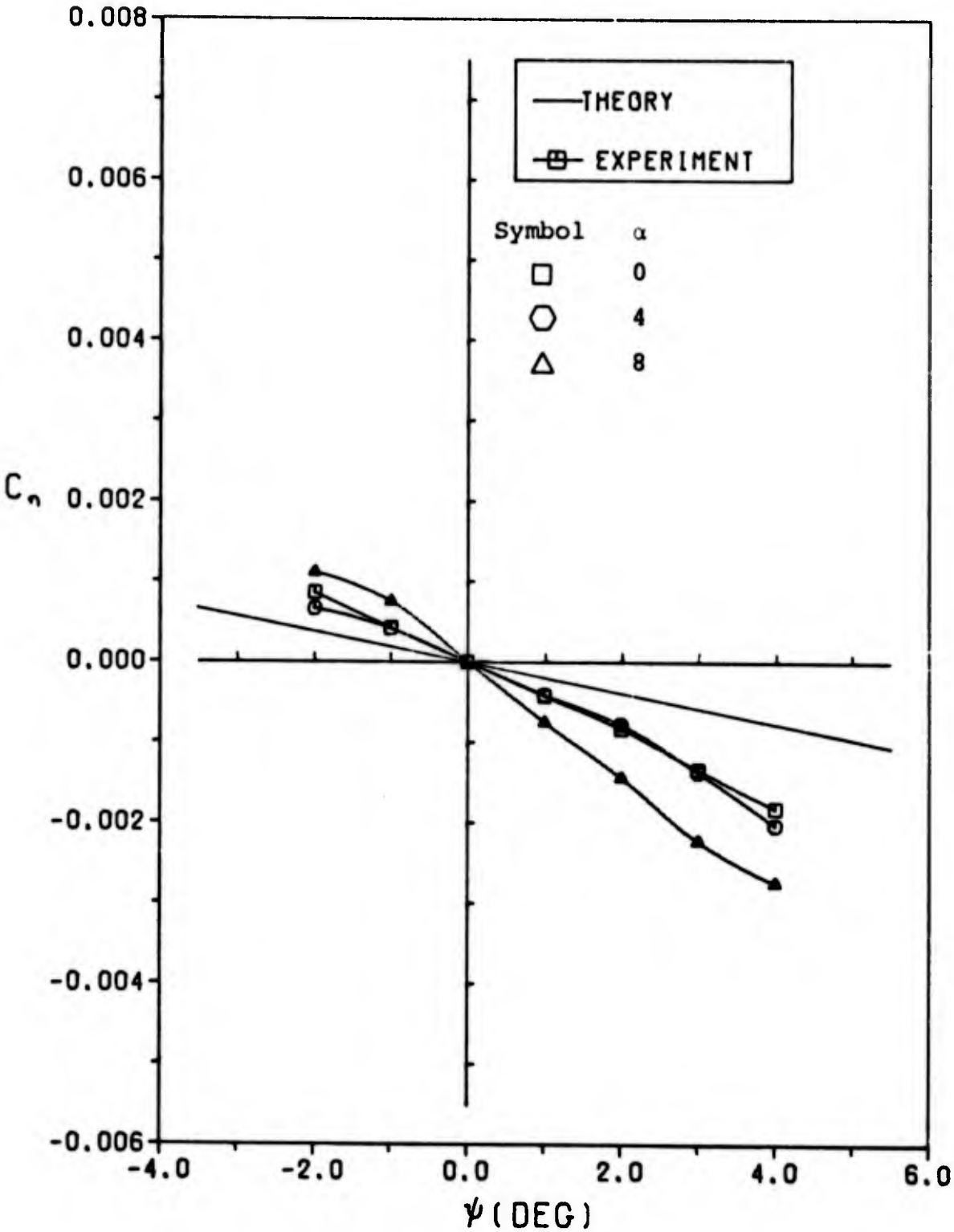

Figure 55. Yaw Moment Coefficient C_n vs Yaw Angle for Config. 5.

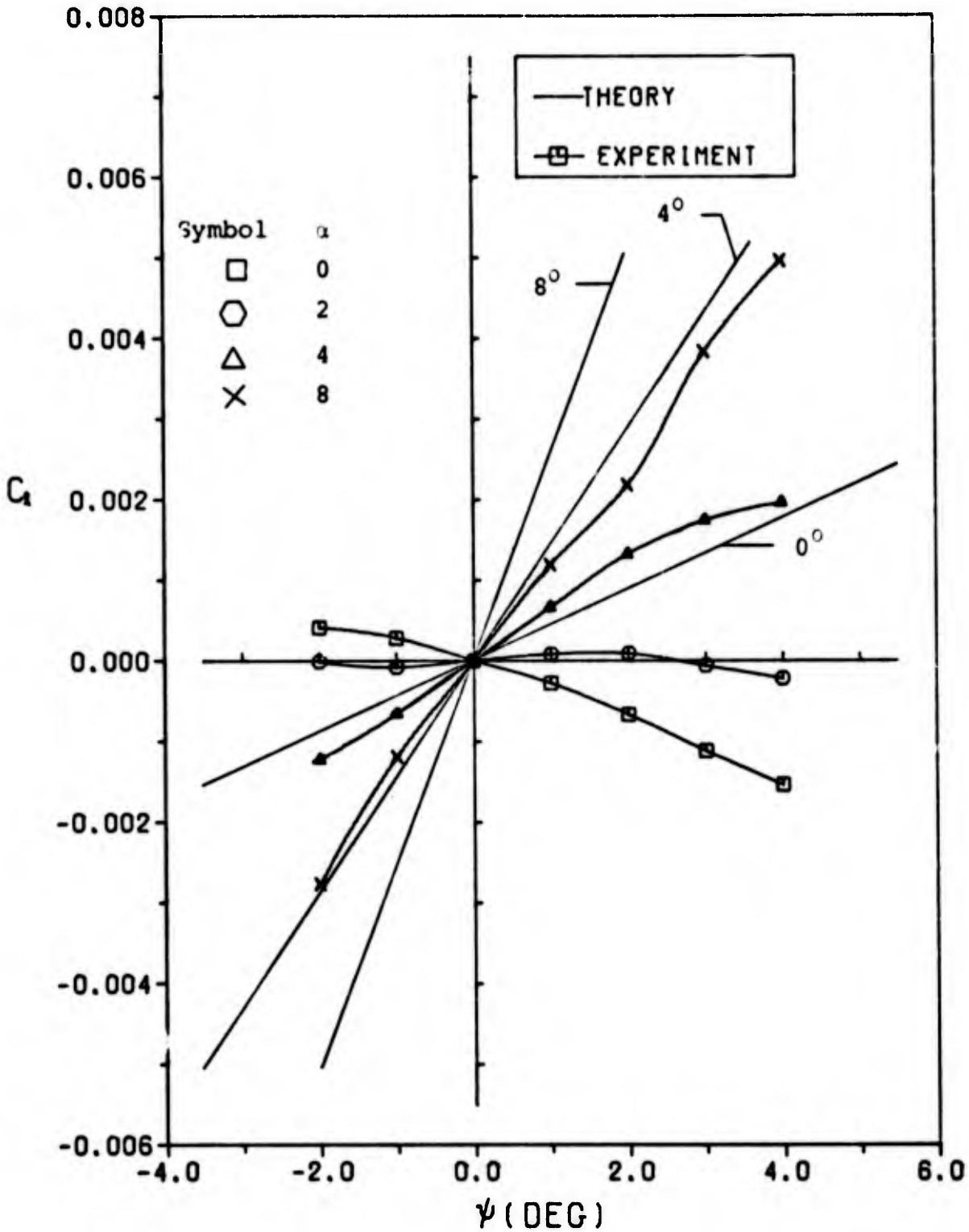

Figure 56. Roll Moment Coefficient C_l vs Yaw Angle for Config. 5.

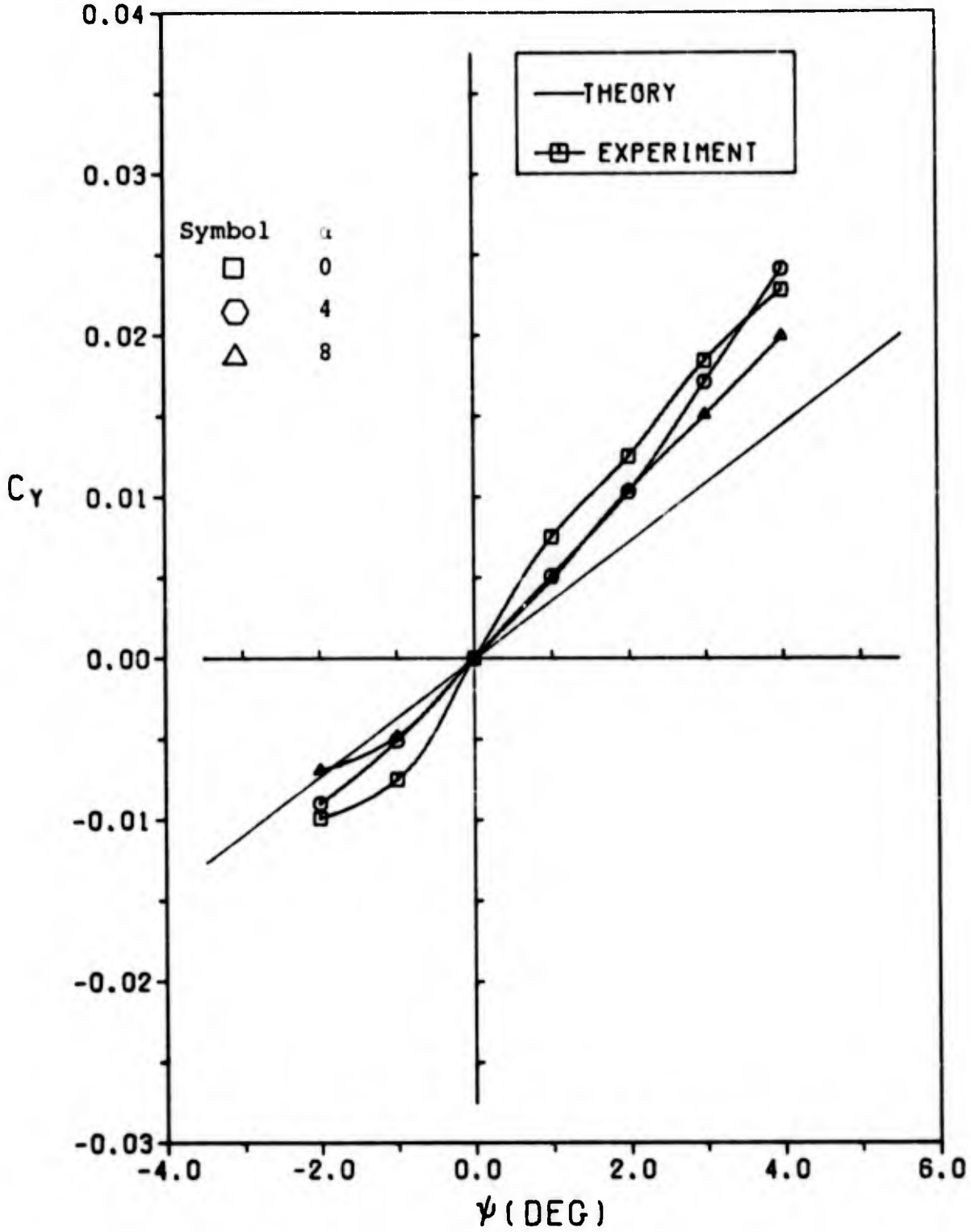

Figure 57. Side Force Coefficient C_Y vs Yaw Angle for Config. 5.

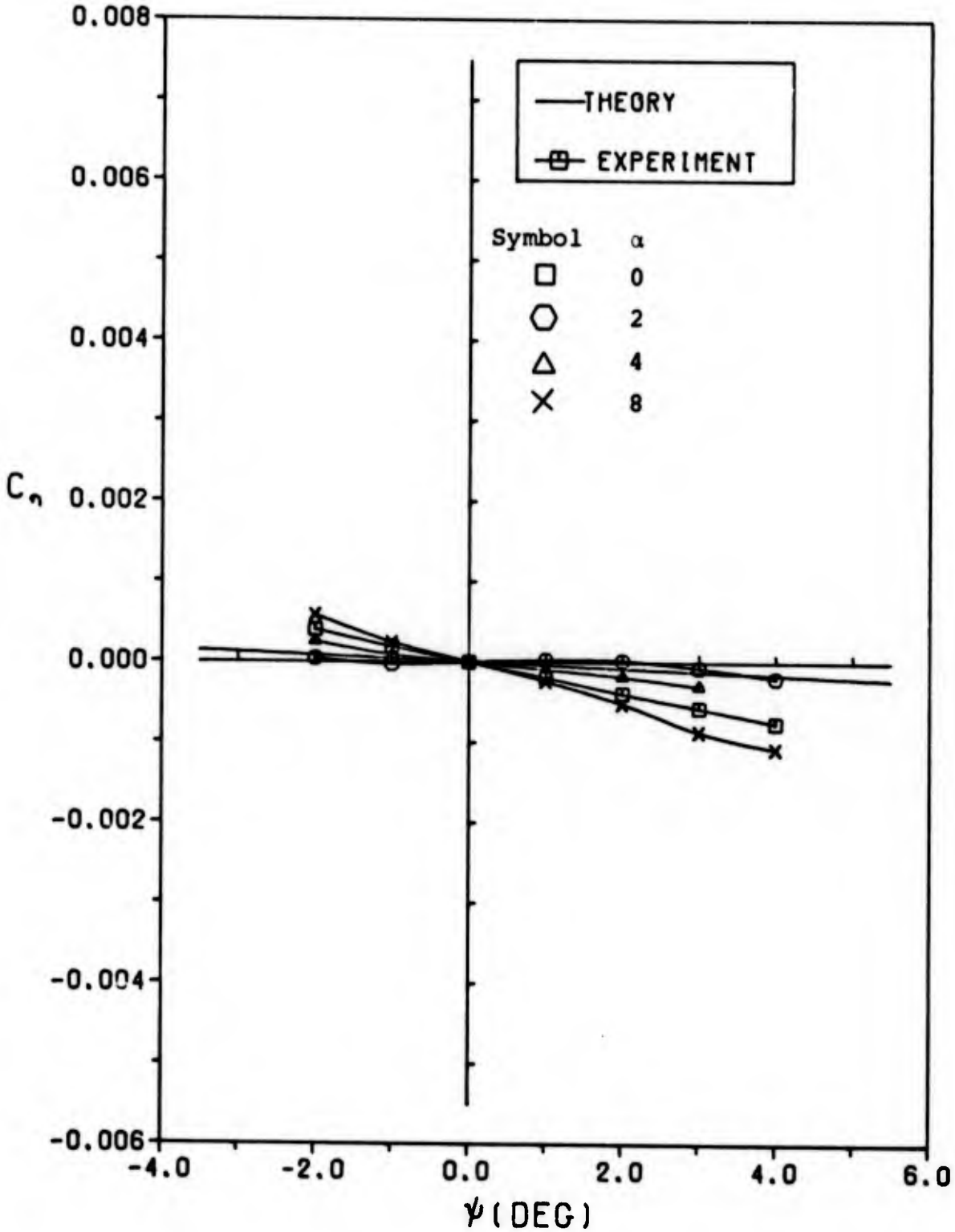

Figure 58. Yaw Moment Coefficient C_n vs Yaw Angle for Config. 6.

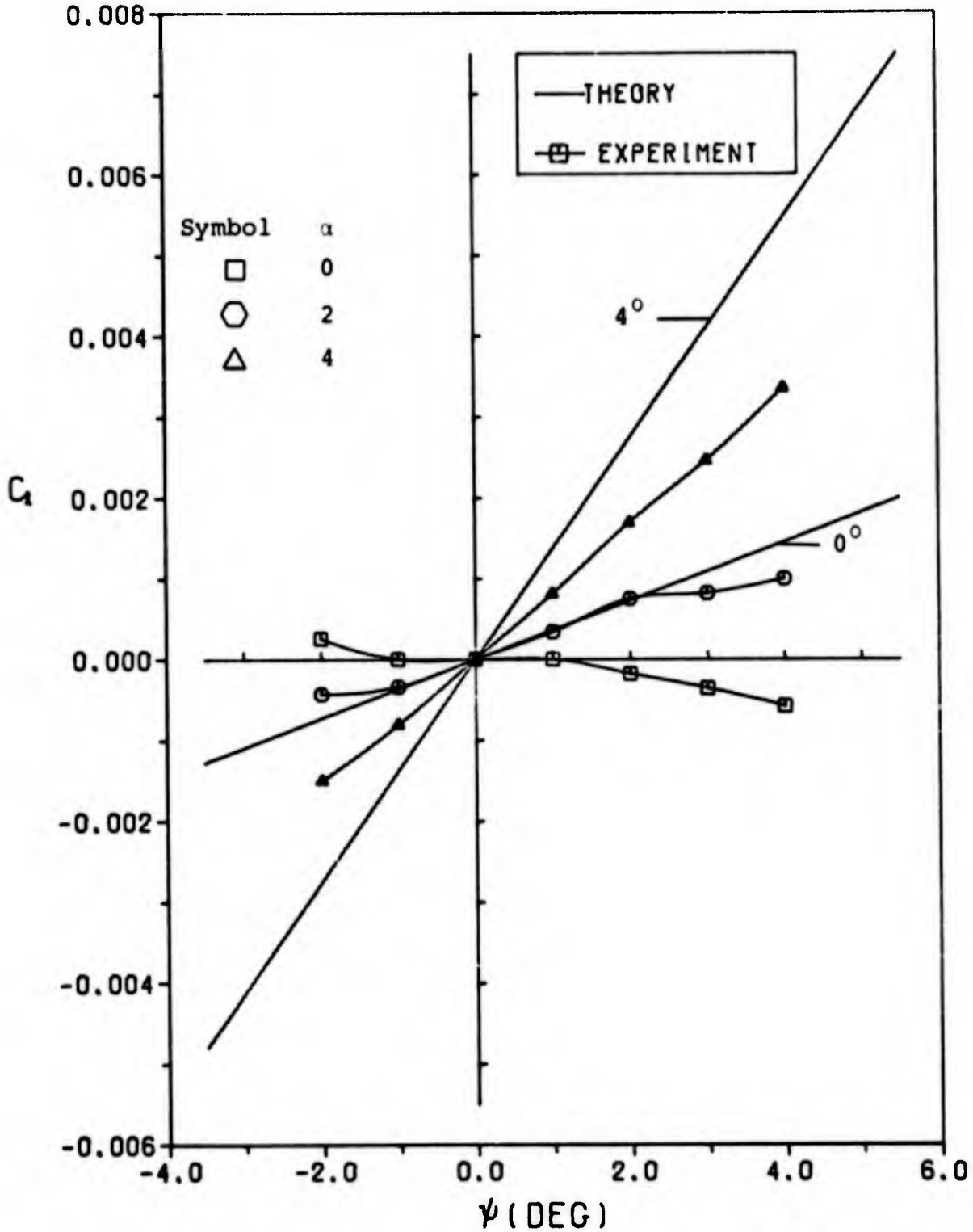

Figure 59. Roll Moment Coefficient C_l vs Yaw Angle for Config. 6.

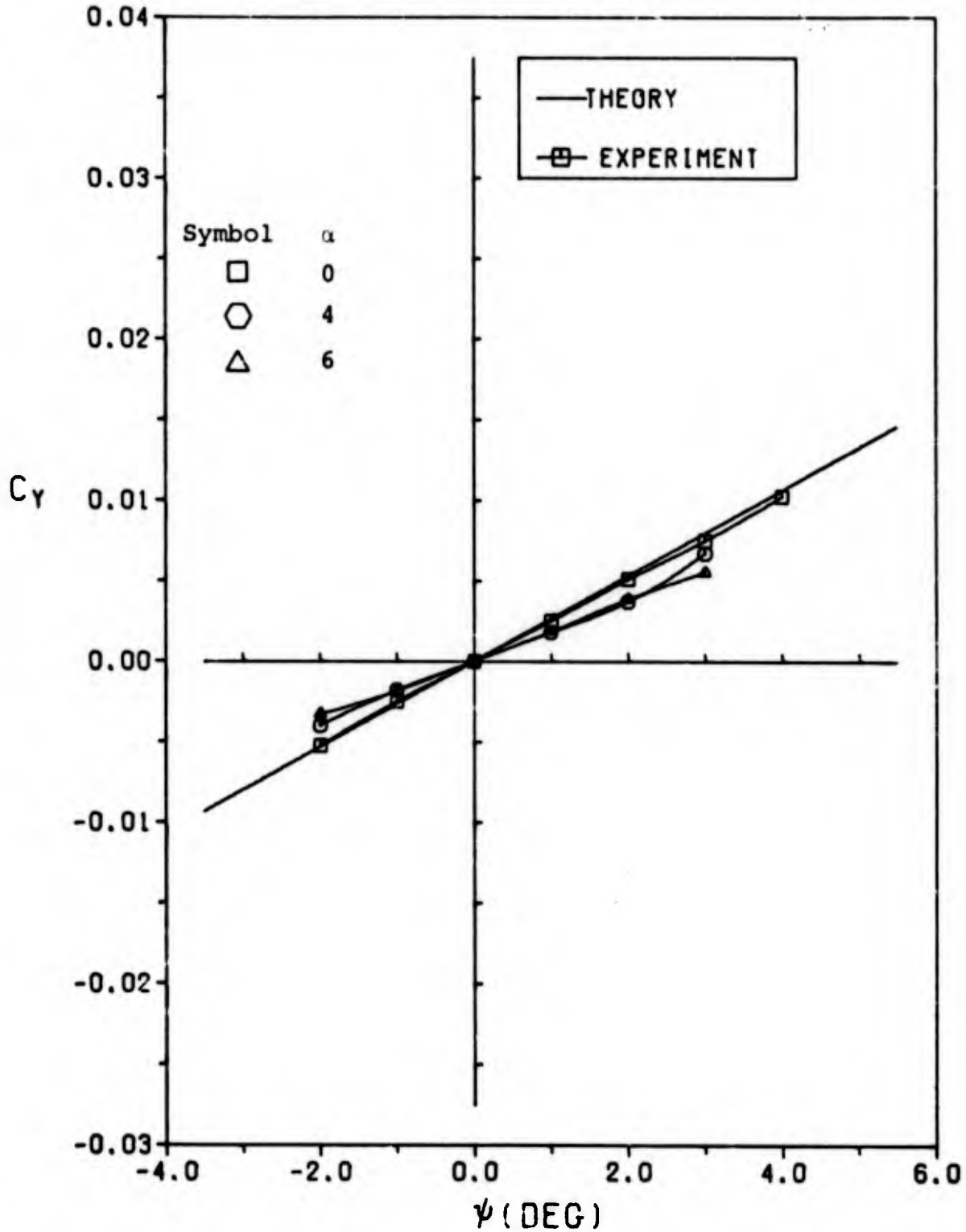

Figure 60. Side Force Coefficient C_Y vs Yaw Angle for Config. 6.

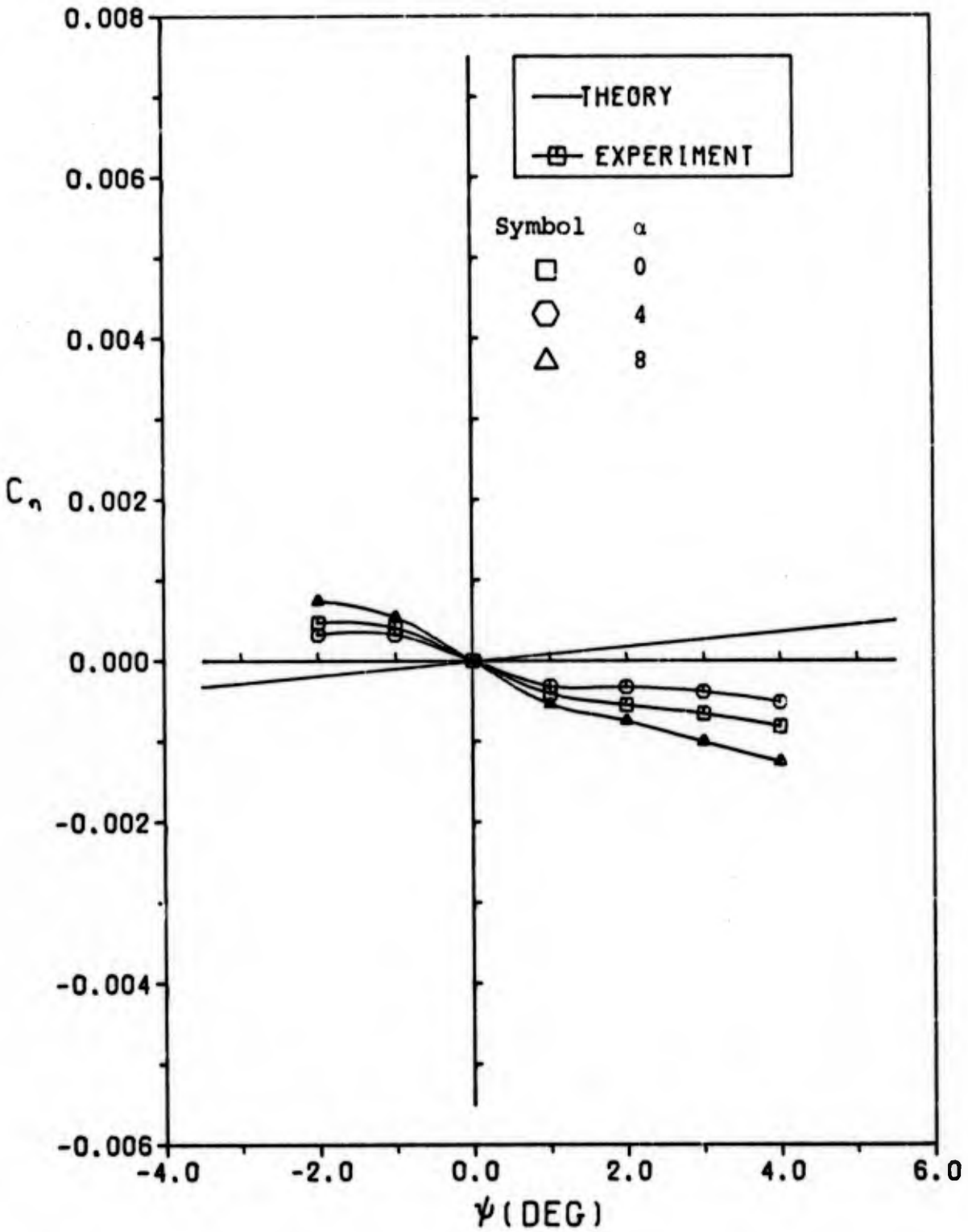

Figure 61. Yaw Moment Coefficient C_n vs Yaw Angle for Config. 7.

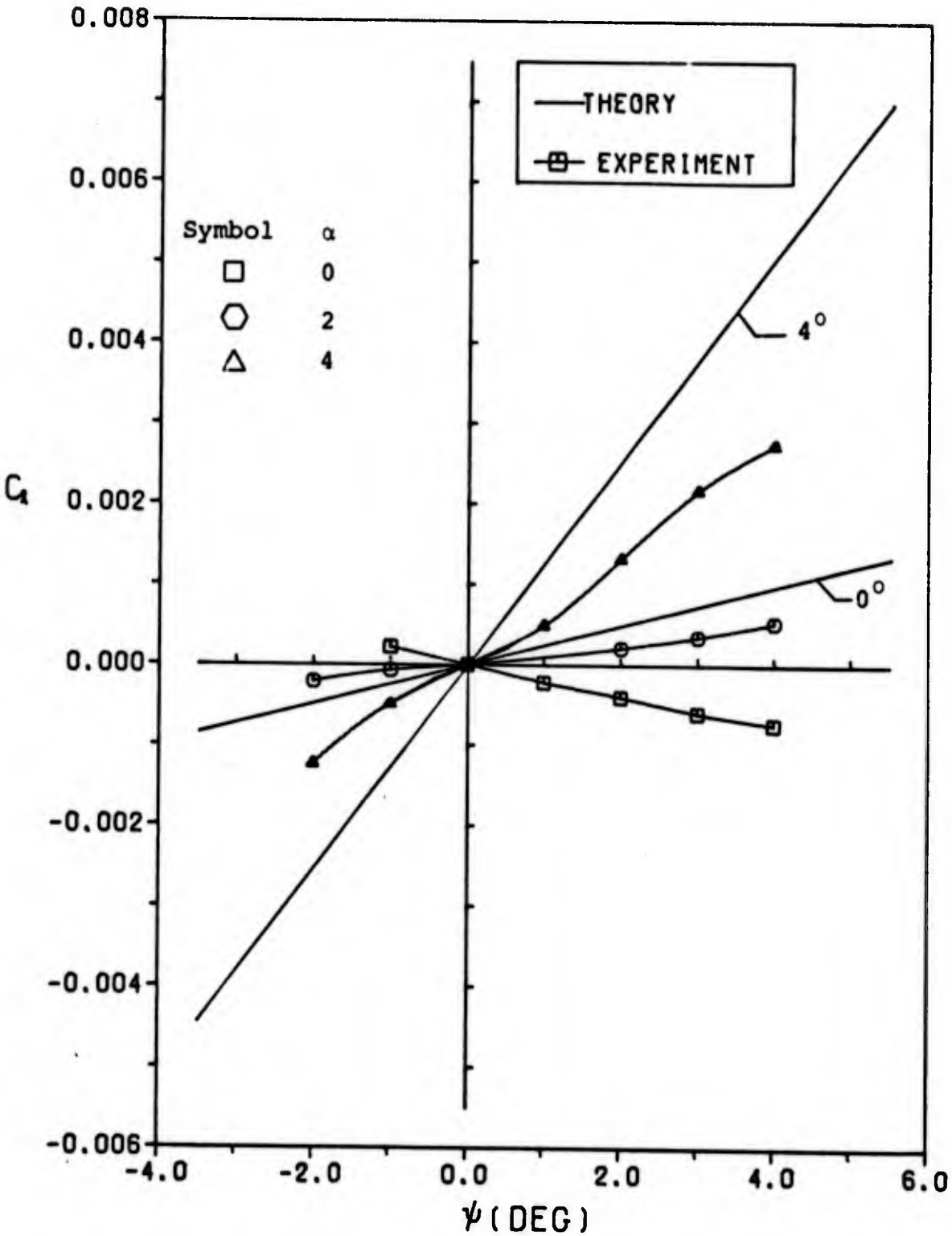

Figure 62. Roll Moment Coefficient C_l vs Yaw Angle for Config. 7.

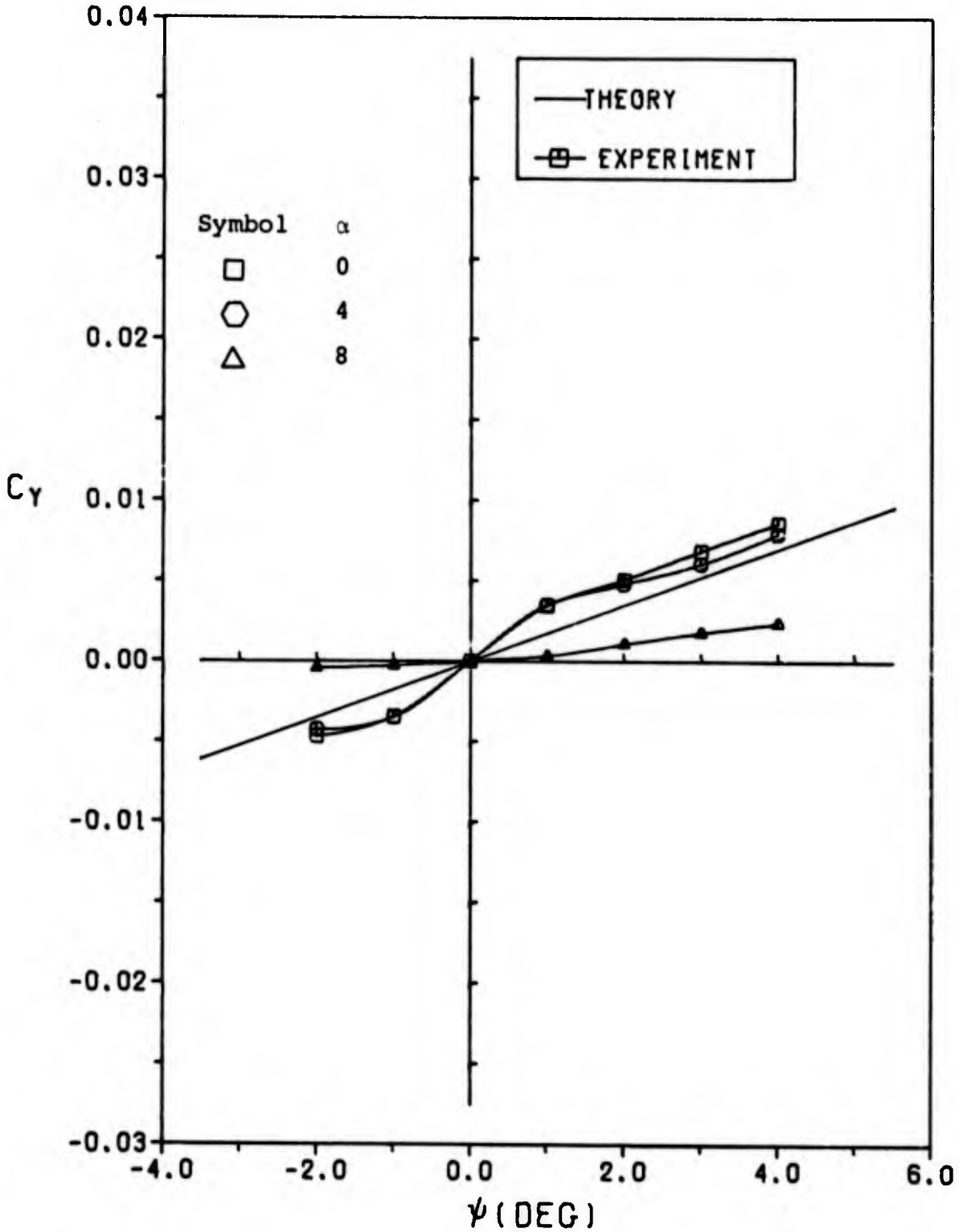

Figure 63. Side Force Coefficient C_Y vs Yaw Angle for Config. 7.

VITA

Leonard Voyd McCommon was born in [redacted], in [redacted]. He graduated from Oklahoma State University with a B.S. in Mechanical-Aerospace Engineering in January 1969. Upon completion of Officers Training School (OTS) in May 1969, he was assigned as a Deputy Missile Combat Crew Commander of a Titan II ICBM launch crew at McConnell Air Force Base, Wichita, Kansas. He progressed within three years to a Senior Instructor Combat Crew Commander and during his last year of duty at McConnell served as Missile Procedures Trainer Operator and Supervisor. He entered the Air Force Institute of Technology in May, 1974.

Permanent Address: [redacted]

This thesis typed by Linda Pearson.